Responses to Comments From Reviewers

Responses to Comments from Anonymous Referee #1

First, we wish to thank this reviewer for their helpful review. We first copy the comments of the reviewer **(in bold)** with our response below. In cases where the text is modified, we show both the original text and the revised text, with the changes shown in blue.

General Comments:

1. This paper extends studies in preparation for a new satellite radio occultation technique to profile atmospheric humidity. In order to explore some aspects of the deployment of this technique between two LEO satellites, the paper describes implementation of the same technique with transmitter and receiver on two mountain tops.

No response required.

2. It is a well-conceived experiment and the ideas and results are interesting. The paper is generally well written. The results are presented concisely but adequately. The discussions of the results and of the future potential of this technology are careful and persuasive.

No response required.

3. There is some problem with Figure 2 – the annotation referred to in the text is missing.

It looks like the wrong figure was uploaded as it is missing the annotations. Below is the figure 2 that should have been included with the paper. Figure 2 in the original document will be changed to the figure below. No change to caption, but it is repeated below the figure.

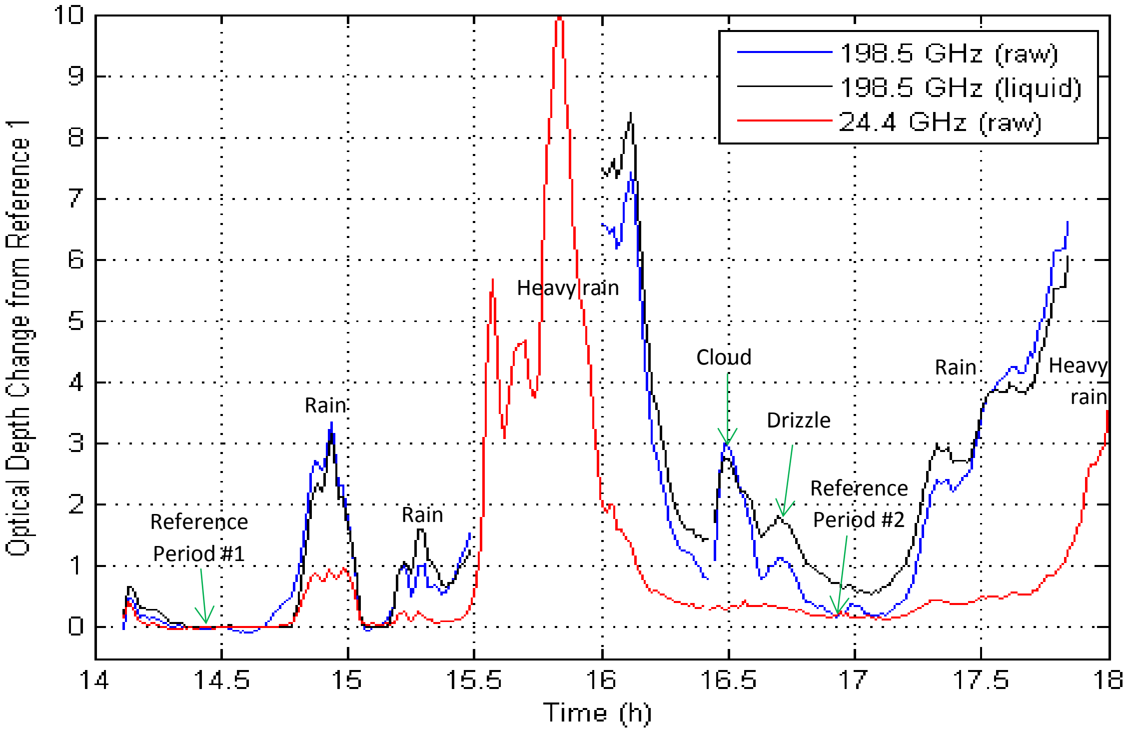

Figure 2. Blue and red lines show observed changes in optical depth at 198.5 GHz and 24.4 GHz relative to reference period 1. The black line shows changes in optical depth at 198.5 GHz due to changes in liquid water after removing the contribution from changes in vapor pressure and temperature.

4. I recommend publication subject to minor revision to address the points below.

No response required.

Specific Comments:

5. p.1, l.24: "precision" and "absolute accuracy". The words "precision" and "precise" are used here and in other places, and it is not clear whether the usage is technical or just general. Also, nowadays, "uncertainty" is usually preferred for "accuracy". So in this case, does "precision" mean "random uncertainty" and does "absolute accuracy" mean "systematic uncertainty"? If so, I suggest to re-write this sentence to clarify this, and to review all other occurrences of "precise" "precision" and "accuracy" throughout.

In the manuscript we use "precision" to mean "random uncertainty" and "accuracy" to mean "systematic uncertainty." We have made the following change.

Page 1, line 24. The word "precision" will be changed to "random uncertainty"

Original Sentence: Using an ATOMMS instrument prototype between two mountaintops, we have demonstrated its ability to penetrate through water vapor, clouds and rain up to optical depths of 17 (7 orders of magnitude reduction in signal power) and still isolate the vapor absorption line spectrum to retrieve water vapor with a precision better than 1%.

Revised Sentence: Using an ATOMMS instrument prototype between two mountaintops, we have demonstrated its ability to penetrate through water vapor, clouds and rain up to optical depths of 17 (7 orders of magnitude reduction in signal power) and still isolate the vapor absorption line spectrum to retrieve water vapor with a random uncertainty less than 1%.

6. p.1, l.25: "constraining processes". This is too brief to be clear. It is well explained on p.2, l.1.

The following sentences will be added at the end of the abstract:

ATOMMS' water vapor retrievals from orbit will not be biased by climatological or first guess constraints, and will be capable of capturing nearly the full range of variability through the atmosphere and around the globe, in both clear and cloudy conditions, and will therefore greatly improve our understanding and analysis of water vapor. This information can be used to improve weather and climate models through constraints on and refinement of processes affecting and affected by water vapor.

7. p.1, l.28: “precise”. See comment 5 above.

This sentence has been eliminated based on the changes spurred by the comment from Reviewer 3, referring to line 26 of page 1.

8. p.2, l.32: “precision”. See comment 5 above

We change the wording of two sentences in the last paragraph on page 2. The sentence beginning on page 2, line 26 contained the word “precisely” in line 27. Eliminate “precisely” by changing that sentence as follows

Original sentence: Profiling both the speed of light like GPS RO as well as the absorption of light, which GPS RO does not measure, enables ATOMMS to precisely profile temperature, pressure and water vapor simultaneously from near the surface to the mesopause (Kursinski et al., 2002).

Revised sentence: Profiling both the speed of light like GPS RO as well as the absorption of light, which GPS RO does not measure, enables ATOMMS to profile temperature, pressure and water vapor simultaneously from near the surface to the mesopause with little random or systematic uncertainties (Kursinski et al., 2002).

The sentence beginning on page 2, line 31 contained the word “precision.” Eliminate the word precision by changing that sentence

Original Sentence: Kursinski et al. (2002) found that such a system could provide water vapor retrievals with a precision of 1 – 3% from near the surface well into the mesosphere.

Revised Sentence: Kursinski et al. (2002) found that such a system could provide water vapor retrievals with a random uncertainty of 1 – 3% from near the surface well into the mesosphere.

9. p.4, l.1: “precise”. See comment 5 above.

We believe the word “precise” is appropriate as it is used on page 4, line 1. However, we do believe a wording change is warranted for “precise” on page 5, line 3. This instance was not specifically mentioned by the reviewer.

Original sentence: This ratio of ratios approach enables precise measurement of water vapor in the presence of clouds and rain as we demonstrate below.

Revised sentence: This ratio of ratios approach enables measurement of water vapor in the presence of clouds and rain with very small random and systematic uncertainty as we demonstrate below.

10. p.4, l.3-4: ". . . attenuation . . . distributed along the path . . . In contrast, . . .". Although this problem is more acute for passive radiometry, it is also present for RO – the attenuation is also distributed along the path and it is not possible to say where exactly along the path it takes place, even in the full RO retrieval context. So "In contrast" is too strong.

In order to address this concern, several wording changes are proposed within the paragraph that begins on page 4, line 1.

Original: ATOMMS functions as a precise, active spectrometer over the propagation path between the transmitter and receiver. Retrievals of water vapor from radiance measurements are inherently ambiguous because both the unknown signal source emission and attenuation, which are distributed along the path, must be solved for, creating an ill-posed problem (e.g., Rodgers, 2000). In contrast, the ATOMMS signal strength is known and the observed quantity is simply the attenuation along the path, which makes the retrievals much more direct and unambiguous. The active approach also enables precise and accurate retrievals under conditions of large path optical depths, which is not possible for passive retrievals.

Revised: ATOMMS functions as a precise, active spectrometer over the propagation path between the transmitter and receiver. Retrievals of water vapor from radiance measurements are inherently ambiguous because both the signal source emission and attenuation along the path are unknown and must be solved for, creating an ill-posed problem (e.g., Rodgers, 2000). In comparison to radiance retrievals, ATOMMS has the advantage that the transmitted signal strength is well known and the observed quantity is simply the attenuation along the path, which makes the retrievals much more direct and less ambiguous. The active approach also enables retrievals with small random and systematic uncertainty under conditions of large path optical depths, which is not possible for passive retrievals.

11. p.4, l.8: "in terms of amplitude rather than intensity". Does this explain the factor of 1 2 in eq.(1)? It may be worth pointing this out. Otherwise it looks like a rather unconventional definition of optical depth.

Add the following sentence after the sentence ending on line 11 of page 4. The factor of ½ multiplying the optical depth comes about because intensity is proportional to amplitude squared.

12. p.6, l.12-26. It would be helpful to say something here about another geometric difference: in this experiment, all the attenuation takes places at ~2600 m in height whereas, even in a single LEO-LEO measurement, it takes place over a range of altitudes characteristic of limb-viewing geometry.

Four wording changes have been made to address this comment.

(a) Add the following sentence after the sentence ending on page 5, line 27.

The attenuation contributed at higher altitudes along the ray path is comparatively much smaller than the contribution near the ray path tangent altitude due to both the limb sounding geometry and the exponential decay in water vapor concentrations with altitude.

(b) Change the sentence that begins on page 5, line 27.

Original Sentence: We note that the Abel transform isolates the contributions of these layers.

New Sentence: We note that the Abel transform isolates the contribution from the lowest altitude portion of the signal path.

(c) Change the sentence that begins on page 5, line 28.

Original Sentence: For a vertical resolution of 100 m, the horizontal length of the lowest layer is approximately 70 km (Eq. 13, Kursinski et al., 2002).

New Sentence: For a vertical resolution of 100 m, the horizontal length of the path through the lowest layer is approximately 70 km (Eq. 13, Kursinski et al., 2002).

(d) Change the wording of the sentence that begins on page 6, line 12.

Original Sentence: “In this mountaintop demonstration, the atmospheric path from transmitter to receiver was only 5.4 km, such that the water vapor attenuation due to absorption by the weak 22 GHz line was too small to measure accurately.”

New Wording (2 sentences): In this mountaintop demonstration, the atmospheric path from transmitter to receiver took place over a narrow altitude range from 2752 m to 2515 m above sea level and was only 5.4 km in length. Over this short path the water vapor attenuation due to absorption by the weak 22 GHz line was too small to measure accurately.

13. p.7, l.2-3: “as indicated by the annotations in Fig.2”. The intended annotations in Fig.2 appear to be missing. See comment 3 above. Similarly, “the First Reference period” (p.2, l.8) is not clear and presumably is intended to be an annotation on Fig.2.

Replacing figure 2, based on general comment #3, eliminates this issue.

14. p.7, l.21 and l.23: 4:30 –> 16:30?

Our mistake. The time should be specified as 16:30 in both instances. Changes will be made.

15. p.7, l.29: “as the calibration tone”. Do you mean fCAL, which you call the “calibration signal” on p.4, l.20? It would be helpful to standardise references to fCAL, calibration signal, calibration frequency and calibration tone throughout.

To avoid confusion and for consistency, we have decided to use the term “calibration signal” throughout. The calibration signal amplitude at a particular selected frequency (typically in the wing of the absorption line) is used to remove or reduce unwanted common mode amplitude variations before using the on line signal frequencies to estimate atmospheric absorption.

Here are all the instances of f_{CAL}, calibration frequency, and calibration tone that have been changed. The changes are shown below. If just a single word is changed, the change is indicated in blue.

page 3, line 11. “ATOMMS performance in cloud and rain is achieved via a differential transmission approach using a calibration ~~tone~~ signal, in contrast to passive IR and microwave sensors systems that work via emission.”

page 4, line 20.

Original sentence: The frequency, f, of one signal is placed on the absorption line of interest while the frequency of the second signal, f_{CAL}, is farther from line center to function as a calibration signal.

Modified sentence. The frequency, f, of one signal is placed on the absorption line of interest while the frequency of the second signal, f_{CAL}, is farther from line center so that signal can function as an amplitude calibration signal.

page 6, line 31. “198.5 GHz was the frequency of the High-Band calibration ~~tone~~ signal during this experiment.”

page 7, line 27. Several changes were made for clarification. This also partially addresses specific comment #16.

Original wording. For this experiment, one transmitter swept through the tunable frequency range generating a tuned tone that was received by a receiver sweeping through the same tuning sequence. The other tone was fixed at 198.5 GHz in order to function as the calibration tone.

Revised wording. For this mountaintop experiment, the frequency of the signal generated by one transmitter was swept through a tuning sequence that spanned the instrument’s tunable frequency range. This signal was received by a narrowband heterodyne receiver whose second local oscillator was simultaneously swept through its matching tuning sequence. The frequency of the other signal was fixed at 198.5 GHz in order to function as the amplitude calibration signal for measuring differential absorption.

page 8, line 4.

Original sentence. Calibration tone amplitudes were computed using the same method.

Modified sentence. The calibration signal amplitudes were computed using the same method.

page 9, line 5.

Original sentence. The liquid optical depth in Fig. 2 is the liquid optical depth at the calibration tone, $f_{CAL} = 198.5$ GHz.

Modified sentence. The liquid optical depth in Fig. 2 is the liquid optical depth measured by the calibration signal, $f_{CAL} = 198.5$ GHz.

page 11, line 24. “These were reduced by almost an order of magnitude via amplitude ratioing with the calibration ~~tone~~ signal (Kursinski et al., 2016).

page 13, line 3. Ratioing of the amplitudes of two signals, as was done here, eliminates the effects of liquid particle extinction to the extent that the liquid extinction is spectrally flat over the ATOMMS tuning range and calibration frequencies. No change needed here.

page 13, starting on line 12. This small 0.8% change in the retrieved vapor pressure provides some indication of how effective the calibration ~~tone~~ signal ratioing is in minimizing the sensitivity of the ATOMMS water vapor retrievals to hydrometeors. In the future, the High Band system will have 4 rather than its present 2 ~~tones~~ signals in order to place calibration ~~tones~~ signals on both the low and high frequency sides of the 183 GHz water vapor line to reveal and compensate for any overall spectral tilt caused by particle extinction as well as other effects.”

page 16, lines 32 and 33.

Original wording. In terms of the number of signal frequencies required to accurately determine the water vapor, we used from 5 to 15 tuned signal frequencies plus a calibration frequency for the water vapor spectral fits. The agreement and consistency of these results indicate that the amplitudes from just a few tuned frequencies and a calibration frequency are needed to produce water vapor retrievals with very small random and absolute uncertainties.

Revised wording. In terms of the number of signal frequencies required to accurately determine the water vapor, we used between 5 and 15 tuned signal frequencies plus a calibration signal at a fixed frequency for the water vapor spectral fits. The agreement and consistency of these results indicate that the amplitudes from just a few tuned frequencies and a fixed frequency amplitude calibration signal are needed to produce water vapor retrievals with very small random and absolute uncertainties.

page 17, line 18.

Original sentence. “The LEO version of ATOMMS will provide the information necessary to observe and account for such non-vapor effects using at least three simultaneous signal frequencies to place calibration tones on both the low and high sides of the absorption line and the third frequency on the line.

Revised sentence. “The LEO version of ATOMMS will provide the information necessary to observe and account for such non-vapor effects using at least three simultaneous signal frequencies to place amplitude calibration signals on both the low and high sides of the absorption line and the third frequency on the line.”

16. p.8, l.1-5. The description of the processing is very compressed and it is not possible for the reader, from this alone, to understand how the processing is done. Can you give a reference to a more complete description?

We propose to significantly change the wording under the heading “Signal Tuning and Detection,” which begins on page 7, line 25. Major changes are shown in blue.

Original text.

The High Band portion of the ATOMMS ground-based prototype instrument simultaneously transmits and receives two continuous wave signals that are tunable from 181 to 206 GHz. For this experiment, one transmitter swept through the tunable frequency range generating a tuned tone that was received by a receiver sweeping through the same tuning sequence. The other tone was fixed at 198.5 GHz in order to function as the calibration tone. There were 122 tuning frequencies in the sweep, separated by 0.25 GHz, except for a gap between 191.5 and 193.5 GHz. This gap is due to the limited receiver response for Intermediate Frequencies (IF) less than one GHz and the first stage local oscillator (LO) being set to 192.5 GHz. This is likely the finest spectral resolution sampling of the 183 GHz line ever achieved in the field.

The dwell time for each frequency of the tuned transmitted tone was 100 ms. The timing of the transmitter-receiver tuning was synchronized using GPS receivers. Each received ATOMMS signal was filtered, down converted in frequency, digitized and recorded. The signal frequency in the final receiver stage ranged from 8 to 35 kHz for each of the 122 tuned frequencies. The frequency and power of the down converted signals were detected using a Fast Fourier Transform (FFT) and the signal amplitude was determined by taking the square root of the integrated signal power from each FFT. The integration time was 50 ms, which is half of the dwell time to allow time for each synthesizer tune to settle. Calibration tone amplitudes were computed using the same method.

One sweep of the frequencies took 12.2 seconds. The instrument cycled through the four combinations of the two transmitters and two receivers before repeating the tuning cycle to help isolate any transmitter or receiver issues. Thus, a full tuning cycle was completed every 48.8 s. The observations from the four different transmit-receive pairs were averaged together to yield new estimates for the ATOMMS signal ratio every 48.8 seconds (Eq. (2)). The resulting integration time for each particular tuned frequency was four times 50 ms or 200 ms.”

Revised text.

The High Band portion of the ATOMMS ground-based prototype instrument simultaneously transmits and receives two continuous wave signals that are tunable from 181 to 206 GHz. For this mountaintop experiment, the frequency of the signal generated by one transmitter was swept through a tuning sequence that spanned the instrument’s tunable frequency range. This signal was received by a narrowband heterodyne receiver whose second local oscillator was simultaneously swept through its matching tuning sequence. The frequency of the other signal was fixed at 198.5 GHz in order to function as the amplitude calibration signal for measuring differential absorption. There were 122 frequencies in the tuning sequence, separated by 0.25 GHz, except for a gap between 191.5 and 193.5 GHz due to the receiver’s limited response for Intermediate Frequencies (IF) less than one GHz and the first stage local oscillator

(LO) being set to 192.5 GHz. ~~This is likely the finest spectral resolution sampling of the 183 GHz line ever achieved in the field.~~

When executing the tuning sequence, the tuned transmitter tone dwelled at a particular frequency in the tuning sequence for 100 ms before moving to the next frequency in the sequence. The timing of the transmitter and receiver tuning sequences were synchronized using GPS receivers. At the receiver, each of the two received ATOMMS signals was filtered, down-converted in frequency, digitized and recorded. The frequency and power of the down-converted signals were determined using a Fast Fourier Transform (FFT), calculated over a 50 ms integration time. The reason that only half of the 100 ms tuning dwell time was used was to allow time for each synthesizer tune to settle. Each FFT-derived signal power estimate was then converted to an amplitude by taking the square root. The calibration signal amplitudes were computed using the same method.

One sweep through the frequency tuning sequence took 12.2 seconds. The instrument cycled through the four combinations of the two transmitters and two receivers before repeating the tuning cycle in order to help isolate any transmitter or receiver issues. Thus, a full tuning cycle was completed every 48.8 s. The observations from the four combinations of transmitter-receiver pairs were then averaged together such that new estimates for the ATOMMS signal amplitude ratios at all of the 122 tuning frequencies were generated every 48.8 seconds (Eq. (2)). As a result, the integration time used to estimate the signal amplitude and frequency for each of the 122 frequencies in the tuning sequence was four times 50 ms or 200 ms.

17. p.8, l.15: “are identified in Fig.2”. See comment 13 above

Taken care of with the correctly annotated Figure 2.

18. p.8, l.22 and elsewhere: “the am Atmospheric Model”. This is not clear; is the name of this forward model the “Atmospheric Model”, abbreviated as “am”. Later it is referred to as “AM” sometimes with a version number. Please make all these references consistent.

Several changes were made for clarification and consistency.

Page 8, line 22, original text. “…we used the *am* Atmospheric Model, version 7.2 [*Paine*, 2011] which was shown to fit the ATOMMS measurements to the 0.3% level in previous work with the ground-based ATOMMS prototype system [*Kursinski et al.*, 2012].”

Revised text. “… we used an atmospheric propagation tool known as the Atmospheric Model (am), version 7.2 (Paine, 2011), which we will refer to as *am7.2*. This model was shown to fit the ATOMMS measurements to the 0.3% level in previous work with the ground-based ATOMMS prototype system (Kursinski et al., 2012).”

Page 12, line 6, original text. “For the conditions of this particular experiment, based on the AM7.2 model, the sensitivity of the change in derived water vapor due to a temperature change relative to the reference period temperature was approximately -0.17 hPa/°C.”

Revised text. “For the conditions of this particular experiment, based on forward calculations made with *am7.2*, the sensitivity of the change in derived water vapor due to a temperature change relative to the reference period temperature was approximately -0.17 hPa/°C.”

Page 12, line 29, original text. “This half range represents a conservative estimate of the random uncertainty of the retrieved vapor pressure changes that includes both measurement and am model errors.”

Revised text. “This half range represents a conservative estimate of the random uncertainty of the retrieved vapor pressure changes that includes both measurement and *am7.2* modeling errors.”

Caption of figure 5, current text. “forward calculated ATOMMS ratio using the am Model, version 7.2.”

Revised text. “forward calculated ATOMMS ratio using *am7.2*.”

19. p.9, l.10-11: “12 different solutions”. At this point the 12 solutions have not been mentioned or explained. Please refer forwards to section 5 for this description.

We have referred to Section 5 already. The current text is “The retrieved path-averaged vapor pressure between the instruments is shown in Fig. 3A. The figure shows 12 different solutions that were used to estimate the random uncertainty in the retrieval of vapor pressure as described in Section 5.”

The following change has been made for clarity: “The figure shows 12 different solutions that were used to estimate the random uncertainty in the retrieval of vapor pressure. The methodology used to compute the 12 solutions is described in Section 5.”

19. p.10, l.4-20. This is a very ingenious solution to the problem – nice piece of work! The only question remaining at this point in the reader’s mind concerns the inherent uncertainties in this method. You discuss this later in section 5, and so I suggest here you refer forward to this discussion.

This is already done on page 10, line 10, where it is stated “The uncertainty associated with this temperature estimation is discussed in Section 5.”

To be clearer that sentence will be moved to the end of the last paragraph of the section “Determining Temperature,” which is page 10, line 20 in the original document.

20. p.12, l.6 and l.26: “AM7.2” and “am”. See comment 18 above.

Changes specified in response to comment #18 above.

21. p.18, l.7-13. In addition to these points, it is worth mentioning that GPS RO loses sensitivity to humidity, typically from the mid-troposphere upwards (at a height dependent on absolute humidity and hence temperature) because of the relatively low absorption coefficient of water vapour at GPS frequencies.

We respectfully disagree with this comment. GPS has very little sensitivity to water vapor via absorption because its frequencies are so low in comparison to the 22 GHz water absorption line. The sensitivity that GPS does have to water vapor is via the propagation delay due to the refractivity of water vapor which is significant basically at temperatures above 240 K (because there is enough water vapor present to see this effect in individual profiles). However, one cannot isolate that water vapor signature directly from the GPS observations alone. One must add additional constraints on the dry part of the refractivity to isolate the wet part of the refractivity buried in the GPS refractivity estimates.

22. p.18, l.1 and l.23: "achieves" –> "would achieve"? "offers" –>"would offer"?

We like use of the word "achieve" on page 18, line 2. No change here.

On page 18, line 23, though, we like the reviewer's suggestion to change "offers" to "would achieve."

Revision to sentence shown: Given this present situation, ATOMMS' precise, all-weather retrieval capability, as demonstrated here, ~~offers~~ would achieve a major advance in remote sensing of the atmosphere.

23. p.19, l.4-6. It would be more conventional to write this sentence as a simple statement with reference "(Holger Vömel, personal communication)".

Thank you.

Original wording. "However, when we discussed validating ATOMMS instruments to 1% with Holger Vömel, a chilled mirror hygrometer expert at NCAR, he indicated that no in-situ measurements can reliably achieve 1% accuracy out in the field."

Revised wording. "However, when we discussed validating ATOMMS instruments to 1% with a chilled mirror hygrometer expert at NCAR, we were told that no in-situ measurements can reliably achieve 1% accuracy out in the field (Holger Vömel, personal communication)."

24. p.19-20. In addition to the arguments presented in this Appendix, I think there is an additional one. If the typical scales that need to be measured are ~13m, then any in situ observing system would

need to be so close to the axis of the ground-based remote sensing system that it would interfere with the measurement. Otherwise it is not measuring the same path.

Thank you. This is a point worth mentioning. The following sentence has been added after the second sentence in the last paragraph that begins of page 19. “It would be difficult, if not impossible, to locate these sensors close enough to the signal propagation path without interfering with signal itself.”

25. Fig.2. See comments 3 and 13 above

Figure 2 will be replaced with the correctly annotated figure.

Editorial Points:

26. p.1, l.2. Title: “mm- wavelength” –> “mm-wavelength”?

We agree. There should probably not be a space between mm- and wavelength. We will have to check with the editorial staff. Change initially will be made to original document.

27. p.3, l.16. “Uncertainty” –> lower case?

The word “Uncertainty” will be changed to lower case “uncertainty.”

28. p.11, l.20. “,” after “seconds”?

Comma will be added after the word “seconds” on page 11, line 20.

29. p.16, l.30: “sought after” –> “sought-after”?

Thanks. A hyphen should be used. “sought after” will be replaced by “sought-after”

Responses to Comments from Anonymous Referee #2

We wish to thank this reviewer for their helpful review. We first copy the comments of the reviewer **(in bold)** with our response below. In cases where the text is modified, we show both the original text and the revised text, with the significant changes shown in blue.

General Comments:
The paper is a very interesting and indeed necessary contribution to investigate the atmosphere based on occultation measurement technique by exploiting the microwave capacity. It describes in detail the ground based experiment by detecting water vapour with microwave signals under clear too very turbulent conditions as pre-study to a microwave occultation satellite mission. Besides a detailed results description an error and validation discussion was done. The discussion in the appendix about the difficulty or even impossability to in-situ validate such an experiment rounds up the paper. I recommend the paper for publication with minor revisions.

In this paper the low band signal is only used to determine whether there are small water particles present or not but it apparently is not used for the retrieval of water vapor, which is done only for the high band signal (Fig. 2). It is though claimed that to derive the water vapor content under stormy conditions when the high band becomes opaque, the low band is needed but it is not done for this experiment.
Did you get results on the 8 fixed frequencies at the 22 GHz region to investigate the heavy rain situation at 15:30, since for such heavy weather situation sufficiant attenuation occured?

Unfortunately, we determined that the measurements taken at the 8 fixed frequencies near 22 GHz on this day could not be used to make accurate retrievals for water vapor. The main reason is that the path length (of only 5.4 km) is too short for accurate determination of water vapor using the weak 22 GHz line as the absorption is so small. While the liquid absorption was strong during the heavy rain period, the additional absorption due to water vapor is quite small across the 22 GHz band.

Specific Comments:
p. 2, line 16—20: Please give a reference to the RO technique including the specifications/limits of this remote technique. Please give references for other studies on microwave occultation technique pre-studies too.

To address this comment, we propose making some wording changes and adding additional references to the two consecutive paragraphs that begin on page 2, line 15.

Original text:

GPS radio occultation (RO) has become an important data source for numerical weather prediction (NWP), despite its relatively sparse coverage to date [e.g., Cardinali and Healy, 2014]. Its high impact comes from its unique combination of ~200 m vertical resolution, all weather sampling and very low random and absolute uncertainties via its direct connection to atomic frequency standards. GPS RO profiles atmospheric refractivity. Two limitations of GPS RO are

(1) its inability to separate the dry air and water vapor contributions to refractivity and (2) its insensitivity to water vapor in the colder regions of the troposphere and above.

In recognition of the strengths and weaknesses of GPS RO and radiance measurements and the need for better information about water vapor, in 1997 research groups at the University of Arizona and the NASA Jet Propulsion Laboratory (Herman et al., 1997 and Hajj et al., 1997) identified and began developing an RO system that is now called the Active Temperature, Ozone and Moisture Microwave Spectrometer (ATOMMS), which is designed to overcome these limitations by transmitting and receiving signals between satellites in low Earth orbit (LEO) near the 22 and 183 GHz water vapor absorption lines as well as nearby ozone absorption lines. Profiling both the speed of light like GPS RO as well as the absorption of light, which GPS RO does not measure, enables ATOMMS to precisely profile temperature, pressure and water vapor simultaneously from near the surface to the mesopause (Kursinski et al., 2002). It will also profile ozone from the upper troposphere into the mesosphere, scintillations produced by turbulence, slant path cloud liquid water and detect larger cloud ice particles, with approximately 100 m vertical resolution and corresponding 70 km horizontal resolution (Eq. 13, Kursinski et al., 1997). Kursinski et al. (2002) found that such a system could provide water vapor retrievals with a precision of 1 – 3% from near the surface well into the mesosphere. Kursinski et al. (2009) estimated the degradation in clouds would be less than a factor of 2.

Revised text, with changes shown in blue:

GPS radio occultation (RO) has become an important data source for numerical weather prediction (NWP), despite its relatively sparse coverage to date [e.g., Cardinali and Healy, 2014]. Its high impact comes from its unique combination of ~200 m vertical resolution, all weather sampling and very low random and absolute uncertainties via its direct connection to atomic frequency standards and relatively simple and direct retrieval method. GPS RO profiles atmospheric refractivity. Two limitations of GPS RO are (1) its inability to separate the dry air and water vapor contributions to refractivity and (2) its insensitivity to water vapor in the colder regions 20 of the troposphere and above (e.g., Kursinski et al., 1997; Kursinski and Gebhardt, 2014).

In recognition of the strengths and weaknesses of GPS RO and radiance measurements and the need for better information about water vapor, in 1997 research groups at the University of Arizona and the NASA Jet Propulsion Laboratory (Herman et al., 1997 and Hajj et al., 1997) identified and began developing an RO system that is now called the Active Temperature, Ozone and Moisture Microwave Spectrometer (ATOMMS), which is designed to overcome these limitations by transmitting and receiving signals between satellites in low Earth orbit (LEO) near the 22 and 183 GHz water vapor absorption lines as well as nearby ozone absorption lines. Profiling both the speed of light like GPS RO as well as the absorption of light, which GPS RO does not measure, enables ATOMMS to precisely profile temperature, pressure and water vapor simultaneously from near the surface to the mesopause (Kursinski et al., 2002). It will also profile ozone from the upper troposphere into the mesosphere, scintillations produced by turbulence, slant path cloud liquid water and detect 30 larger cloud ice particles, with approximately 100 m vertical resolution and corresponding 70 km horizontal resolution (Eq. 13, Kursinski et al., 1997). Kursinski et al. (2002) found that such a system could provide water vapor retrievals with a precision of 1 – 3% from near the surface well into the mesosphere. Kursinski et al. (2009) estimated the degradation in clouds would be less than a factor of 2. A summary of LEO to LEO occultation measurement concept studies and demonstrations to date at microwave and IR wavelengths is given in Liu et al. (2017).

The following two new references will be added to the reference list.

Kursinski, E.R., and T. Gebhardt (2014). A Method to Deconvolve Errors in GPS RO-Derived Water Vapor Histograms. *J. Atmos. Ocean. Technol.*, **31**(12):2606–2628, *https://doi.org/10.1175/JTECH-D-13-00233.1*

Liu, C.L., G. Kirchengast, S. Syndergaard, E. R. Kursinski, Y. O. Sun, W. H. Bai and Q. F. Du (2017), A review of LEO-LEO occultation techniques using microwave and infrared-laser signals[J]. *Advances in Space Research*.

p. 3, line 710: Please give a reference to this statement.

We will make a slight change to the text of the sentence in question and add a reference. The text update is more precise with respect to the information in the new reference. Changes are highlighted in blue.

Original text: The smaller than 1% discrepancies between the measured ATOMMS spectra and the forward modeled water vapor spectra, in clear, cloudy and rainy condition are unprecedented and one to two orders of magnitude smaller than present discrepancies between AIRS and ECMWF, which are limited to conditions of relatively low cloud opacity.

Revised text: The smaller than 1% discrepancies between the measured ATOMMS spectra and the forward modeled water vapor spectra, in clear, cloudy and rainy condition are unprecedented and more than one order of magnitude smaller than the 25% to 70% uncertainties in AIRS retrievals reported in Wong et al. (2015).

The following new reference will be added to the reference list.

Wong, S., E. J. Fetzer, M. Schreier, G. Manipon, E. F. Fishbein, B. H. Kahn, Q. Yue, and F. W. Irion (2015), Cloud-induced uncertainties in AIRS and ECMWF temperature and specific humidity, J. Geophys. Res. Atmos., 120, 1880–1901, doi:10.1002/2014JD022440.

p. 5, line 1—4: Did you do investigations in terms of distance of frequency to the calibration frequency and the remaining error if unwanted sources (scintillation, ..) of errors show a frequency dependency?

No formal (published) investigations have been done, though we have done internal simulations. The reference to Kursinski et al. (2016) that we suggest to add based on the next comment addresses this question for our ground-based retrievals.

p. 5, line 7: If the demonstration of these key aspects are published please give a reference.

In order to address this comment, we propose to add text and references to published work for our ground-based retrievals. The new text is rather long, but there is a lot to summarize. These references to past publications concerning ground-based retrievals probably should be contained in this paper.

We suggest to break the first paragraph in Section 3 after the second sentence and include a summary of our published findings from previous experiments using the ground-based ATOMMS system. The remaining sentences currently in the first paragraph will be moved to a new paragraph beginning after the suggested insertion given below.

Here is the revised beginning of Section 3. Again, only the first sentence is carried over.

New text to begin section 3:

~~With funding from NSF~~, ~~w~~We designed and built a ground-based, prototype ATOMMS instrument and then used it to demonstrate some key aspects of ATOMMS capabilities and performance in several fixed geometries in southern Arizona with path lengths ranging from 800 m to 84 km. The prototype ATOMMS High-Band system transmits and receives two simultaneous continuous wave (CW) signals tunable from 181 to 206 GHz. The prototype Low-Band system consists of eight CW transmitters and receivers at fixed frequencies from 18.5 to 25.5 GHz spaced approximately one GHz apart, 10 centered approximately on the 22 GHz water vapor absorption line. Below we summarize the content of previous published work based on field experiments with the ATOMMS ground-based prototype.

In terms of ATOMMS water vapor retrievals, Kursinski et al. (2012) demonstrated agreement at the 2% level between water vapor measurements derived along an 820 m path using the ATOMMS High-Band instrument and a nearby, capacitive-type hygrometer. High-Band mountaintop measurements yielded the first detection by ATOMMS of $H_2{}^{18}O$ via its 203 GHz absorption line (Kursinski et al., 2016). Such measurements in the upper troposphere will determine isotopic ratios to constrain the hydrological cycle (Kursinski et al., 2004).

In terms of spectroscopy, ATOMMS measured lineshape across the 4 GHz interval above the 183 GHz line center agreed with the HITRAN line shape with a standard deviation of 0.3% (Kursinski et al. 2012), some 8 times better than the previously best estimate of Payne et al. (2008). ATOMMS mountaintop measurements between 5 and 25 GHz above the line center revealed discrepancies with the HITRAN line shape (Kursinski et al., 2016) which may help explain inconsistencies in 183 GHz derived water vapor estimates (Brogniez et al., 2016) and may be associated with atmospheric turbulence (Calbet et al., 2018). The ATOMMS measurements also revealed the shape of the 183 GHz line as represented in the Liebe et al., (1993) model is incorrect (Kursinski et al., 2012). The Liebe model is popular, having been referenced more than 600 times in the literature, and is still being used.

Kursinski et al. (2012) combined ATOMMS High-Band measurements with precipitation radar measurements to derive cloud liquid water content (LWC) along the ATOMMS signal path. Kursinski et al. (2016) demonstrated the ability to derive both cloud LWC and rainfall rates by combining the ATOMMS Low-Band and High-Band measurements.

Kursinski et al. (2016) derived the strength of atmospheric turbulence from scintillations of the ATOMMS signal amplitudes and demonstrated the ability to significantly reduce these turbulent amplitude variations via amplitude ratioing, in order to derive accurate water vapor estimates in turbulent conditions.

The last paragraph in the overview portion for Section 3 will be the end of the original paragraph:

On August 18, 2011, we collected approximately four hours of data with the instruments located on Mt. Lemmon Ridge (2752 m altitude) and Mt. Bigelow (2515 m altitude), separated by approximately 5.4 km. The observing geometry is shown in Fig. 1. The water vapor pressure derived from these ATOMMS measurements represents an average over the 5.4 km path which runs above a valley between the mountaintops on which the instruments sit.

This change also requires the following additional references to be added to the reference list:

Kursinski, E. R., D. Feng, D. Flittner, G. Hajj, B. Herman, F. Romberg, S. Syndergaard, D. Ward, and T. Yunck (2004), An Active Microwave Limb Sounder for Profiling Water Vapor, Ozone, Temperature, Geopotential, Clouds, Isotopes and Stratospheric Winds, in *Occultations for Probing Atmosphere and Climate* (OPAC-1), Springer-Verlag, Berlin, ISBN 978-3-540-22350-4, p. 173-188.

Calbet, X., N. Peinado-Galan, S. DeSouza-Machado, E.R. Kursinski, P. Oria, D. Ward, A. Otarola, P. Rípodas, and R Kivi (2018), Can turbulence within the field of view cause significant biases in radiative transfer modelling at the 183 GHz band? *Submitted to Atmos. Meas. Tech.* doi.org/10.5194/amt-2018-181.

Liebe, H.J., G.A. Hufford, and M.G. Cotton (1993), Propagation Modeling of Moist Air and Suspended Water/Ice Particles at Frequencies Below 1000 GHz. AGARD Conference Proc. 542, Atmospheric Propagation Effects through Natural and Man-Made Obscurants for Visible to MM-Wave Radiation, pp.3.1-3.10.

p. 5, line12: Please determine here already on wich of these locations the transmitter and receivers are located.

The following sentence will be added before the first sentence begins on page 5, line 13 of the originally submitted document. The paragraph that includes that sentence will be moved down in the introductory portion of section 3 as described in the previous response. It will begin after the sentence ending with “shown in Fig. 1.

The Mt. Lemmon instrument contained the 183 GHz transmitter and 22 GHz receiver and the Mt. Bigelow instrument contained the 22 GHz transmitter and 183 GHz receiver.

p. 7, line 8: What is the reference period exactly. For a faster understanding it would helpt too if the reference period is marked in Fig. 2.

See response to general comment #3 from anonymous reviewer #1. We originally submitted the wrong figure 2 without the annotations. Reference periods are marked with annotations in the correct figure.

p. 8, line 15: Please mark the second reference period in the Fig.2 too.

The second reference period is marked on the correct figure 2.

p. 8, line 22: Please give a clear acronym for your Atmospheric Model, version 7.2 e.g. AM7.2 and make the notation consistent in the entire document.

This was addressed in response to specific comment #18 from reviewer #1.

p. 9, line 5: Please give the color code in the text too you are using in the figures for a faster understanding. It is not explained in the text what „raw" in the figure label means? Why is the blue line not always higher then the black line? To my understanding the blue lines contains all atmospheric effects and the black line only the liquid optical depth part.

Figure 2 is introduced in the text beginning on page 6, line 32. We propose to make clarifying changes to the text at that point, rather than on page 9.

Original text: The observed variations in optical depth at 198.5 GHz and 24.4 GHz are shown in Fig. 2. 198.5 GHz was the frequency of the High Band calibration tone during this experiment. Also shown are the derived changes in liquid optical depth at 198.5 GHz, which was computed by subtracting the optical depth changes due to variations in the retrieved vapor 7 pressure and temperature from the total observed optical depth change.

Revised text: The measured changes in optical depth at 198.5 GHz (blue line, raw) and 24.4 GHz (red line, raw) are shown in Fig. 2. 198.5 GHz was the frequency of the High Band calibration tone during this experiment. Also shown are the derived changes in liquid optical depth at 198.5 GHz (black line) , which was computed by subtracting the optical depth changes due to variations in the retrieved vapor pressure and temperature from the total observed optical depth change. The change in optical depth relative to reference period 1 will always be positive for liquid (rain and clouds), since there was no rain or clouds during the reference period. However, the change in optical depth due to changes in vapor pressure and temperature can be negative, which means that the overall change in optical depth relative to the reference period can be less than the optical depth change due to liquid alone.

p. 9, line 19: Please give a reference to this publications.

Reference will be added. This paper is already in our reference list. We also noticed a reference to the wrong section at the beginning of the sentence, which will also be changed.

Original Sentence: In Section 5 we note that similar advection of dry air following summertime thunderstorms in this region have been observed in previously published work and show that our estimation of the minimum vapor pressure was consistent with the nearby radiosonde observations from Tucson.

New Sentence: In Section 6 we note that similar advection of dry air following summertime thunderstorms in this region have been observed in previously published work (Kursinski et al., 2008) and show that our estimation of the minimum vapor pressure was consistent with the nearby radiosonde observations from Tucson.

p. 10, line 3: Why where the tempearature sensors so close to the ATOMMS instruments positioned? Why not in a seperate small tent, if protection due to heavy rainfall was needed, to avoide temperature bias due to lost heat by the ATOMMS instrument?

In retrospect, this was a mistake on our part. If we were to repeat this experiment, we would definitely position in-situ sensors slightly away from the operating instruments. However, as you say, these instruments would still have to be protected from the heavy rain and winds in a tent and therefore, not as tightly tied to the environmental conditions as one would like.

p. 10, line 19: Please use the color code of the graph when explaining the figures to gurantee no confusion with the graphs.

The following change will be made to the text.

Original Sentence: Figure 4 shows the derived air temperature between the instruments that was used in the retrievals, as well as the nearby, in-situ thermometer observations.

New Sentence: Figure 4 shows the derived air temperature between the instruments that was used in the retrievals in black, as well as the nearby, in-situ thermometer observations, which are shown in red, green, and blue.

p. 10, line 19: How do the aire pressure graphs look like including the one hour running mean of the air pressure?

The differences between the one hour running mean of air pressure and the higher time resolution observations of pressure are almost imperceptible when plotted on the same graph. Yet, these small variations over short time scales (relative to each other) do create noise in the hydrostatic temperature estimates when not using the time smoothed pressure. We have not made any changes to the text based on this comment. Below is a figure that shows both the high time resolution measurements of air pressure and the one hour running mean. We do not plan to include the figure in the final document.

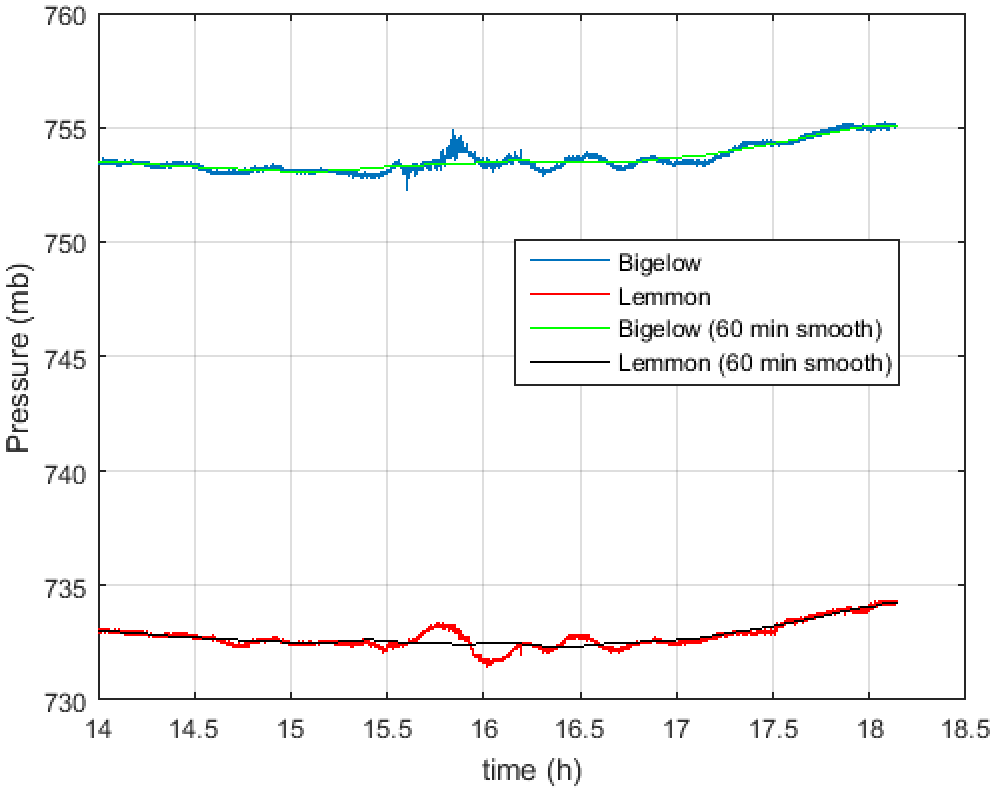

p. 11, line 25: Did you estimate the residual error due to turbulences?

The largest peaks in Fig. 3B are near 14.6 hours. As stated in our revised text, these peaks are due to momentary noise in the calibration signal, and therefore not due to turbulence. Outside of those peaks, the maximum residual to the fit is about 1.8% between 16 and 16.5 hours based on Figure 3B. As stated in the text, we think this is mostly due to residual turbulence, and thus is an estimate of the residual error due to turbulence.

Therefore, we propose to modify the paragraph beginning on page 11, line 23. The original text is shown in black with modifications shown in blue. Please also note the change to the caption for Fig. 3B, which is shown below in response to a comment specifically concerning Fig. 3B.

Turbulence-induced amplitude scintillations (Category 2) were quite significant during the periods of strong convection. These were reduced by almost an order of magnitude via amplitude ratioing with the calibration signal (Kursinski et al., 2016). The strong peaks near 14.6 hours in Fig. 3B are caused by momentary noise in the calibration signal, which influences the frequency ratioing. Outside of this peak the largest fractional uncertainty is about 1.8% of the vapor pressure (green line). We attribute most of this to turbulent-induced scintillations that remain after the frequency ratioing. Thus, for the conditions of this field experiment, the upper bound for the random error in the vapor pressure retrieval due to turbulence is about 1.8% of the vapor pressure. ~~Residual amplitude scintillations may be the largest source of random error in the least square fits.~~

p. 12, line 8: How did you get the value of -0.17 hPa/C? Could you give a short explanation to this?

This was estimated by running forward simulations of the *am7.2* model for the approximate temperature and vapor pressure conditions observed during this experiment. This was partially addressed in one of the changes made to address comment 18 from Reviewer 1. We will add the additional underlined blue text to address this concern as well.

Page 12, line 6, original text. “For the conditions of this particular experiment, based on the AM7.2 model, the sensitivity of the change in derived water vapor due to a temperature change relative to the reference period temperature was approximately -0.17 hPa/°C.”

Revised text. “For the conditions of this particular experiment, based on forward calculations made with *am7.2* for the range of temperature and vapor pressure conditions observed during the experiment, the sensitivity of the change in derived water vapor due to a temperature change relative to the reference period temperature was approximately -0.17 hPa/°C.”

p. 13, line 11: Please give a reference to the Mie cloud model you where applying?

We will add the following citation at the end of the sentence … Mie cloud model (Bohren and Huffman, 1983).

And the following reference in our list of references.

Bohren, Craig F., and Donald R. Huffman. 1983. *Absorption and scattering of light by small particles*. New York: Wiley.

p. 14, line 22: Do you have information/graphs on the wind speeds correlating with the shift in time too e.g. by using the radar data?

Unfortunately we did not estimate wind speed. Our goal was simply to estimate wind direction in order to determine if the sign of the lags between the ATOMMS water vapor measurements and the *in situ* water vapor measurements on Mt. Bigelow made sense.

p. 15, line 2: Do you have a reference on the Tucson WSR-88 RADAR?

The Tucson radar type should have been specified as WSR-88D instead of WSR-88. We will add the following citation. However, reviewer #3 pointed out that we first reference radar data on page 7, so the citation will be placed there as well.

Original: "… Tucson WSR-88 RADAR"

Revised: "…Tucson WSR-88D radar (Crum and Alberty, 1993)."

And reference

Crum, T.D. and R.L. Alberty, 1993: The WSR-88D and the WSR-88D Operational Support Facility. *Bull. Amer. Meteor. Soc.*, **74**, 1669–1688, https://doi.org/10.1175/1520-0477(1993)074<1669:TWATWO>2.0.CO;2

p. 15, line 20: What was the horizontal distance of the radiosond to the actual microwave path, when passing through the mountain height levels of Mt. Bigelow and Mt. Lemmon? Was the radiosond actually passing the microwave path or was it very close or even far away from the microwave path?

The original text incorrectly states that the launch point for the radiosonde is about 20 km south of the observation path. The location of the radiosonde is estimated to be about 20 km south of the observation path during the time it crosses the observation path ascending through the altitudes of Mt. Bigelow and Mt. Lemmon. The sentence will be changed as indicated below.

Original Sentence: The sonde launched between 16:30 and 16:45 from a location about 20 km south of the experiment and ascended through the Mt. Bigelow to Mt. Lemmon altitude interval between 16:35 and 16:50.

Revised Sentence: The sonde launched between 16:30 and 16:45 from a location about 28 km southwest of the experiment and ascended through the Mt. Bigelow to Mt. Lemmon altitude interval between 16:35 and 16:50 at a location approximately 20 km south of the observation path.

p. 19, line 25. Please explain shortly the other colored lines according to the altitude levels. It is not clear why e.g. the black and red lines show a less high ratio than the green and pink lines and they show even different linear dependencies within the length of the integration path.

We have decided to make a few changes based on this comment. One of the changes is to make some slight changes to Figure A1.

First, though, here is the response to the question based on the original figure, which is the last figure in the original document and incorrectly labeled as Figure A2.

The results are based on observations from aircraft observations. The black and red lines, referenced by the reviewer, are at the highest altitudes (lowest pressure) lines on the plot, which correspond with the driest part of the atmosphere. For these altitudes, there is a change in the slope of the ratio std(q)/mean(q) (<q-std>/<q-mean>) when the separation distance becomes smaller than about 10 km. This is likely because when the water vapor content is low, the observed ratio is more affected by instrumental effects. Under these dry conditions, we need separation distances larger than 10 km to be able to observe the effects of anisotropy in the absolute humidity field. Thus in the original figure, at separation distances between measurements longer than 10 km, we start to see the effects of anisotropy in the absolute humidity field for these highest altitude (lowest pressure) lines.

We have updated Figure A1 to show just the 447, 550 and 839 hPa pressure levels which are the only levels of relevance to us and the only levels shown and discussed in Otarola et al. (2011). This removes the odd behavior at the two lowest pressure levels that we believe is tied somehow to the performance of the aircraft hygrometer. We also cleaned up the figure so that the line that is interpolated to the ATOMMS horizontal distance separation does not extend beyond the y axis. The new figure and with an updated caption is shown below.

In carefully reproducing the figure, we also found that the original 13 m estimated length is actually 10 m. This requires that we change the document text references from 13 m to 10 m as listed below. The change to 10 is shown in blue.

Page 19, line 27: Given this power-law exponent and the requirement to keep uncertainties smaller than 1%, the path length required to achieve std(q)/mean(q) = 1% is approximately ~~13~~ 10 m.

Page 19, line 31: Thus, in situ sensors, accurate to 1% each, would need to be placed every ~~13~~ 10 m along a 5.4 km path to achieve an in situ-based path average consistent with the ATOMMS measurements to the 1% level.

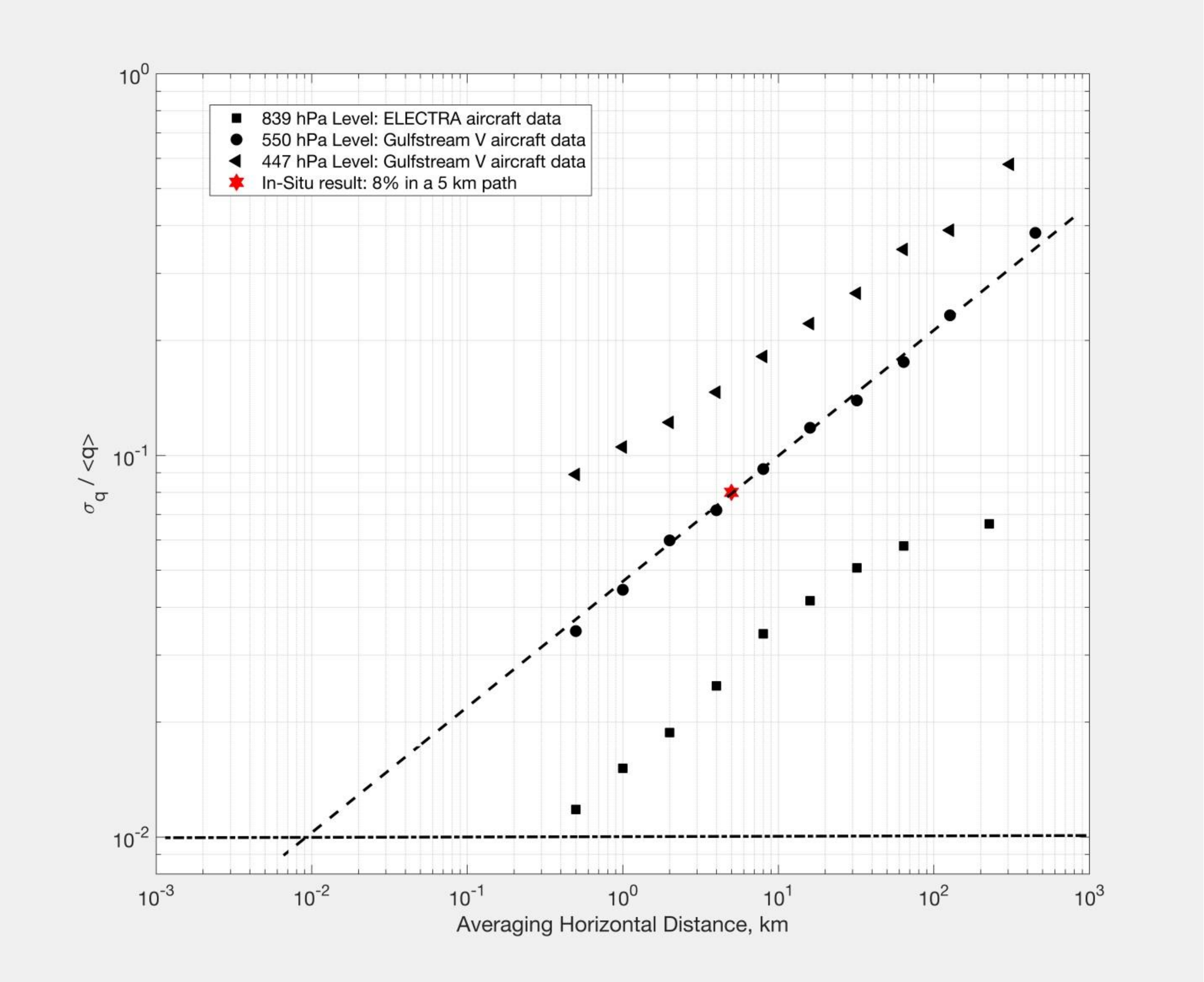

Figure A1: Ratio of the standard deviation of absolute humidity to the mean absolute humidity based on aircraft data taken at different altitudes, which is indicated by the air pressure along different flight paths. The red star on the dashed line constructed for the 550 hPa altitude observations corresponds with the value calculated from the three in-situ sensors operating during the ATOMMS mountaintop experiment (ratio of 8% for a 5 km path). The slope of the dashed line corresponds with a power law exponent of 0.35 for the dependence of std(q)/mean(q) with the length of the path, which is consistent with Kolomogorov turbulence. Extrapolation of this line to a std(q)/mean(q) value equal to 1% indicates that in-situ observations are required every 10 m in order to validate the 1% accuracy of the ATOMMS retrievals. Adapted from Otarola et al. (2011).

Fig. 1: Is it possible to mark the position of the radiosond when passing through the altitude level of the two mountains?

Unfortunately, this is not possible. Figure 1 is about 3 km by 5 km, which zooms on the instrument locations. The sonde was approximately 20 km to the south of the observation path.

Typo Comments:

p. 2, line 9--10: I would recommend to be consistence with the entire paper to write everything in hPa than in mb.

We will search for all remaining instances of ‘mb’ and change it to ‘hPa’ for consistency.

p. 4, line 30: Please change hydrometers to hydrometeors.

This typo is actually on line 13 of page 4. Change will be made.

p. 7, line 21: Please make the notation for the time consistence in the entire document and figures. Sometime 4:30, then 4,5 or even the 12 hour notation is used.

This was addressed in comment 14 from reviewer 1. We will use 24 hour notation, e.g., 16:30 for all such references to time.

p. 10, line 25: The +-1% signe is underlined. Please remove the underline.

The underline will be removed.

p. 14, line 24 – 27: Please make the time consistent. They do not agree with the given times in the legend of Fig. 8B.

The text providing the time ranges on page 14 will be changed to be consistent with the figure and a 24 hour clock time that will be used throughout.

p. 15, line 19: Please make the notation of the Tucson radiosond consistent with legend in Fig. 7.

The text on line 19 will be changed to match the text in the figure caption

Original text: 00Z Tucson radiosonde

Revised text: 00 UTC Tucson radiosonde

Fig. 3A: Please use the consisten units e.g. hPa instead of mb and h instead of hours (in Fig 3A and 3B)

The axis labels will be changed to always use hPa (instead of mb) and h (instead of hours). Below is the updated Fig. 3A. The updated Fig. 3B is included below to address the next comment regarding the right axis labeling of Fig. 3B.

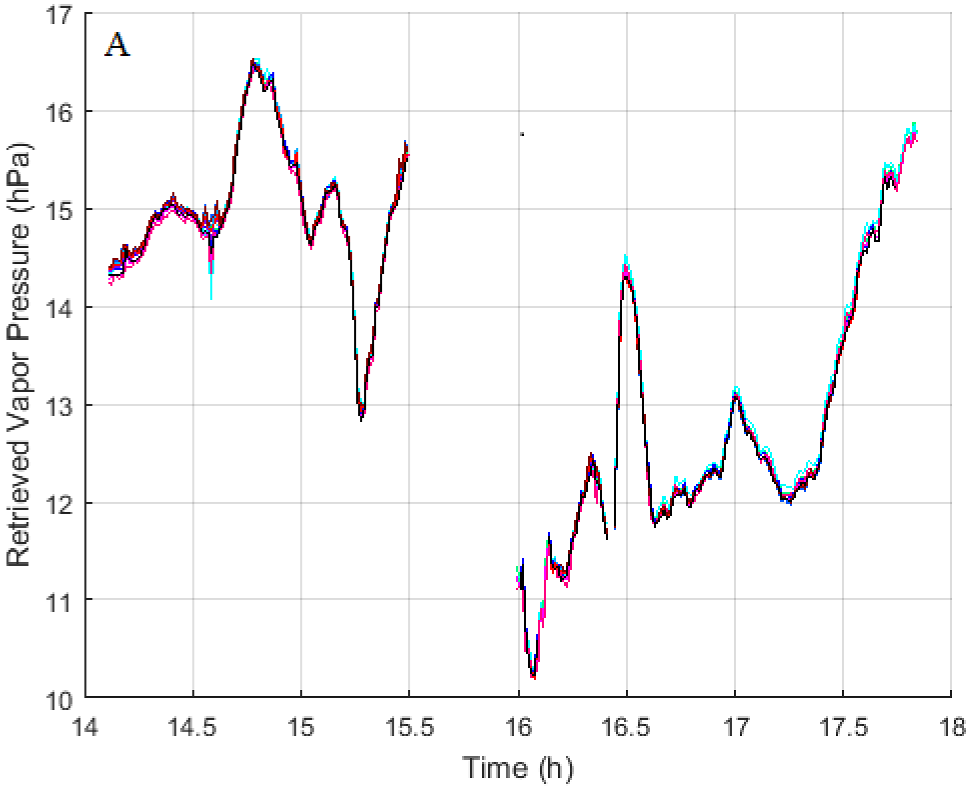

Fig. 3B: What is the strong peak at about 14.6? In the text % is used but in the figure you use fraction for the right y-axes. Please make it consistent.

Below is the updated Fig. 3B in which the right axis has been labeled in percent. We added text to the caption for Fig 3B in two places for clarification. One change is to clarify that the right axis is expressed in percent. The other change is to address the comment related to page 11, line 25 above. The added text is shown in blue.

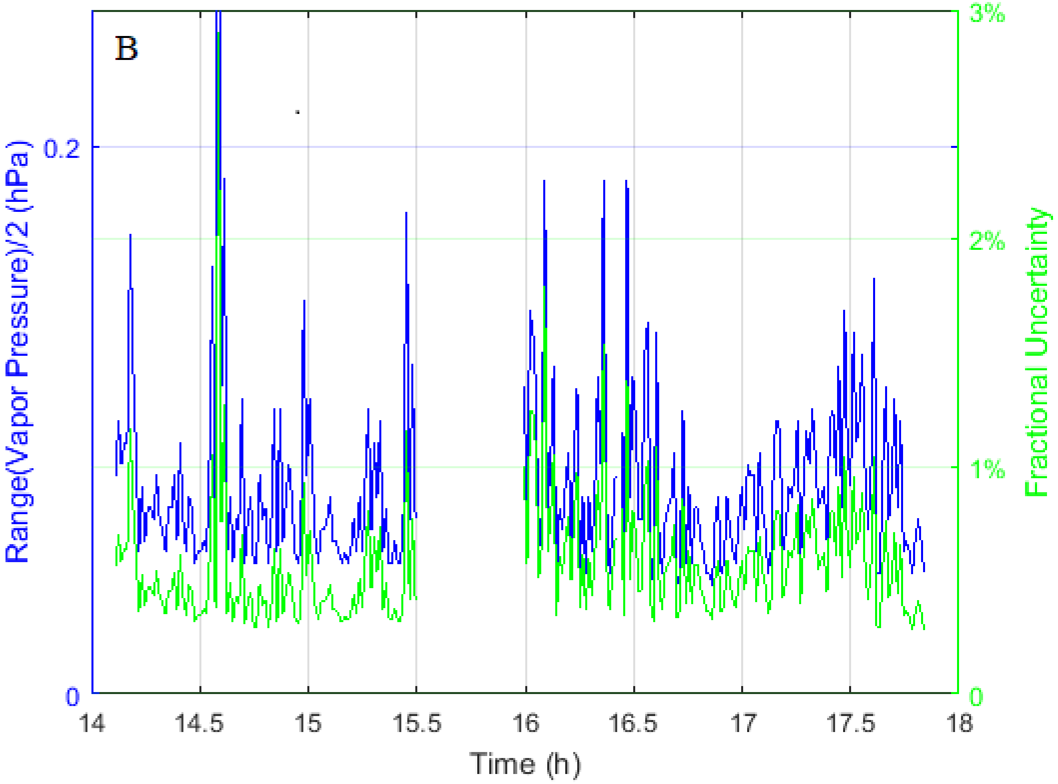

Figure 3: A. Retrieved vapor pressure for the 12 retrieval test cases described in the text. Each line is a different color. B. Blue line and left axis indicate the half range, which is one half of the maximum minus minimum vapor pressure from the 12 retrieval cases; green line and right axis is the half range divided by the absolute vapor pressure at each retrieval point expressed in percent. The strong peaks near 14.6 hours are due to momentary noise in the calibration signal.

Fig. 8B: Please make the time in the label, legend and text consistent. Please give units?

The text in the caption referring to the time will be changed to a 24 hour clock formation as shown in the figure legend. Original caption shown with changes highlighted in blue.

Figure 8: A. Vapor pressure derived from ATOMMS observations (blue) and measured with an in-situ sensor on Mt. Bigelow (red). Also shown in other colors are four time segments of the in-situ observations shifted in time (as described in text) to highlight correlation between the two vapor pressure data sets. The time shift for each colored line is indicated in panel (B). B. 5 **Cross-correlation coefficients as a function of sample lags between the ATOMMS-derived vapor pressure and in-situ measurements of water vapor taken on Mt. Bigelow. The four lines correspond with the four time segments described in the text: green (14:03 – 14.47 hours), black (14:59 to 15:30 hours), cyan (16:00 to 16:25 hours), and magenta (16:45 to 17:23 hours).**

Fig. A1: Please remove the title of the plot or make the symbols for standard deviation and mean value consistent. Please correct the x-axes label.

These issues have been fixed with our changes to figure A1 as described in our response to the comments related to page 19, line 25 above.

COMMENTS FROM DAVE ADAMS (REVIEWER 3).

We wish to thank Dave Adams for his helpful review. We first copy the comments of the reviewer **(in bold)** with our response below. In cases where the text is modified, we show both the original text and the revised text, with the significant changes shown in blue.

Minor Comments.

Line 26 You can probably be a bit more emphatic here. Water is the most important greenhouse gas, critical in the energy balance, responsible for storms etc... Line 29 Should be Sherwood et al., (2010) And you should probably include a few more "big picture" type references related to water vapor in the climate system.

To address this comment, we will make substantial changes to the first paragraph in section 1.

Original text:

Water vapor is an important constituent in Earth's atmosphere and its distribution in space and time must be known to understand and predict weather and climate. Despite its importance, we do not have precise observations of its distribution in the atmosphere, its trend with time, or a good understanding of the factors controlling these (Sherwood et al., 2013). Water vapor is challenging to measure because of the wide range of concentrations and scales across which it varies. Water vapor observations must be unbiased and capture the full range of variability in clear and cloudy conditions across the globe in order to improve the understanding and analysis of water vapor, which is used to initialize weather prediction systems, to monitor trends and variations and to improve weather and climate models through constraints on and refinement of processes affecting and affected by water vapor (e.g., Bony et al., 2015).

Revised text:

Water vapor is an important constituent in Earth's atmosphere and its distribution in space and time must be known to understand and predict weather and climate. Water vapor is fundamental to the radiative balance of the Earth, both as the most important greenhouse gas and indirectly through clouds. Through its latent heat, water vapor is crucial to formation and evolution of severe weather, transport of energy both upward and poleward in the troposphere and transfer of energy between the surface and atmosphere. Furthermore, water vapor dominates tropospheric radiative cooling which drives convection (Sherwood et al., 2010). Uncertainty in modeled cloud feedback results in the factor of 3 spread in predictions in the surface temperature response to a doubling of atmospheric CO_2 concentrations and the cloud feedback depends critically on the strength of the water vapor feedback (Held and Soden, 2000). Predicted amplification of extreme precipitation with warmer temperatures is tied directly to predicted increases in extreme water vapor concentrations and it may be underestimated (e.g., Allan and Soden, 2008).

Water vapor is challenging to measure because of the wide range of concentrations and scales across which it varies. Water vapor observations must be unbiased and capture the full range of variability in clear and cloudy conditions across the globe in order to improve the understanding and analysis of water vapor, which is used to initialize weather prediction systems, to monitor trends and variations and to improve weather and climate models through constraints on and refinement of processes affecting and affected by water vapor (e.g., Bony et al., 2015).

The date on this reference item was incorrectly listed as 2013 and will be changed to 2010.

Sherwood, S. C., R. Roca, T. M. Weckwerth, and N. G. Andronova (2010), Tropospheric water vapor, convection, and climate, Rev. Geophys., 48, RG2001, doi:10.1029/2009RG000301

The following new references will be added to the reference list:

Held, Isaac M. and Soden, Brian J. (2000), Water vapor feedback and global warming, Annu Rev Energy Environ., 25, 441 – 475, doi: 10.1146/annurev.energy.25.1.441.

Allan, R.P., and B.J. Soden (2008), Atmospheric warming and the amplification of precipitation extremes. Science, 321, 1481-1484, doi: 10.1126/science.1160787.

Line 30 Water vapor observations must be unbiased and capture the full range of variability in clear and cloudy conditions across the globe... This sentence is a bit awkward, it could be written in a more concise manner or turn into two sentences.

This sentence has been modified as follows.

Original Text

Water vapor observations must be unbiased and capture the full range of variability in clear and cloudy conditions across the globe in order to improve the understanding and analysis of water vapor, which is used to initialize weather prediction systems, to monitor trends and variations and to improve weather and climate models through constraints on and refinement of processes affecting and affected by water vapor (e.g., Bony et al., 2015).

Revised text:

Water vapor observations must be unbiased and capture the full range of variability in clear and cloudy conditions across the globe in order to improve the understanding and analysis of water vapor. This information is used to initialize weather prediction systems, to monitor trends and variations and to improve weather and climate models through constraints on and refinement of processes affecting and affected by water vapor (e.g., Bony et al., 2015).

Page 2.

Satellite systems typically do not have sufficient temporal or spatial resolution to capture many of the important processes related to the distribution of water vapor (such as deep convection in the Tropics). And if the satellite systems do have this appropriate temporal and spatial resolution (e.g. GOES water vapor channels), they only provide column water vapor and not its vertical structure. You should include a bit more detail in this paragraph to give greate force to your proposed system.

To fully address this comment, we propose to make substantial changes and additions to Section 1 of the paper, Introduction/Motivation. We show the original text of the three paragraphs that begin on line 3 of page 2. After that, we show the proposed new text that will replace those paragraphs.

Original Text (starting on line 3 of page 2):

Satellite observations are required to gain a global perspective for weather prediction and climate monitoring and constraining the critical processes at work in different regions across the globe. Unfortunately, present satellite observations provide limited constraints on the water vapor field, particularly when clouds are present, which in turn limits the skill of the weather forecasts and our detailed knowledge of water vapor across the globe. Yue et al. (2013) compared the water vapor estimates from the NASA's AIRS retrievals and ECMWF analyses and found large fractional differences between the two data sets in terms of both biases and centered, root mean-square differences (CRMSD) that were associated with clouds and surface conditions. Biases were +/-10% near the surface and 35% dry at 200 mb. CRMSD ranged from 15% to 40% near the surface to 45% to 80% at 200 mb, where the range at each pressure level reflects the dependence on cloud type and surface conditions. The point is that present state-of-the-art, radiance-based satellite water vapor remote sensing systems have serious limitations in terms of performance and sampling biases associated with clouds and surface conditions, accuracy, vertical resolution and the ambiguity inherent in the conversion of radiances to the atmospheric state (Rodgers 2000).

GPS radio occultation (RO) has become an important data source for numerical weather prediction (NWP), despite its relatively sparse coverage to date [e.g., Cardinali and Healy, 2014]. Its high impact comes from its unique combination of ~200 m vertical resolution, all weather sampling and very low random and absolute uncertainties via its direct connection to atomic frequency standards. GPS RO profiles atmospheric refractivity. Two limitations of GPS RO are (1) its inability to separate the dry air and water vapor contributions to refractivity and (2) its insensitivity to water vapor in the colder regions of the troposphere and above.

In recognition of the strengths and weaknesses of GPS RO and radiance measurements and the need for better information about water vapor, in 1997 research groups at the University of Arizona and the NASA Jet Propulsion Laboratory (Herman et al., 1997 and Hajj et al., 1997) identified and began developing an RO system that is now called the Active Temperature, Ozone and Moisture Microwave Spectrometer (ATOMMS), which is designed to overcome these limitations by transmitting and receiving signals between satellites in low Earth orbit (LEO) near the 22 and 183 GHz water vapor absorption lines as well as nearby ozone absorption lines. Profiling both the speed of light like GPS RO as well as the absorption of light, which GPS RO does not measure, enables ATOMMS to precisely profile temperature, pressure and water vapor simultaneously from near the surface to the mesopause (Kursinski et al., 2002). It will also profile ozone from the upper troposphere into the mesosphere, scintillations produced by turbulence, slant path cloud liquid water and detect larger cloud ice particles, with approximately 100 m vertical resolution and corresponding 70 km horizontal resolution (Eq. 13, Kursinski et al., 1997). Kursinski et al. (2002) found that such a system could provide water vapor retrievals with a precision of 1 – 3% from near the surface well into the mesosphere. Kursinski et al. (2009) estimated the degradation in clouds would be less than a factor of 2.

Revised text:

Satellite observations are required to gain a global perspective for weather prediction and climate monitoring and for constraining the critical processes at work ~~across the~~ in different regions ~~of~~ across the globe. Unfortunately, present satellite observations provide limited constraints on the water vapor field, particularly when clouds are present, which in turn limits the skill of weather forecasts and our detailed knowledge of water vapor across the globe. ~~Yue et al. (2013) compared the water vapor estimates from the NASA's AIRS retrievals and ECMWF analyses and found large fractional differences between the two data sets in terms of both biases and centered, root mean-square differences (CRMSD) that were associated with clouds and surface conditions. Biases were +/-10% near the surface and 35% dry at 200 mb. CRMSD ranged from 15% to 40% near the surface to 45% to 80% at 200 mb, where the range at each pressure level reflects the dependence on cloud type and surface conditions.~~ For example, GOES observations provide high time and horizontal resolution but very limited vertical information. While hyperspectral IR on polar orbiting satellites provide more information, their temporal sampling is limited and their water vapor estimates are quite noisy with fractional, root mean-square (RMS) differences ranging from 25% in the lower troposphere to 70% around 400 hPa and a tendency toward dry biases up to 30%, depending on cloud type (Wong et al., 2015). While downward looking microwave radiance measurements are particularly useful for determining the column water over the ocean (e.g., Wang et al., 2016), they provide significantly less vertical information than IR and are inherently ambiguous over land, snow and ice due to surface emissivity variations. The point is that present state-of-the-art, radiance-based satellite water vapor remote sensing systems have serious limitations in terms of performance and sampling biases associated with clouds and surface conditions, accuracy, vertical resolution and the ambiguity inherent in the conversion of radiances to the atmospheric state (Rodgers 2000).

Because of these satellite limitations, balloon-borne sondes and dropsondes continue to be the measurement of choice for field campaigns focused on answering key questions about the atmosphere. In fact, the globe would be covered with sondes if the cost to do so were not so completely prohibitive. Operational global weather observing systems therefore rely primarily on more affordable but vertically coarse satellite radiance measurements and the inherent ambiguities in the information they provide. Unfortunately, this limits how much understanding we can gain from these observations about important atmospheric processes like those associated with clouds, convection and surface exchange.

In this context, GPS radio occultation (RO) has provided a welcome advance in satellite remote sensing through its ability to profile the atmosphere with ~200 m vertical resolution, approaching that of sondes, in all-weather conditions, with very small random and absolute uncertainties. As such, GPS RO has become an important data source for numerical weather prediction (NWP), despite its relatively sparse coverage to date (e.g., Cardinali and Healy, 2014). Its high impact comes from its unique combination of ~200 m vertical resolution, all weather sampling and very low random and absolute uncertainties via its direct connection to atomic frequency standards and relatively simple and direct retrieval method. GPS RO profiles atmospheric refractivity. Two limitations of GPS RO are (1) its inability to separate the dry air and water vapor contributions to refractivity and (2) its insensitivity to water vapor in the colder regions of the troposphere and above (e.g., Kursinski et al., 1997; Kursinski and Gebhardt, 2014).

In recognition of the strengths and weaknesses of GPS RO and radiance measurements and the need for better information about water vapor, in 1997 research groups at the University of Arizona and the NASA Jet Propulsion Laboratory (Herman et al., 1997 and Hajj et al., 1997) identified and began developing an RO system that is now called the Active Temperature, Ozone and Moisture Microwave Spectrometer (ATOMMS), which is designed to overcome these GPS limitations by transmitting and receiving signals between satellites in low Earth orbit (LEO) near the 22 and 183 GHz water vapor absorption lines as well as nearby ozone absorption lines. Profiling both the speed of light, like GPS RO, as well as the absorption of light, which GPS RO does not measure, enables ATOMMS to precisely profile temperature, pressure and water vapor simultaneously from near the surface to the mesopause with little random or systematic uncertainties (Kursinski et al., 2002). It will also profile ozone from the upper troposphere into the mesosphere, scintillations produced by turbulence, slant path cloud liquid water and ~~detect~~ larger cloud ice particles, with approximately 100 m vertical resolution and corresponding 70 km horizontal resolution (Eq. 13, Kursinski et al., 1997). Kursinski et al. (2002) found that such a system could provide water vapor retrievals with a precision of 1 – 3% from near the surface well into the mesosphere. Kursinski et al. (2009) estimated the degradation in clouds would be less than a factor of 2. A summary of LEO to LEO occultation measurement concept studies and demonstrations to date at microwave and IR wavelengths is given in Liu et al. (2017).

Regarding the sampling densities that can be achieved with ATOMMS, Kursinski et al. (2016b) noted that a constellation of 60 very small satellites, carrying both ATOMMS and GNSS RO sensors, would produce approximately 26,000 ATOMMS and 170,000 GNSS occultations profiles each day, for a fraction of the cost of a single, operational, polar orbiting weather satellite. These numbers of profiles are approximately 10 and 100 times present GPS RO and radiosonde sampling densities. Such an orbiting ATOMMS constellation providing dense, very high vertical resolution, precision and accuracy water and temperature profiling via radio occultation will complement existing observations of clouds, precipitation and energy fluxes and tie the entire weather and climate system together. This combination will also dramatically improve the realism and utility of global analyses for climate as well as forecasting (increasingly extreme) weather (Kursinski et al., 2016b).

With regard to constraining processes, we briefly discuss three important and representative application areas: moist convection, weather fronts and polar weather and climate.

Moist convection is ubiquitous across the globe but inadequately understood which leads to inaccurate representation in models. Environmental variables critical for understanding and predicting moist convection and associated severe weather include temperature, water vapor, stability, and conditional instability in particular, the level of free convection, convective available potential energy (CAPE), convective inhibition (CIN), winds and divergence. Unfortunately, coarse vertical resolution and ambiguities inherent in converting radiance spectra to the atmospheric state limit the ability of satellite radiances to provide detailed constraints on convection related processes. GPS RO provides much needed vertical information across the globe and is particularly useful for determining temperatures and stability in the upper troposphere where conditions are very dry. However, the ambiguity of the wet and dry gas contributions to refractivity under the warmer, moister conditions deeper in the troposphere limit the utility of GPS RO refractivity profiles there.

In contrast, ATOMMS will be the first orbiting remote sensing system to simultaneously profile temperature and water vapor with very high ~100 m vertical resolution and very small uncertainties needed to tightly constrain these environmental quantities relevant to convection, in clear and cloudy conditions, through the troposphere, across the entire globe. While ATOMMS profiles will not resolve detailed horizontal structure at scales much below 70 km, they are sensitive to these scales via the phase and amplitude scintillations that small scale turbulence produces on the ATOMMS signals (Kursinski et al., 2016b). Furthermore, 100 km, which is approximately the horizontal resolution of ATOMMS, is the scale most important for forecasting severe convection in the form of thunderstorms (Durran and Weyn, 2016).

Weather fronts are another fundamental class of severe weather poorly constrained by satellite radiance measurements. Unlike radiances, RO measurements can profile fronts from orbit because RO profiles readily penetrate through clouds and the vertical and horizontal resolutions of RO are well matched to the vertical and horizontal scales of weather fronts. While GPS RO can profile fronts in the upper troposphere (e.g. Kuo et al., 1998), the lack of refractivity contrast between the warm-wet and the cold-dry sides of fronts deeper in the troposphere limits GPS RO profiling of fronts there (Hardy et al., 1994). ATOMMS high precision temperature, pressure and water vapor profiles in clear and cloudy conditions will readily distinguish between the warm and cold sides of fronts down through the lower troposphere and precisely determine the location of any frontal surface that crosses an ATOMMS profile (Kursinski et al., 2002).

This unprecedented capability to measure fronts globally will also enable detailed characterization of the dynamics and moisture fluxes of atmospheric rivers out over remote ocean regions to better predict and prepare for the torrential rainfall and flooding they produce following landfall. These observations will also guide refinements in model representations of atmospheric rivers to increase and extend the accuracy of weather forecasts and the climatologically important mid-latitude water vapor transport in reanalyses and climate models (e.g., Guan and Waliser, 2016).

Profiling in Polar regions, particularly the near-surface environment, is critical to understanding the causes of ongoing and future climatic changes there. Reducing uncertainty due to our limited knowledge about the critical processes at work there requires quantitative, process-resolving observations that span the entire range of environmental conditions and behavior across these remote regions. Present understanding comes largely from operational sondes and a small number of field campaigns (e.g., Esau and Sorokina, 2010). While satellites radiance measurements already provide dense sampling of these remote, high latitude regions, they have yielded relatively little insight due to intrinsic ambiguities associated with poor vertical resolution, frequent clouds, near-surface inversions and variations in surface emissivity. As a result, many "global" satellite products do not extend to the poles (e.g. Chen et al., 2008). While GPS RO has much needed very high vertical resolution, cloud penetration and insensitivity to surface conditions, its impact is also limited, because of the unknown contributions of water vapor and the bulk dry gas to the measured refractivity profiles.

In this context, ATOMMS' precise and very high vertical resolution profiling of temperature, stability, water vapor, pressure gradients, clouds and turbulence, down to the surface, over all types of surfaces, in clear and cloudy conditions, across the diurnal and seasonal cycles, will bring unprecedented information about the high latitudes and, in particular, the lowermost troposphere, to constrain and reduce presently large uncertainties in surface fluxes and the surface energy budget there.

ATOMMS will simultaneously probe through clouds to determine the gas state as well as the cloud properties themselves, including their phase (liquid, ice and mixed) which are critical in the surface energy budget (e. g., Klingebiel et al., 2015) and fundamental to calculating upward and downward short and long wave radiative fluxes through the atmosphere. ATOMMS will profile the frequent polar boundary layer clouds too close to the surface to be characterized by CloudSat (Kay and Gettleman, 2009).

ATOMMS will constrain winds via horizontal pressure gradients to further constrain wind shear and moisture fluxes. This wind and cloud information together with ATOMMS' simultaneous profiling of stability and turbulent scintillations will provide a new set of observational constraints over the entire high latitude region to expose flaws in and guide improvements to presently inaccurate and poorly constrained model parameterizations of sensible and latent heat fluxes. The ability to estimate turbulence and radiative cooling at cloud top are also critical to determining cloud lifetimes and the radiative budget because turbulent entrainment rates influence droplet size and therefore albedo (Esau and Sorokina, 2010). ATOMMS global perspective would provide critical information for understanding why the two poles are evolving so differently.

The preceding examples reveal inadequacies in our present observing system that limit our understanding, and the substantial increase that ATOMMS promises in our observationally based knowledge and understanding. The performance of ATOMMS profiles approach that of sondes and, when implemented as a constellation such as in Kursinski et al. (2016b), would provide far denser coverage across the globe. For example, the vast Amazon rainforest which is presently profiled twice a day by only 8 sondes (Itterly et al., 2016), would be sampled by approximately 300 ATOMMS profiles and 1,800 GNSS RO profiles each day via the ATOMMS satellite constellation noted above.   Thus, an ATOMMS constellation would create a continuous, dense, global data set, with performance approaching that of sondes, that researchers could divide up as they like into smaller domains (creating essentially their own regional (field) campaigns) to better understand and model key processes and reduce weather and climate prediction uncertainty across the globe.

The last two paragraphs of section 1 remain unchanged.

These changes require the following new items in our reference list.

Chen, J., A. D. del Genio, B. E. Carlson and M. G. Bosilovich, (2008), The Spatiotemporal Structure of Twentieth-Century Climate Variations in Observations and Reanalyses. Part I: Long-Term Trend. *J. Climate, 21(11)*, 2611-2633.

Durran, D. R., and J. A. Weyn (2016), Thunderstorms Do Not Get Butterflies, *Bull. Amer. Met. Soc.,* February 2016, P. 237-244, doi.org/10.1175/BAMS-D-15-00070.1.

Esau, I. and S. Sorokina (2010), Climatology of the Arctic Planetary Boundary Layer, in Atmospheric Turbulence, Meteorological Modeling and Aerodynamics, Editors: P. R. Lang and F. S. Lombargo, 2009 Nova Science Publishers, Inc., ISBN 978-1-60741-091-1.

Guan, B., and D. E. Waliser (2015), Detection of atmospheric rivers: Evaluation and application of an algorithm for global studies. *J. Geophys. Res. Atmos.*, **120**, 12 514–12 535, doi:10.1002/2015JD024257.

Hardy, K. R., Hajj, G. A. and Kursinski, E. R. (1994), Accuracies of atmospheric profiles obtained from GPS occultations. Int. J. Satell. Commun., 12: 463-473. doi:10.1002/sat.4600120508

Itterly, K. F., P. C. Taylor, J. B. Dodson, and A. B. Tawfik (2016), On the sensitivity of the diurnal cycle in the Amazon to convective intensity, J. Geophys. Res. Atmos., 121, 8186–8208, doi:10.1002/2016JD025039.

Kay, J. E., and A. Gettelman (2009), Cloud influence on and response to seasonal Arctic sea ice loss, *J. Geophys. Res*., **114**, D18204, doi:10.1029/2009JD011773.

Klingebiel, M., A. de Lozar, S. Molleker, R. Weigel, A. Roth, L. Schmidt, J. Meyer, A. Ehrlich, R. Neuber, M. Wendisch, and S. Borrmann (2015), Arctic low-level boundary layer clouds: in situ measurements and simulations of mono- and bimodal supercooled droplet size distributions at the top layer of liquid phase clouds, *Atmos. Chem. Phys*., **15**, 617–631, doi:10.5194/acp-15-617-2015.

Kuo, Y.-H., et al. (1998), A GPS/MET Sounding through an Intense Upper-Level Front, *Bull. Amer. Meteor. Soc.*, **79**, 617-626.

Kursinski, E. R., D. Ward, A. C. Otarola, A. L. Kursinski and C. McCormick (2016a), Reducing Climate and Weather Prediction Uncertainty via cm- and mm-Wavelength Satellite to Satellite Occultations, *White Paper Submitted to 2017 ESAS Decadal Survey In Applications\ of\ ATOMMS\ 072118.docx response to RFI#1, January 2016,* http://surveygizmoresponseuploads.s3.amazonaws.com/fileuploads/15647/2289356/183-ea6d9954df8cfcbdb60a500c254348c4_KursinskiEmilR.pdf .

Uttal, T., et al. (2002), Surface heat budget of the Arctic Ocean. *Bull. Amer. Meteor. Soc.*, **83,** 255–275.

Wang, J., A. Dai and C. Mears (2016), Global Water Vapor Trend from 1988 to 2011 and Its Diurnal Asymmetry Based on GPS, Radiosonde, and Microwave Satellite Measurements, *J. Clim*., **29**, p. 5205-5222, DOI: 10.1175/JCLI-D-15-0485.1.

Line 19 Can you be specific as to what you mean here by insensitivity "(2) its insensitivity to water vapor in the colder regions of the troposphere and above."

We will add the following sentence to the end of the sentence in question. The new sentence begins on line 20 of page 2.

New Text:

Two limitations of GPS RO are (1) its inability to separate the dry air and water vapor contributions to refractivity and (2) its insensitivity to water vapor in the colder regions of the troposphere and above (e.g., Kursinski et al., 1997; Kursinski and Gebhardt, 2014). The insensitivity occurs when there is so little water vapor that the majority of the refractivity is dominated by the dry air component.

Line 28 I think you should write "It can also profile ozone ..."

The statement about profiling ozone is provided in the very next sentence. No change here.

Page 3

Line 2 Probably not necessary to include this "...we developed with funding from NSF,..."

That part of the sentence will be removed. Instead, this information will be included in an acknowledgement section placed immediately before the references section.

Change to original sentence:

Using ground-based ATOMMS prototype instrumentation ~~that we developed with funding from NSF~~, we demonstrate the ability of ATOMMS to retrieve changes in the path-averaged water vapor between the instruments operating between two mountaintops in Southern Arizona to within 1%, during weather conditions that ranged from clear to cloudy to thunderstorms with heavy rain.

And add the following acknowledgement section:

Acknowledgments

We want to thank Jeff Kingsley for his support in making critical resources available at the University of Arizona's Steward Observatory needed to complete the ATOMMS instrumentation, and Chris Walker for sharing the Steward Observatory Radio Astronomy Laboratory (SORAL) facilities with us during development of the prototype ATOMMS instrument. We also want to thank Jim Grantham for providing access and modifications to the Mt Bigelow and Mt Lemmon facilities to support these observations. We thank David Adams and two anonymous reviewers whose constructive criticism improved the presentation of this paper considerably. This work was supported by the National Science Foundation Major Research Instrumentation (MRI) Program grant 0723239 and the National Science Foundation, Division of Atmospheric and Geospace Sciences (GEO/AGS) grants 0946411 and 1313563. In particular, we want to thank Jay Fein, program scientist and manager at NSF, who passed away in 2016. Without Jay's insight and relentless effort and support, this research would never have been funded and taken place.

Line 6 Clarify what you are referring to here "..and the forward modeled water vapor spectra,.."

This line is in the introductory section. We do not believe that a detailed explanation belongs here. We will add a note that this is described in section 4.

Original text: The smaller than 1% discrepancies between the measured ATOMMS spectra and the forward modeled water vapor spectra …

New text: The smaller than 1% discrepancies between the measured ATOMMS spectra and the forward modeled water vapor spectra (described in Section 4) …

Line 10 Don' t use contractions in formal writing. "...simply do not work."

We will change don't on line 10 to do not.

Line 16 Write "Sources of uncertainty ..."

This typo (capitalized letter U) will be changed

Original text: Sources of Uncertainty

Revised text: Sources of uncertainty

Line 30 Write Refractivity and "the" extinction coefficient (or write coefficients)

The word "the" will be added in front of extinction coefficient in the sentence.

Original sentence: From these, occultation profiles of bending angle and absorption are derived and then used to derive radial profiles of refractivity and extinction coefficient using Abel Transforms [*Kursinski et al.*, 2002].

Revised sentence: From these, occultation profiles of bending angle and absorption are derived and then used to derive radial profiles of refractivity and the extinction coefficient using Abel Transforms (Kursinski et al., 2002).

The hydrostatic assumption would be very dubious during deep convective activity

As the manuscript notes, based on ATOMMS 100 to 200 m vertical resolution and equation 13 of Kursinski et al. (1997), the horizontal resolution of an orbiting ATOMMS system is approximately 100 km. At the 100 km horizontal scale, hydrostatic equilibrium should be a good approximation.

We also note that NWP systems using non-hydrostatic models can assimilate the ATOMMS LEO observations of bending angle and path-integrated absorption, prior to the Abel transform and hydrostatic equilibrium steps in the retrieval process, to avoid the assumption of hydrostatic equilibrium. Non-hydrostatic NWP systems already do this with GPS RO bending angle profiles.

Page 4

Line 11. This is a bit unclear. "The gas phase optical depth is due to water vapor and dry air absorption, which introduces temperature and pressure dependence, and any attenuation due to hydrometers." You are saying the gas phase optical depth is also dependent up the presence of non-gas constituents like hydrometeors?

Yes, this does seem confusing. The sentence in question will be changed.

Original: The gas phase optical depth is due to water vapor and dry air absorption, which introduces temperature and pressure dependence, and any attenuation due to hydrometers.

Revised: The total optical depth is due to the gas phase optical depth plus the attenuation due to hydrometeors. The gas phase optical depth includes water vapor and dry air absorption, which depend on temperature and pressure. The hydrometeor attenuation also depends on temperature (Kursinski et al., 2009).

Page 5

Again, not sure if this is necessary to state. "With funding from NSF,..."

That part of the sentence will be removed. Instead, this information will be included in an acknowledgement section placed immediately before the references section. The new acknowledgement is shown above in response to a similar comment.

Change to original sentence:

~~With funding from NSF, w~~We designed and built a ground-based, prototype ATOMMS instrument and then used it to demonstrate some key aspects of ATOMMS capabilities and performance in several fixed geometries in southern Arizona with path lengths ranging from 800 m to 84 km.

Page 6.

Line 14 "ATOMMS High Band signals" should be

The original paper is inconsistent with references to the ATOMMS High Band signals.

We will search for all occurrences and change them to ATOMMS High-Band signals for consistency.

Page 7.

Line 13. Which radar data are you referring to? You need to clarify this point.

This is similar to a comment from reviewer 2 above. However, this reference to radar data precedes the one pointed out by reviewer 2. Thus, we will specify the radar here and include the reference in both places.

Original Sentence: The RADAR data and field observations indicated that rain was still falling over portions of the path between the two instruments.

Revised sentence: Radar data from the Tucson WSR-88D radar (Crum and Alberty, 1993) and field observations indicated that rain was still falling over portions of the path between the two instruments.

As mentioned in our reply to reviewer #2, the following reference will be added.

Crum, T.D. and R.L. Alberty, 1993: The WSR-88D and the WSR-88D Operational Support Facility. *Bull. Amer. Meteor. Soc.*, **74**, 1669–1688, https://doi.org/10.1175/1520-0477(1993)074<1669:TWATWO>2.0.CO;2

Line 13 Write "By 16:30, the rain was considerably lighter"

We will change the sentence in question by adding the comma after 16:30.

Original: By 16:30 the rain was considerably lighter.

Revised: By 16:30, the rain was considerably lighter.

Line 33. Can you back this statement up with any citations or some references. "This is likely the finest spectral resolution sampling of the 183 GHz line ever achieved in the field."

Revised text: ~~This is likely the finest spectral resolution sampling of the 183 GHz line ever achieved in the field.~~

Page 8.

Line 22 Should this be capitalized AM

References to the am7.2 microwave propagation model have been standardized based on comment #18 from reviewer 1 as *"am7.2"*

Below is the revised text on page 8, line 22, where we first mention the model and define our terminology. All subsequent references to the model will use *"am7.2"* for consistency.

"… we used an atmospheric propagation tool known as the Atmospheric Model (am), version 7.2 (Paine, 2011), which we will refer to as *am7.2*.

Page 9.

Line 30. What size of error should we expect given the use of local pressure measurements at each of the sites? That is, across the line of site, there should be some small variability of pressure given updrafts and downdrafts.

Background: The figure below shows the in-situ pressure observations at both instrument locations and the one hour running mean that we used to determine the air temperature using a hydrostatic approximation. This figure is also included above in our response to reviewer #2 concerning **p. 10, line 19.** The figure shows that the unsmoothed pressure variations at each observation site were up to 2 hPa during the time of the convection as shown in the figure below. When we initially thought to use the hydrostatic pressure scale height to infer the average temperature over the path, these short term pressure variations mapped into unphysical temperature variations. As a result, we recognized immediately that these pressure variations must be non-hydrostatic. These 2 hPa variations are consistent with non-hydrostatic pressure variations of up to 2 hPa expected during convection.

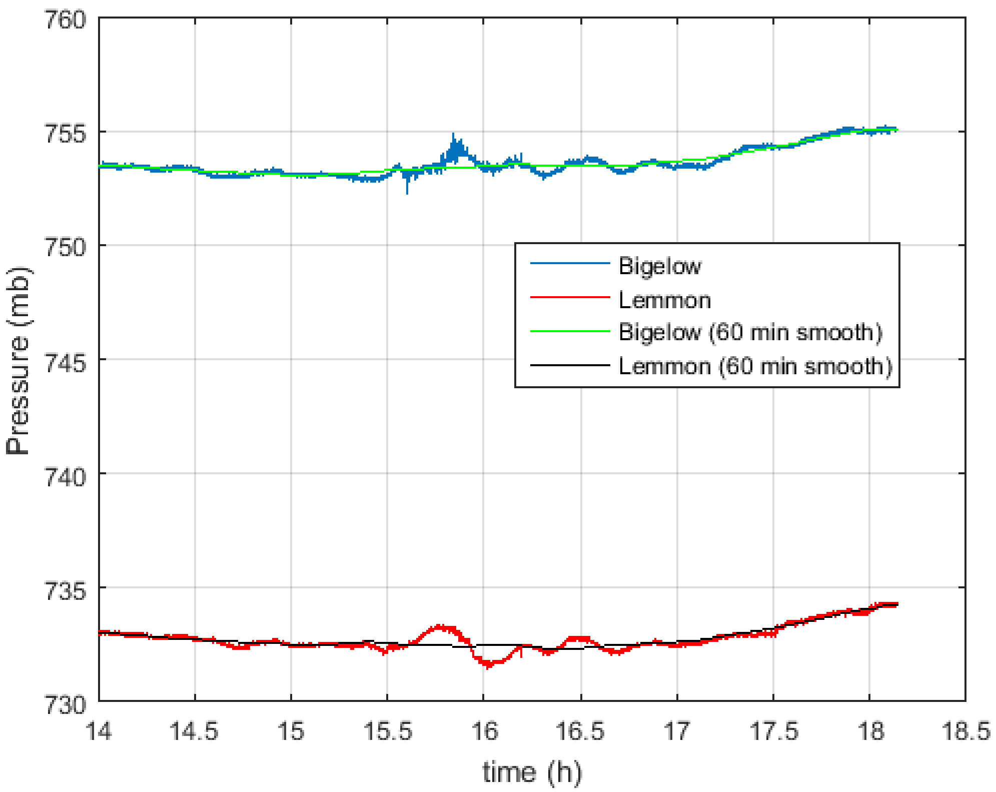

That figure also shows that there were slower varying, highly correlated pressure variation of about 2 hPa over the duration of the experiment. As a result of these considerations, we ended up using a 60 minute running mean of pressure to estimate the average air temperature along the signal path.

Response: We interpret this question as asking, what is the impact of pressure variations along the path relative to the retrieval of water vapor**.** While variations in air pressure do impact the water vapor line shape, the resulting changes are quite small. The figure below, which we do not plan to include in the paper**,** shows the variations in the ATOMMS amplitude ratio over the 187.5 to 191.5 GHz range of signal frequencies that were used in our retrievals. The changes in the ATOMMS amplitude ratio that result from ±2 hPa changes in pressure are comparable to changes due to ± 0.2% changes in vapor pressure. The calculations for the figure assumed reference period one conditions, namely vapor pressure = 15 hPa, air temperature = 20° C, and air pressure = 743 hPa. Thus, the non-hydrostatic pressure variations during the convective period are insignificant relative to 1% variations in water vapor and therefore do not impact our conclusion that ATOMMS observations enabled water vapor retrievals to within 1%.

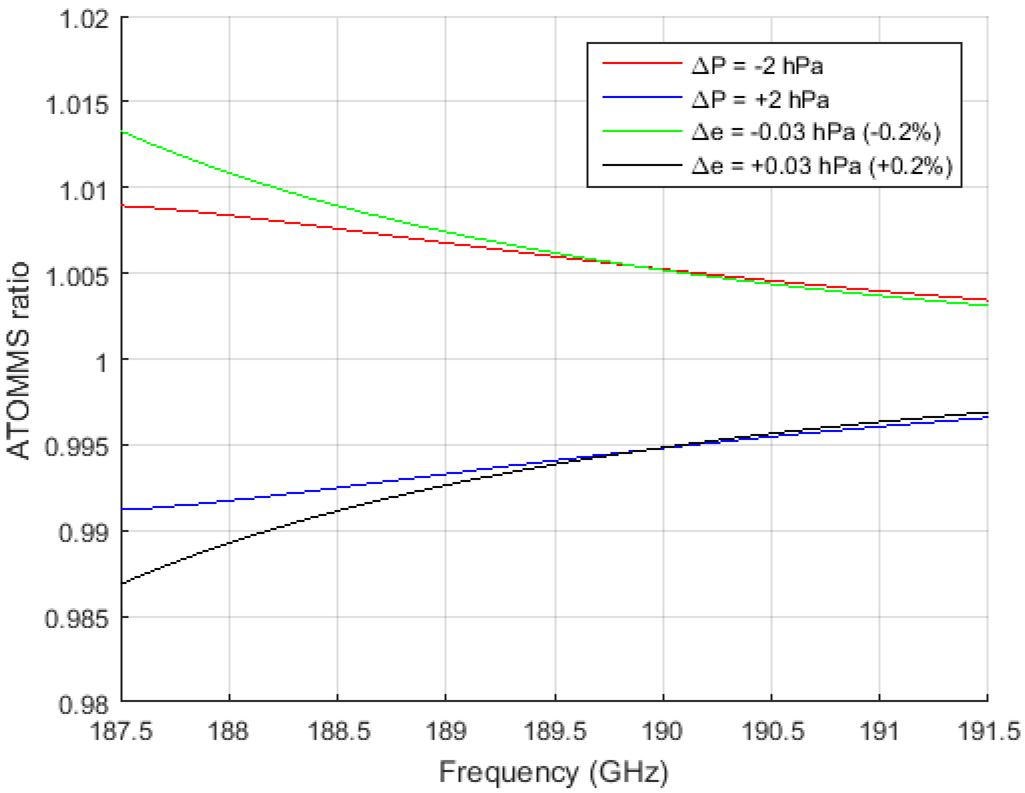

Manuscript changes: In response to this comment from Dave Adams about the impact of pressure variations on the retrievals, we intend to add a line in Figure 6 that represents the change in amplitude ratio that results from a change in pressure of +10 hPa relative to the reference conditions. The point is to show that even for pressure variations much larger than those that were observed, the impact on the water vapor retrieval is insignificant.

Below is the revised Fig. 6 and caption. This is followed by corresponding changes to the text on page 12 beginning with the sentence that starts on line 8, which is where we describe Fig. 6. Those changes are shown below the revised figure and caption.

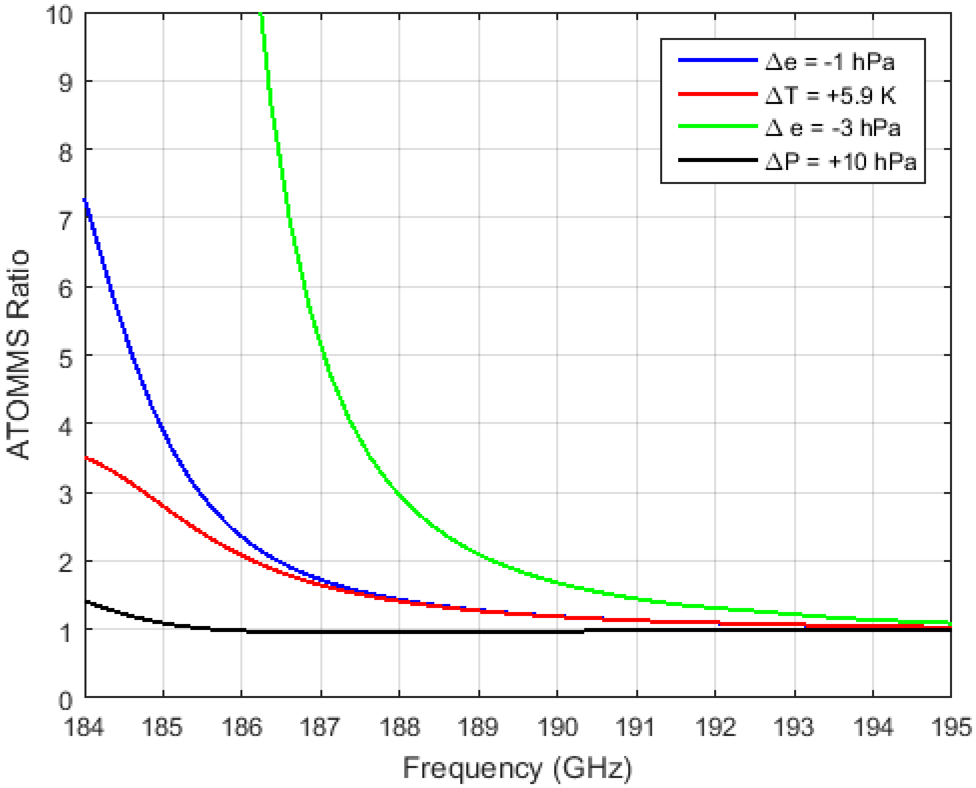

Figure 6: ATOMMS ratio for four changes in the atmospheric conditions along the 5.4 km observation path relative to reference conditions: vapor pressure decreased by 1 hPa (blue), temperature increased by 5.9 K (red), vapor pressure decreased by 3 hPa (green), and air pressure increased by 10 hPa (black). The reference conditions were air pressure = 743 hPa, air temperature = 20° C, and vapor pressure = 15 hPa.

Original text beginning on page 12, line 8:

Examples of the sensitivity of the ATOMMS ratio, Eq. (2), to changes in vapor pressure and temperature relative to the reference conditions for this experiment are shown in Fig. 6. The figure plots the forward-computed ATOMMS ratio spectrum for three different changes relative to the reference conditions. For the conditions of the field experiment, we were able to measure amplitudes for signal frequencies of 187.861 GHz and higher. Lower frequencies closer to line center were too attenuated to track. As the figure shows, for frequencies greater than 187.861 GHz, a one hPa decrease in vapor pressure produced approximately the same ATOMMS amplitude ratio spectrum as a 5.9° C increase in air temperature does. Larger changes in vapor pressure, such as the 3 hPa in the figure, are easily distinguished from changes in air temperature. Based on Fig. 4, the uncertainty in the change in temperature relative to the reference period temperature during this experiment was less than 3°C, which places an upper bound of a 0.5 hPa water vapor uncertainty due to the temperature uncertainty.

Revised text, with changes highlighted in blue:

Examples of the sensitivity of the ATOMMS ratio, Eq. (2), to changes in vapor pressure, temperature, and air pressure relative to the reference conditions for this experiment are shown in Fig. 6. The figure plots the forward-computed ATOMMS ratio spectrum for ~~three~~ four different changes relative to the reference conditions. For the conditions of the field experiment, we were able to measure amplitudes for signal frequencies of 187.861 GHz and higher. Lower frequencies closer to line center were too attenuated to track. The figure shows the change in the ATOMMS ratio spectrum resulting from a change in air pressure of 10 hPa, which is much larger than the ±2 hPa changes in air pressure that were observed during the experiment. Therefore, the sensitivity of the ATOMMS ratio to changes in air pressure is quite small relative to changes in vapor pressure. As the figure shows, for frequencies greater than 187.861 GHz, a one hPa decrease in vapor pressure produced approximately the same ATOMMS amplitude ratio spectrum as a 5.9° C increase in air temperature ~~does~~. Larger changes in vapor pressure, such as the -3 hPa line in the figure, are easily distinguished from changes in air temperature. Based on Fig. 4, the uncertainty in the change in temperature relative to the reference period temperature during this experiment was less than 3° C, which places an upper bound of a 0.5 hPa water vapor uncertainty due to the temperature uncertainty.

Page 11

Line 10 Probably more common “signal-to-noise ratio”

signal to noise ratio will be changed to signal-to-noise-ratio

Page 13

Line 23 Write “comparison with independent, in-situ moisture...”

The comma will be added as suggested.

Original: “comparison with independent in-situ moisture...”

Revised: “comparison with independent, in-situ moisture...”

Page 14

Line 1-3 Maybe you could be a little bit more specific here referring to the map “ between the mountaintops on which instruments sit, while in-situ sensors are located on the ground at each end of the observation path and another in a valley below the observation path.”

The noted changes to the text will be made to be more specific.

Original: The observation geometry in Fig. 1, shows that the ATOMMS-derived vapor pressure is an average over the 5.4 km path that runs above a valley between the mountaintops on which instruments sit, while in-situ sensors are located on the ground at each end of the observation path and another in a valley below the observation path.

Revised: The observation geometry in Fig. 1, shows that the ATOMMS-derived vapor pressure is an average over the 5.4 km path that runs above a valley between the mountaintops on which the instruments sit. The High-Band transmitter was located at the position marked and labeled as "Physics/Atmos bldg Radio Ridge" at an altitude of 2752 m and the High-Band receiver was located at the position marked and labeled as "Catalina Station Steward Observatory" at an altitude of 2515 m. In-situ sensors were located on the ground at the two instrument sites, with another at the location marked and labeled as "Summerhaven," which is about 830 m from the observation path in a valley at an elevation of 2439 m.

Page 15

Line 17. Such behavior where moisture at the surface varies little while air aloft becomes significantly drier following summertime thunderstorms is common in this region (e.g., Fig. 4 in Kursinski et al. [2008]). You can probably find a few more references that describe theromdynamic conditions after T-storms during the NAM

We will add the following sentence after the sentence that ends on line 17. The sentence ending on line 17 is repeated first, followed by the new sentence, which contains a few new citations.

Revised wording. Such behavior where moisture at the surface varies little while air aloft becomes significantly drier following summertime thunderstorms is common in this region (e.g., Fig. 4 in Kursinski et al., 2008). It is also common in the Amazon (e.g., Fig. 7 in Schiro et al., 2016) and may be associated with mid-level inflow of drier air into the precipitating region that results in evaporative cooling and descent of this air (e.g., Leary, 1980 and Houze, 2004).

This requires the following additions to the reference list

Schiro, K. A., J. D, Neelin, D. K. Adams and B. R. Lintner (2016), Deep Convection and Column Water Vapor over Tropical Land versus Tropical Ocean: A Comparison between the Amazon and the Tropical Western Pacific, *J. Atmos. Sci*., 73, p. 4043-4063, DOI: 10.1175/JAS-D-16-0119.1.

Leary, C. A. (1980), Temperature and humidity profiles in mesoscale unsaturated downdrafts, *J. Atmo. Sci*., 37, p. 1005-1012.

Houze, R. A., Jr. (2004), Mesoscale convective systems, *Rev. Geophys*., 42, RG4003, doi:10.1029/2004RG000150.

Page 16

Line 21 "The nearby Tucson radiosonde indeed indicated that..." With all of the reference in the paper to this sounding, you should include it in the figures.

Based on this recommendation, we performed a closer examination of the afternoon sonde profile of August 18, 2011, and we have found that we can infer a bit more than we had previously understood about what happened that afternoon.

Therefore the figure, below will be added to the paper. It shows specific humidity, *q*, and potential temperature, *θ*, derived from the afternoon sonde. In the absence of sources and sinks, *q* and *θ* are conserved variables that can provide additional insight into what happened that afternoon. The figure shows the 3,000 meters above the Tucson valley floor in order to see the boundary layer structures and the ATOMMS' height interval.

Revisions: The new figure, which will be Figure 9 in the paper, is shown immediately below with its proposed caption. We also propose to make changes to the text to describe the figure and its significance. The text changes are shown below the new figure.

Figure 9.

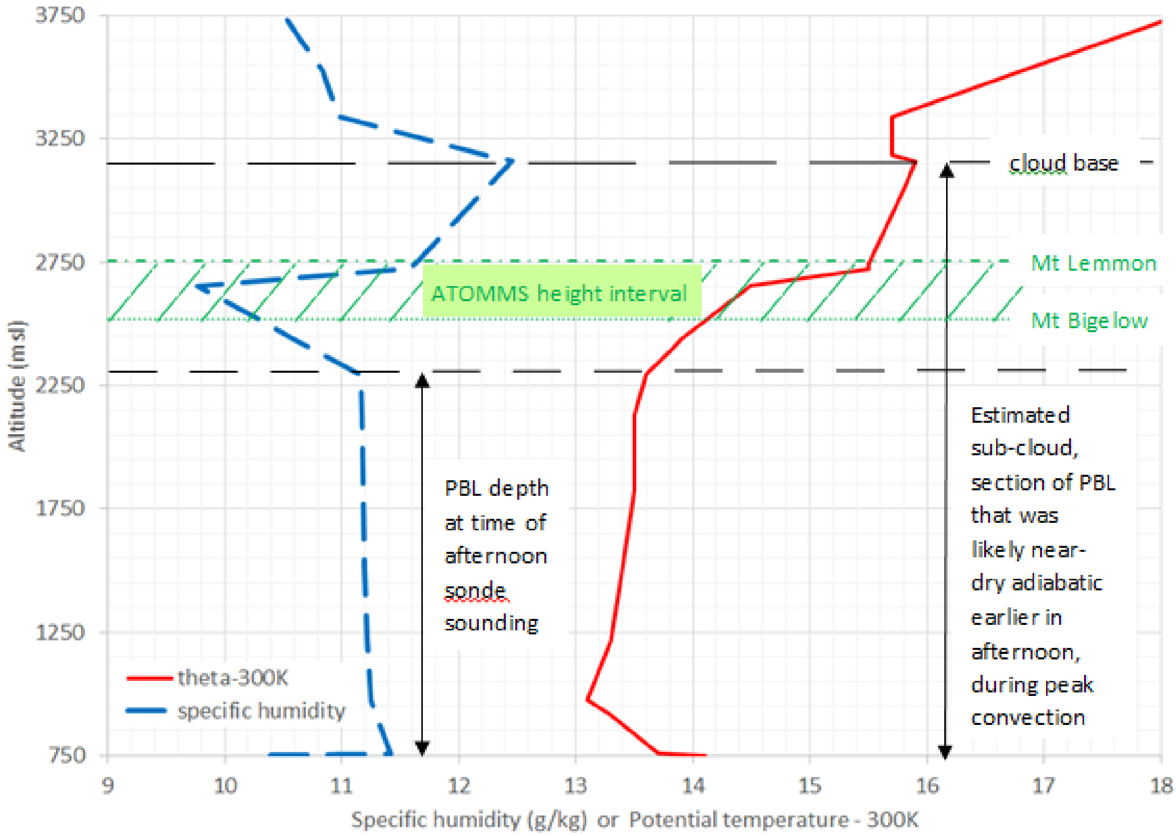

Figure 9: Vertical profiles of specific humidity and potential temperature minus 300 K calculated from the 00 UTC Tucson sonde. The local time of the sonde launch was approximately 16:30 on August 18. Theta label for the red line stands for potential temperature and PBL stands for planetary boundary layer.

To provide the reviewers with some context for the modified text, we first repeat the two paragraphs at the end of Section 6, starting on line 9 of page 15, with minor changes indicated with strikethrough marks for deletion and blue for text changes. Below that, the paragraph shown in entirely in blue is a new paragraph.

Revised text:

Another issue in validating the ATOMMS water vapor retrievals against the in-situ sensor results is a moist bias in the ground measurements relative to the overlying air after the period of heavy rain. The bias is due to evaporation from the wet surface moistening the near-surface air, which is the air whose properties were measured by the in-situ sensors. As a result, with the exception of the cloud around 16:30, the retrieved ATOMMS water vapor amounts over the 80 minutes following the heavy rain were systematically lower than the surface measurements. This continued until approximately 17:20 when the steady increase in water vapor and rain began and continued through the end of the experiment. The largest differences occurred shortly after the most intense rain, when ATOMMS measured a vapor pressure of 10.2 hPa, the smallest of the entire experiment. This value is approximately 25% lower than water vapor measured at the surface stations. Such behavior where moisture at the surface varies little while air aloft becomes significantly drier following summertime thunderstorms is common in this region (e.g., Fig. 4 in *Kursinski et al.*, 2008). It is also common in the Amazon (e.g., Fig. 7 in Schiro et al., 2016) and may be associated with mid-level inflow of drier air into the precipitating region that results in evaporative cooling and descent of this air (e.g., Leary, 1980 and Houze, 2004).

For the period of relatively dry air following the cloud, the 00Z Tucson radiosonde profile provides perhaps the best validation of the ATOMMS results. The sonde launched between 16:30 and 16:45 from a location about ~~20 km south~~ 28 km southwest of the experiment and ascended through the Mt. Bigelow to Mt. Lemmon altitude interval between 16:35 and 16:50 at a location approximately 20 km south of the ATOMMS' observation path. According to the sonde, the average vapor pressure in the layer between Mt. Bigelow and Mt. Lemmon was about 12.3 hPa which is within a few percent of the ATOMMS water vapor retrievals following the cloud's passage. We also note that moisture concentrations measured on Mt. Lemmon decreased steadily through this period reaching a minimum of 12.7 hPa at 17:25, a value essentially identical to the ATOMMS moisture retrieval at this time (Fig. 7). This decrease, despite the evaporative moistening from the wet surface, suggests that dry air was indeed advecting over Mt. Lemmon. Thus, the combination of the sonde profile, the ATOMMS measurements and Mt Lemmon surface measurements all indicate passage of a relatively dry, horizontally extended, air layer following the heavy rain.

Further examination of the operational sonde profiles launched in Tucson that morning around 4:30 AM and particularly that afternoon, around 4:30 PM, provide additional clues as to what happened that afternoon. Figure 9 shows the specific humidity and potential temperature calculated from the Tucson August 19, 00 UTC sonde for the lowest 3,000 m above Tucson. The green hatched region shows the altitude interval across the ATOMMS observation path. In the afternoon sonde profile, the potential temperature, θ, and specific humidity, q, are nearly constant between the surface and 2,300 m above sea level (msl), indicating that the boundary layer (BL) near 16:30 local time extended to about 2,300 msl. In contrast, cloud base at 3,150 msl where the dew point equals the temperature in the sonde profile, and the 500 m near-adiabatic layer immediately below it, further indicate that earlier in the afternoon, the well mixed, dry adiabatic, sub-cloud BL very probably extended up to 3,150 msl. Between 2,300 and

2,750 msl is a thermal inversion layer that is noticeably drier than the air immediately above and below it. The ATOMMS measurements were made within this altitude interval. The relatively low moisture concentrations in this layer measured by both ATOMMS and the afternoon sonde combined with the fact that the θ of this inversion layer is lower than the θ of the peak afternoon BL indicates this air was likely cooled diabatically by evaporation of precipitation falling through it during the turbulent period of heavy rain. The net effect of this process was to increase its q and reduce its θ, causing it to descend from a higher altitude to where it was measured by ATOMMS. Similarly, the fact that the θ of the late afternoon boundary layer below the ATOMMS layer, is 2.5 K lower than that of the peak afternoon BL also indicates that air has also been evaporative cooled and descended. Such evaporative cooling and descent and moistening of dry air layers is a well-known feature of squall lines (e.g., Houze, 2004) and cause microbursts which are well known in Arizona (e.g. Willingham et al., 2010). Further understanding of the details of what happened that afternoon will require detailed modeling with a convection resolving model, which is beyond the scope of the present research.

This change requires adding the following new references to our reference list.

Houze, R. A., Jr. (2004), Mesoscale convective systems, *Rev. Geophys.*, **42**, RG4003, doi:10.1029/2004RG000150.

Willingham, K. M. , E. J. Thompson, K. W. Howard and C. L. Demspey (2010), Characteristics of Sonoran Desert Microbursts, *Weather and Forecasting*, 26, p. 94-108, DOI: 10.1175/2010WAF2222388.1.

Page 18

Frequency of observations will always be an issue to some extent with the RO technique, particularly when the scales are of the time and space scales need for weather prediction.

Below we respond to the reviewer's comment. We have proposed text changes to address these points in Section 1, which are in response to your second overall comment with respect to page 2 of the original document. We are not planning to make any additional changes to the text of the paper on page 18 as these have been addressed in Section 1.

The reviewer raises an important point that we have thought about since the conception of ATOMMS. ATOMMS measurements from low Earth orbit (LEO) will profile the atmosphere with very high, 100-200 m vertical resolution with a corresponding horizontal resolution of approximately 100 km as noted in the manuscript. As the results of this paper imply, ATOMMS profiling from LEO will work quite well in both clear and cloudy conditions which is critical for sampling convection. The vertical information that ATOMMS sensors in LEO will provide promises to provide information across the globe on atmospheric stability and particularly conditional instability that are critical for predicting the onset and evolution of atmospheric convection. We also note that ATOMMS' ~100 km horizontal resolution matches the 100 km scale that Durran and Weyn (2016) argue is the most important scale for forecasting thunderstorms.

Thus, ATOMMS LEO data promises to be very useful with regard to convection IF we can create sufficiently dense ATOMMS sampling densities. This issue was discussed in Kursinski et al. (2016) who noted that a constellation of 60 very small satellites, carrying both ATOMMS and GNSS RO sensors, would produce approximately 25,000 ATOMMS occultations and 170,000 GNSS occultations each day, for a fraction of the cost of a NOAA polar orbiting weather satellite. The orbits they noted would sample the entire globe every 6 hours to support the 6 hour update cycle of global weather prediction centers. The average spacing between ATOMMS and GNSS occultations every 6 hours would be approximately 320 and 120 km respectively which is quite dense compared to present GNSS RO and radiosonde sampling. To further put that into perspective from the standpoint of convection, such a system would provide approximately 300 ATOMMS profiles and 1,800 GNSS RO profiles respectively over the Amazon basin, each day.

Thus, an eventual large ATOMMS+GNSS RO constellation, which can be implemented relatively cost effectively, promises to be quite enlightening for improving our understanding and ability to predict atmospheric convection.

These points are made in the updated text in response to Dave Adams comment on page 2.

Retrieval of Water Vapor using Ground-based Observations from a Prototype ATOMMS Active cm- and mm-–Wavelength Occultation Instrument

Dale M. Ward[1], E. Robert Kursinski[2], Angel C. Otarola[1,3], Michael Stovern[4], Josh McGhee[2], Abe Young[5], Jared Hainsworth[6], Jeff Hagen[7], William Sisk[8] and Heather Reed[9]

[1]Department of Atmospheric Sciences, University of Arizona, Tucson, AZ 85721, USA
[2]Space Sciences and Engineering, Boulder, CO, 80301, USA
[3]TMT International Observatory, LLC~~Inc~~., Pasadena, CA 91105, USA
[4]Environmental Protection Agency, Denver, CO 80202-1129, USA
[5]Department of Physics, University of Arizona, Tucson, AZ 85721, USA
[6]Hill Air Force Base, A-10 Mechanical Systems, Ogden, UT 84056, USA
[7]Lithe Technology, Tucson, AZ 85721, USA
[8]Department of Astronomy, University of Arizona, Tucson, AZ 85721, USA
[9]LASP, University of Colorado, Boulder, CO 80303, USA

Correspondence to: Dale M. Ward (dward@email.arizona.edu)

Abstract. A fundamental goal of satellite weather and climate observations is profiling the atmosphere with in situ-like precision and resolution with absolute accuracy and unbiased, all-weather, global coverage. While GPS radio occultation (RO) has come perhaps closest in terms of profiling the gas state from orbit, it does not provide sufficient information to simultaneously profile water vapor and temperature. We have been developing the Active Temperature, Ozone and Moisture Microwave Spectrometer (ATOMMS) RO system that probes the 22 and 183 GHz water vapor absorption lines to simultaneously profile temperature and water vapor from the lower troposphere to the mesopause. Using an ATOMMS instrument prototype between two mountaintops, we have demonstrated its ability to penetrate through water vapor, clouds and rain up to optical depths of 17 (7 orders of magnitude reduction in signal power) and still isolate the vapor absorption line spectrum to retrieve water vapor with a ~~precision better~~random uncertainty less than 1%. This demonstration represents a key step toward an orbiting ATOMMS system for weather, climate and constraining processes. ATOMMS' water vapor retrievals from orbit will not be biased by climatological or first guess constraints, and will be capable of capturing nearly the full range of variability through the atmosphere and around the globe, in both clear and cloudy conditions, and will therefore greatly improve our understanding and analysis of water vapor. This information can be used to improve weather and climate models through constraints on and refinement of processes affecting and affected by water vapor.

Formatted: Font: 10 pt

1. Introduction/Motivation

Water vapor is an important constituent in Earth's atmosphere and its distribution in space and time must be known to understand and predict weather and climate. Water vapor is fundamental to the radiative balance of the Earth, both as the most important greenhouse gas and indirectly through clouds. Through its latent heat, water vapor is crucial to formation and evolution of severe weather, transport of energy both upward and poleward in the troposphere and transfer of energy between the surface and atmosphere. Furthermore, water vapor dominates tropospheric radiative cooling which drives convection (Sherwood et al., 2010). Uncertainty in modeled cloud feedback results in the factor of 3 spread in predictions in the surface temperature response to a doubling of atmospheric CO_2 concentrations and the cloud feedback depends critically on the strength of the water vapor feedback (Held and Soden, 2000). Predicted amplification of extreme precipitation with warmer temperatures is tied directly to predicted increases in extreme water vapor concentrations and it may be underestimated (e.g., Allan and Soden, 2008).

~~Despite its importance, we do not have precise observations of its distribution in the atmosphere, its trend with time,~~ Water vapor observations must be unbiased and capture the full range of variability in clear and cloudy conditions across the globe in order to improve the understanding and analysis of water vapor, This information ~~which~~ is used to initialize weather prediction systems, to monitor trends and variations and to improve weather and climate models through constraints on and refinement of processes affecting and affected by water vapor (e.g., Bony et al., 2015).

Satellite observations are required to gain a global perspective for weather prediction and climate monitoring and for constraining the critical processes at work in ~~in~~ different regions across ~~across~~ the globe. Unfortunately, present satellite provide limited constraints on the water vapor field, particularly when clouds are present, which in turn limits the skill of ~~the the~~ weather forecasts and our detailed knowledge of water vapor across the globe. For example, GOES observations provide time and horizontal resolution but very limited vertical information. While hyperspectral IR on polar orbiting satellites provide more information, their temporal sampling is limited and their water vapor estimates are quite noisy with fractional, root mean-square (RMS) differences ranging from 25% in the lower troposphere to 70% around 400 hPa and a tendency toward dry biases up to 30%, depending on cloud type (Wong et al., 2015). While downward looking microwave radiance measurements are particularly useful for determining the column water over the ocean (e.g., Wang et al., 2016), they provide significantly less vertical information than IR and are inherently ambiguous over land, snow and ice due to surface emissivity variations. ~~Yue~~ point is that present state-of-the-art, radiance-based satellite water vapor remote sensing systems have serious limitations in terms of performance and sampling biases associated with clouds and surface conditions, accuracy, vertical resolution and the ambiguity inherent in the conversion of radiances to the atmospheric state (Rodgers 2000).

Because of these satellite limitations, balloon-borne sondes and dropsondes continue to be the measurement of choice for field campaigns focused on answering key questions about the atmosphere. In fact, the globe would be covered with sondes if the cost to do so were not so completely prohibitive. Operational global weather observing systems therefore rely primarily on more affordable but vertically coarse satellite radiance measurements and the inherent ambiguities in the information they provide. Unfortunately, this limits how much understanding we can gain from these observations about important atmospheric processes like those associated with clouds, convection and surface exchange.

In this context, GPS radio occultation (RO) has provided a welcome advance in satellite remote sensing through its ability to profile the atmosphere with ~200 m vertical resolution, approaching that of sondes, in all-weather conditions, with very small random and absolute uncertainties. As such, GPS RO ~~GPS radio occultation (RO)~~ has become an important data source for numerical weather prediction (NWP), despite its relatively sparse coverage to date (~~[~~e.g., Cardinali and Healy, 2014)~~]~~. Its high impact comes from its unique combination of ~200 m vertical resolution, all weather sampling and very low random and absolute uncertainties via its direct connection to atomic frequency standards and relatively simple and direct retrieval method. GPS RO profiles atmospheric refractivity. Two limitations of GPS RO are (1) its inability to separate the dry air and water vapor contributions to refractivity and (2) its insensitivity to water vapor in the colder regions of the troposphere and above (e.g., Kursinski et al., 1997; Kursinski and Gebhardt, 2014). The insensitivity occurs when there is so little water vapor that the majority of the refractivity is dominated by the dry air component.

In recognition of the strengths and weaknesses of GPS RO and radiance measurements and the need for better information about water vapor, in 1997 research groups at the University of Arizona and the NASA Jet Propulsion Laboratory (Herman et al., 1997 and Hajj et al., 1997) identified and began developing an RO system that is now called the Active Temperature, Ozone and Moisture Microwave Spectrometer (ATOMMS), which is designed to overcome these GPS limitations by transmitting and receiving signals between satellites in low Earth orbit (LEO) near the 22 and 183 GHz water vapor absorption lines as well as nearby ozone absorption lines. Profiling both the speed of light like GPS RO as well as the absorption of light, which GPS RO does not measure, enables ATOMMS to ~~precisely~~ profile temperature, pressure and water vapor simultaneously from near the surface to the mesopause with little random or systematic uncertainty (Kursinski et al., 2002). It will also profile ozone from the upper troposphere into the mesosphere, scintillations produced by turbulence, slant path cloud liquid water and detect larger cloud ice particles, with approximately 100 m vertical resolution and corresponding 70 km horizontal resolution (Eq. 13, Kursinski et al., 1997). Kursinski et al. (2002) found that such a system could provide water vapor retrievals with a ~~precision~~ random uncertainty of 1 – 3% from near the surface well into the mesosphere. Kursinski (2009) estimated the degradation in clouds would be less than a factor of 2. A summary of LEO to LEO occultation measurement concept studies and demonstrations to date at microwave and IR wavelengths is given in Liu et al. (2017).

Regarding the sampling densities that can be achieved with ATOMMS, Kursinski et al. (2016b) noted that a constellation of 60 very small satellites, carrying both ATOMMS and GNSS RO sensors, would produce approximately 26,000 ATOMMS and 170,000 GNSS occultations profiles each day, for a fraction of the cost of a single, operational, polar orbiting weather satellite. These numbers of profiles are approximately 10 and 100 times present GPS RO and radiosonde sampling densities. Such an orbiting ATOMMS constellation providing dense, very high vertical resolution, precision and accuracy water and temperature profiling via radio occultation will complement existing observations of clouds, precipitation and energy fluxes and tie the entire weather and climate system together. This combination will also dramatically improve the realism and utility of global analyses for climate as well as forecasting (increasingly extreme) weather (Kursinski et al., 2016b).

With regard to constraining processes, we briefly discuss three important and representative application areas: moist convection, weather fronts and polar weather and climate.

Moist convection is ubiquitous across the globe but inadequately understood which leads to inaccurate representation in models. Environmental variables critical for understanding and predicting moist convection and associated severe weather include temperature, water vapor, stability, and conditional instability in particular, the level of free convection, convective available potential energy (CAPE), convective inhibition (CIN), winds and divergence. Unfortunately, coarse vertical resolution and ambiguities inherent in converting radiance spectra to the atmospheric state limit the ability of satellite radiances to provide detailed constraints on convection related processes. GPS RO provides much needed vertical information across the globe and is particularly useful for determining temperatures and stability in the upper troposphere where conditions are very dry. However, the ambiguity of the wet and dry gas contributions to refractivity under the warmer, moister conditions deeper in the troposphere limit the utility of GPS RO refractivity profiles there.

In contrast, ATOMMS will be the first orbiting remote sensing system to simultaneously profile temperature and water vapor with very high ~100 m vertical resolution and very small uncertainties needed to tightly constrain these environmental quantities relevant to convection, in clear and cloudy conditions, through the troposphere, across the entire globe. While ATOMMS profiles will not resolve detailed horizontal structure at scales much below 70 km, they are sensitive to these scales via the phase and amplitude scintillations that small scale turbulence produces on the ATOMMS signals (Kursinski et al., 2016b). Furthermore, 100 km, which is approximately the horizontal resolution of ATOMMS, is the scale most important for forecasting severe convection in the form of thunderstorms (Durran and Weyn, 2016).

Weather fronts are another fundamental class of severe weather poorly constrained by satellite radiance measurements. Unlike radiances, RO measurements can profile fronts from orbit because RO profiles readily penetrate through clouds and the vertical and horizontal resolutions of RO are well matched to the vertical and horizontal scales of weather fronts. While GPS RO can profile fronts in the upper troposphere (e.g. Kuo et al., 1998), the lack of refractivity contrast between the warm-wet and the cold-dry sides of fronts deeper in the troposphere limits GPS RO profiling of fronts there (Hardy et al., 1994). ATOMMS high precision temperature, pressure and water vapor profiles in clear and cloudy conditions will readily distinguish between the warm and cold sides of fronts down through the lower troposphere and precisely determine the location of any frontal surface that crosses an ATOMMS profile (Kursinski et al., 2002).

This unprecedented capability to measure fronts globally will also enable detailed characterization of the dynamics and moisture fluxes of atmospheric rivers out over remote ocean regions to better predict and prepare for the torrential rainfall and flooding they produce following landfall. These observations will also guide refinements in model representations of atmospheric rivers to increase and extend the accuracy of weather forecasts and the climatologically important mid-latitude water vapor transport in reanalyses and climate models (e.g., Guan and Waliser, 2016).

Profiling in Polar regions, particularly the near-surface environment, is critical to understanding the causes of ongoing and future climatic changes there. Reducing uncertainty due to our limited knowledge about the critical processes at work there requires quantitative, process-resolving observations that span the entire range of environmental conditions and behavior across these remote regions. Present understanding comes largely from operational sondes and a small number of field campaigns (e.g., Esau and Sorokina, 2010). While satellites radiance measurements already provide dense sampling of these remote, high latitude regions, they have yielded relatively little insight due to intrinsic ambiguities associated with poor vertical resolution, frequent clouds, near-surface inversions and variations in surface emissivity. As a result, many "global" satellite products do not extend to the poles (e.g. Chen et al., 2008). While GPS RO has much needed very high vertical resolution, cloud penetration and insensitivity to surface conditions, its impact is also limited, because of the unknown contributions of water vapor and the bulk dry gas to the measured refractivity profiles.

In this context, ATOMMS' precise and very high vertical resolution profiling of temperature, stability, water vapor, pressure gradients, clouds and turbulence, down to the surface, over all types of surfaces, in clear and cloudy conditions, across the diurnal and seasonal cycles, will bring unprecedented information about the high latitudes and, in particular, the lowermost troposphere, to constrain and reduce presently large uncertainties in surface fluxes and the surface energy budget there.

ATOMMS will simultaneously probe through clouds to determine the gas state as well as the cloud properties themselves, including their phase (liquid, ice and mixed) which are critical in the surface energy budget (e. g., Klingebiel et al., 2015) and fundamental to calculating upward and downward short and long wave radiative fluxes through the atmosphere. ATOMMS will profile the frequent polar boundary layer clouds too close to the surface to be characterized by CloudSat (Kay and Gettleman, 2009).

ATOMMS will constrain winds via horizontal pressure gradients to further constrain wind shear and moisture fluxes. This wind and cloud information together with ATOMMS' simultaneous profiling of stability and turbulent scintillations will provide a new set of observational constraints over the entire high latitude region to expose flaws in and guide improvements to presently inaccurate and poorly constrained model parameterizations of sensible and latent heat fluxes. The ability to estimate turbulence and radiative cooling at cloud top are also critical to determining cloud lifetimes and the radiative budget because turbulent entrainment rates influence droplet size and therefore albedo (Esau and Sorokina, 2010). ATOMMS global perspective would provide critical information for understanding why the two poles are evolving so differently.

The preceding examples reveal inadequacies in our present observing system that limit our understanding, and the substantial increase that ATOMMS promises in our observationally based knowledge and understanding. The performance of ATOMMS profiles approach that of sondes and, when implemented as a constellation such as in Kursinski et al. (2016b), would provide far denser coverage across the globe. For example, the vast Amazon rainforest which is presently profiled twice a day by only 8 sondes (Itterly et al., 2016), would be sampled by approximately 300 ATOMMS profiles and 1,800 GNSS RO profiles each day via the ATOMMS satellite constellation noted above. Thus, an ATOMMS constellation would create a continuous, dense, global data set, with performance approaching that of sondes, that researchers could divide up as they like into smaller domains (creating essentially their own regional (field) campaigns) to better understand and model key processes and reduce weather and climate prediction uncertainty across the globe.

Our work here is focused on a mountaintop demonstration of ATOMMS' ability to measure water vapor through rain and clouds. Using ground-based ATOMMS prototype instrumentation ~~that we developed with funding from NSF~~, we demonstrate the ability of ATOMMS to retrieve changes in the path-averaged water vapor between the instruments operating between two mountaintops in Southern Arizona to within 1%, during weather conditions that ranged from clear to cloudy to thunderstorms with heavy rain. The ATOMMS mountaintop retrievals worked up to optical depths of 17. The smaller than 1% discrepancies between the measured ATOMMS spectra and the forward modeled water vapor spectra (described in Section 4), in clear, cloudy and rainy condition are unprecedented and more than one order of magnitude smaller than the 25% to 70% uncertainties in AIRS retrievals reported in Wong et al. (2015). ~~one to two orders of magnitude smaller than present discrepancies between AIRS and ECMWF, which are limited to conditions of relatively low cloud opacity.~~ At still higher cloud and rain opacities such as the conditions encountered during our ATOMMS mountaintop experiment, IR and microwave emission-based water vapor retrievals simply do not~~n't~~ work. ATOMMS performance in cloud and rain is achieved via a differential transmission approach using a calibration signal ~~tone~~, in contrast to passive IR and microwave sensors systems work via emission. In addition, the vertical resolution attainable via active occultation observing systems is at least an order of magnitude better than that of passive sensors.

The structure of the paper is as follows. Section 2 summarizes the ATOMMS concept for satellites operating in low Earth orbit (LEO) and Section 3 describes this mountaintop experiment. In Section 4, we discuss the water vapor retrievals from the measured mountaintop data. Sources of u~~U~~ncertainty are covered in Section 5, while Section 6 examines validation the water vapor retrievals with available in-situ measurements. Finally, in S~~s~~ection 7 the encouraging results from the ATOMMS ground-based system lead us to a discussion of the unique capabilities of a future ATOMMS satellite occultation system for improving numerical weather forecasts, monitoring climate changes, and improving our understanding and model representation of processes related to water vapor.

2. ATOMMS Concept

ATOMMS is a natural extension of the GPS RO concept. It extends the capabilities and overcomes several limitations of GPS RO by simultaneously measuring atmospheric bending and absorption at several essentially monochromatic signal frequencies in two frequency bands centered on the 22 GHz and 183 GHz water absorption lines, referred to as Low-Band and High-Band respectively. The High-Band includes several ozone absorption lines used to profile ozone. During ATOMMS satellite to satellite occultations, signals transmitted from one satellite are received by the other which yields measurements of the signal phase and amplitude during the occultation. From these, occultation profiles of bending angle and absorption are derived and then used to derive radial profiles of refractivity and the extinction coefficient using Abel Transforms (~~[~~*Kursinski et al.*, 2002)~~]~~. These are then combined with knowledge of spectroscopy together with the equations of refractivity and hydrostatic equilibrium to derive profiles of air temperature, pressure, water vapor, ozone, and some properties of condensed water.

ATOMMS functions as a precise, active spectrometer over the propagation path between the transmitter and receiver. Retrievals of water vapor from radiance measurements are inherently ambiguous because both the unknown signal source emission and attenuation along the path are unknown and ~~, which are distributed along the path,~~ must be solved for, creating 2000). In comparison to radiance retrievals, ATOMMS has the advantage that the transmitted signal strength is well ~~contrast,~~ and the observed quantity is simply the attenuation along the path, which makes the retrievals much more direct and less unambiguous. The active approach also enables ~~precise and accurate~~ retrievals retrievals with small random and systematic conditions of large path optical depths, which is not possible for passive retrievals.

Because ATOMMS uses phase coherent signals to measure Doppler shift and bending angle like GPS RO, we write the signal attenuation in terms of amplitude rather than intensity as follows,

$$A(f) = \mathrm{A}_0(f)e^{-\tau/2} \tag{1}$$

where *A* is the measured signal amplitude after the absorption, A_0 is the amplitude of the signal that would be measured in the absence of atmospheric attenuation and τ is the optical depth at the signal frequency, *f*. The factor of ½ multiplying the optical depth comes about because intensity is proportional to amplitude squared. The total optical depth is due to the gas phase optical depth plus the attenuation due to hydrometeors. The gas phase optical depth includes water vapor and dry air absorption, which depend on temperature and pressure. The hydrometeor attenuation also depends on temperature (Kursinski et al., 2009).

~~The gas phase optical depth is due to water vapor and dry air absorption, which introduces temperature and pressure dependence, and any attenuation due to hydrometers.~~

Differential Absorption

A key to ATOMMS performance is its double differential absorption approach (~~[~~Kursinski et al., 2002)~~]~~. First, the amplitude observable is the *change* in signal amplitude over an occultation relative to the amplitude measured at time, t_0, when the signal path between the two spacecraft is entirely above the atmosphere. Second, the amplitudes of two (or more) signals are measured simultaneously during each occultation. The frequency, *f*, of one signal is placed on the absorption line of interest while the frequency of the second signal, f_{CAL}, is farther from line center so that signal can ~~to~~ function as ~~a~~an amplitude signal.

The quantity used in the ATOMMS retrievals is the ratio of two amplitude ratios,

$$R(f, f_{CAL}, t, t_0) = \left.\frac{A(f,t)}{A(f_{CAL},t)}\right/\frac{A(f,t_0)}{A(f_{CAL},t_0)} \tag{2}$$

The amplitude ratio in the denominator represents the ratio of the amplitude of the tuned signal to the amplitude of the calibration signal at reference time, t_0, when the signal is nominally above the atmosphere. The amplitude ratio in the numerator represents the ratio of the amplitude of the tuned signal to the amplitude of the calibration signal at measurement time, *t*, during the occultation. Taking the natural logarithm of *R* and multiplying by two yields the change in the difference between the optical depths at frequencies *f* and f_{CAL}, from the reference time, t_0, to time, *t*.

$$2\log(R) = \tau(f,t) - \tau(f_{CAL},t) - [\tau(f,t_0) - \tau(f_{CAL},t_0)] \tag{3}$$

If the signal path is entirely above the atmosphere at reference time, t_0, as will be the case in a LEO-LEO occultation geometry, then the optical depths at time t_0 are zero and Eq. (3) simplifies to

$$2\log(R) = \tau(f,t) - \tau(f_{CAL},t) \tag{4}$$

The frequency separation between f and f_{CAL} is chosen such that R retains most of the absorption signature while cancelling unwanted common sources of error such as gain variations due to pointing errors, scintillations due to atmospheric turbulence and attenuation due to scattering by hydrometeors. This ratio of ratios approach enables precise measurement of water vapor in the presence of clouds and rain with very small random and systematic uncertainty as we demonstrate below.

3. Overview of the ATOMMS Mountaintop Experiment

W~~ith funding from NSF, w~~e designed and built a ground-based, prototype ATOMMS instrument and then used it to demonstrate some key aspects of ATOMMS capabilities and performance in several fixed geometries in southern Arizona with path lengths ranging from 800 m to 84 km. The prototype ATOMMS High-Band system transmits and receives two simultaneous continuous wave (CW) signals tunable from 181 to 206 GHz. The prototype Low-Band system consists of eight CW transmitters and receivers at fixed frequencies from 18.5 to 25.5 GHz spaced approximately one GHz apart, centered approximately on the 22 GHz water vapor absorption line. Below we summarize the content of previous published work based on field experiments with the ATOMMS ground-based prototype.

In terms of ATOMMS water vapor retrievals, Kursinski et al. (2012) demonstrated agreement at the 2% level between water vapor measurements derived along an 820 m path using the ATOMMS High-Band instrument and a nearby, capacitive-type hygrometer. High-Band mountaintop measurements yielded the first detection by ATOMMS of $H_2^{18}O$ via its 203 GHz absorption line (Kursinski et al., 2016b). Such measurements in the upper troposphere will determine isotopic ratios to constrain the hydrological cycle (Kursinski et al., 2004).

In terms of spectroscopy, the ATOMMS measured line shape across the 4 GHz interval above the 183 GHz line center agreed with the HITRAN line shape with a standard deviation of 0.3% (Kursinski et al. 2012), some 8 times better than the previously best estimate of Payne et al. (2008). ATOMMS mountaintop measurements between 5 and 25 GHz above the line center revealed discrepancies with the HITRAN line shape (Kursinski et al., 2016b) which may help explain inconsistencies in 183 GHz derived water vapor estimates (Brogniez et al., 2016) and may be associated with atmospheric turbulence (Calbet et al., 2018). The ATOMMS measurements also revealed the shape of the 183 GHz line as represented in the Liebe et al., (1993) model is incorrect (Kursinski et al., 2012). The Liebe model is popular, having been referenced more than 600 times in the literature, and is still being used.

Kursinski et al. (2012) combined ATOMMS High-Band measurements with precipitation radar measurements to derive cloud liquid water content (LWC) along the ATOMMS signal path. Kursinski et al. (2016b) demonstrated the ability to derive both cloud LWC and rainfall rates by combining the ATOMMS Low-Band and High-Band measurements.

Kursinski et al. (2016b) derived the strength of atmospheric turbulence from scintillations of the ATOMMS signal amplitudes and demonstrated the ability to significantly reduce these turbulent amplitude variations via amplitude ratioing, in order to derive accurate water vapor estimates in turbulent conditions.

On August 18, 2011, we collected approximately four hours of data with the instruments located on Mt. Lemmon Ridge (2752 m altitude) and Mt. Bigelow (2515 m altitude), separated by approximately 5.4 km. The observing geometry is shown in Fig. 1. The Mt. Lemmon instrument contained the 183 GHz transmitter and 22 GHz receiver and the Mt. Bigelow instrument contained the 22 GHz transmitter and 183 GHz receiver. The water vapor pressure derived from these ATOMMS measurements represents an average over the 5.4 km path which runs above a valley between the mountaintops on which the instruments sit.

Differences between mountaintop and LEO measurements

The mountaintop-to-mountaintop geometry differs from the satellite-to-satellite geometry in several important aspects. In the satellite-to-satellite occultation geometry, the ATOMMS differential absorption measurements yield *absolute* water vapor concentrations because the reference signal strength is measured above the atmosphere where there is no absorption. Since we cannot evacuate the path between the two mountaintops, mountaintop-to-mountaintop observations are limited to measuring *changes* in water vapor relative to a selected reference period as defined in Eq. (3). In the satellite geometry, a profile of water vapor is retrieved as a function of altitude via an Abel Transform (Kursinski et al., 2002). In the mountaintop experiment, the signal path is fixed and the retrieved quantity is the change in the average water vapor along the fixed path as a function of time.

In the satellite to satellite occultation geometry, the majority of the signal attenuation occurs along the lowest altitude portion of the signal path centered at the ray tangent point which is 100 to 500 km in length. The attenuation contributed at higher altitudes along the ray path is comparatively much smaller than the contribution near the ray path tangent altitude due to both the limb sounding geometry and the exponential decay in water vapor concentrations with altitude. We note that the Abel transform isolates the contribution~~s~~ from the lowest altitude portion of the signal path. ~~of these layers.~~ For a vertical the horizontal length of the path through ~~of~~ the lowest layer is approximately 70 km (Eq. 13, Kursinski et al., 2002). Because large water vapor concentrations in the lower and middle troposphere produce impenetrably high opacities near the 183 GHz line when integrated over such long signal paths, this portion of the troposphere must be profiled using the weak 22 GHz absorption line and the ATOMMS Low-~~–~~Band system from space. This is also the altitude region where liquid water clouds most common. To achieve our goal of an all-weather observing system, the observations must provide enough information for the inversion routine to be able to separate the signal attenuation due to liquid water absorption from that due to water vapor absorption. *Kursinski et al.* (~~[~~2009)~~]~~ showed that the spectral shape of the cloud liquid water absorption at the Low-Band frequencies depends primarily on the cloud liquid water path and cloud temperature. Simultaneously measuring the amplitudes of four Low-~~–~~Band signals, with at least one of the signal frequencies on the high side of the 22 GHz line, in addition to refractivity plus application of a hydrostatic constraint, enables water vapor, cloud liquid water path and effective cloud temperature to be estimated simultaneously. Thus, with absorption information from at least four Low ~~-~~Band frequencies, we can isolate liquid water clouds from water vapor and unwanted variations due to instrumental noise and turbulence. Simulations in *Kursinski et al*. (2009) showed the uncertainty in cloudy conditions should increase by no more than a factor of 2 relative to clear sky conditions. We also note that Kursinski et al. (2009) recommended using at least 5 signal frequencies in order to expose spectral modeling errors and provide the quantitative information needed to refine the modeling of both the water vapor and liquid water spectra.

In this mountaintop demonstration, the atmospheric path from transmitter to receiver took place over a narrow altitude range from 2752 m to 2515 m above sea level and was only 5.4 km in length. Over this short path, the water vapor attenuation due to absorption by the weak 22 GHz line ~~, such that the water vapor attenuation due to absorption by the weak 22 GHz line~~ was too small to measure accurately. Therefore, in this experiment, we used the ATOMMS High ~~-~~Band signals to probe near the stronger 183 GHz water line to retrieve changes in water vapor along the path. Below we show that the liquid attenuation has a relatively flat spectral response across the H~~h~~igh-B ~~b~~and frequencies utilized for the mountaintop retrieval of water vapor and essentially ratios out. In the satellite case, at altitudes where liquid clouds commonly occur, the combined attenuation from liquid water and water vapor will make the atmosphere too opaque to probe with the High ~~-~~Band frequencies and ATOMMS will therefore profile these conditions with the Low ~~-~~Band signals near the 22 GHz line as noted above.

Another difference is that in the LEO-LEO geometry, profiles of atmospheric refractivity and temperature are derived from a Doppler shift proportional to atmospheric bending (~~[~~e.g., Kursinski et al., 1997)~~]~~. In a fixed geometry, there is no equivalent Doppler shift and we therefore had to determine the air temperature via another method which is described in Section 4.

A final point relates to instrument stability. The duration of a typical LEO-LEO occultation is approximately 100 seconds, which allows little time for instrument drift, while mountaintop measurements can continue ~~go on~~ for hours or days. Therefore, to maintain instrument stability over the four hour mountaintop observation period, we used water chillers to minimize temperature variations of critical portions of the transmitters and receivers.

In spite of the differences noted above, this ground-based experiment clearly demonstrates the ability of an ATOMMS-type system to probe through and accurately retrieve changes in water vapor under conditions of large total optical depths with liquid water present along the path.

Observed Optical Depths

The measured changes ~~observed variations~~ in optical depth at 198.5 GHz (blue line, raw) and 24.4 GHz (red line, 2. 198.5 GHz was the frequency of the High ~~-~~Band calibration ~~to~~signal ~~ne~~ during this experiment. Also shown are the derived changes in liquid optical depth at 198.5 GHz (black line), which was computed by subtracting the optical depth changes due to variations in the retrieved vapor pressure and temperature from the total observed optical depth change. The change in optical depth relative to reference period 1 will always be positive for liquid (rain and clouds), because there was no rain or clouds during the reference period. However, the change in optical depth due to changes in vapor pressure and temperature can be negative, which means that the overall change in optical depth relative to the reference period can be less than the optical depth change due to liquid alone.

The instruments were housed in tents to protect them from weather conditions that spanned from clear to cloudy to thunderstorms with heavy rain, as indicated by the annotations in Fig. 2. This wide range of conditions and associated optical depths provided an excellent field test to evaluate and demonstrate several key ATOMMS capabilities. In-situ measurements of temperature, pressure and water vapor were made at each tent. Web cameras in each tent pointed at the opposite ATOMMS instrument site, providing periodic images of weather conditions and visible opacity.

Fig. 2 indicates that when the ATOMMS observations began, a light rain was falling. The rain ended prior to the First Reference period. A brief rain shower was observed from about 14:43 to 15:02 PM. The sharp peak in the 198.5 GHz liquid optical depth just before 15:00 and absence of a peak in the 24.4 GHz liquid optical depth likely indicates an increase in the number of smaller raindrops. This was followed by a brief clear period before the next rain shower began at 15:10. This rain was initially light, but became a heavy thunderstorm at 15:30. From 15:30 to 16:00 the 198.5 GHz tone was too attenuated to be observed at the receiver. During the heavy rain, the 24.4 GHz liquid optical depth reached a peak value of 10. The 198.5 GHz signal was detected again at 16:00 as the rain lightened. By 16:30, the rain was considerably lighter. The radar data from the Tucson WSR-88D radar (Crum and Alberty, 1993) ~~RADAR data~~ and field observations indicated that rain was still falling over portions of the path between the two instruments. Note that the liquid optical depths did not return to zero before the next heavier rain shower began around 17:15.

Between 16:28 and 16:31, a cloud advected through the observation path. Field notes and images taken every 30 seconds show a cloud moving into and through the field of view. Initially the cloud extended only part way across the observation path. It then apparently spanned the entire path for a brief period of less than 2 minutes before gradually clearing out of the observation path. The presence of smaller cloud droplets caused the 198.5 GHz liquid optical depth to increase around 16~~4~~:30, while little if any change was apparent in the 24.4 GHz liquid optical depth. The fact that the 24.4 GHz optical depth did not drop to 0 indicates some light rain was present as well. The decrease in 198.5 GHz liquid optical depth after the peak at 16~~4~~:30 likely indicates that cloud droplets or drizzle obscured only part of the observation path.

Signal Tuning and Detection

The High~~-~~Band portion of the ATOMMS ground-based prototype instrument simultaneously transmits and receives two continuous wave signals that are tunable from 181 to 206 GHz. For this mountaintop experiment, the frequency of the signal generated by one transmitter was swept through a tuning sequence that spanned the instrument's tunable frequency range. This signal was received by a narrowband heterodyne receiver whose second local oscillator was simultaneously swept through its matching tuning sequence. The frequency of the other signal ~~swept through the tunable frequency range generating a tuned tone that was received by a receiver sweeping through the same tuning sequence. The other tone~~ was fixed at 198.5 GHz in order to function as the amplitude calibration signal for measuring differential absorption. ~~calibration tone.~~ There were frequencies in the sweep, separated by 0.25 GHz, except for a gap between 191.5 and 193.5 GHz. This gap is due to the limited receiver response for Intermediate Frequencies (IF) less than one GHz and the first stage local oscillator (LO) being set to 192.5 GHz.

~~This is likely the finest spectral resolution sampling of the 183 GHz line ever achieved in the field.~~ When executing sequence for 100 ms before moving to the next frequency in the sequence. ~~The dwell time for each frequency of the tuned~~ synchronized using GPS receivers. Each received ATOMMS signal was filtered, down converted in frequency, digitized and recorded. The signal frequency in the final receiver stage ranged from 8 to 35 kHz for each of the 122 tuned frequencies. The frequency and power of the down-converted signals were determined using a Fast Fourier Transform (FFT), calculated over a 50 ms integration time. The reason that only half of the 100 ms tuning dwell time was used was to allow time for each synthesizer tune to settle. Each FFT-derived signal power estimate was then converted to an amplitude by taking the square root. The calibration signal amplitudes were computed using the same method. ~~The frequency and power of the down converted~~

One sweep through the frequency tuning sequence ~~of the frequencies~~ took 12.2 seconds. The instrument cycled combinations of the two transmitters and two receivers before repeating the tuning cycle in order to help isolate any transmitter or receiver issues. Thus, a full tuning cycle was completed every 48.8 s. The observations from the four combinations of transmitter-receiver pairs were then averaged together such that new estimates for the ATOMMS signal amplitude ratios at all of the 122 tuning frequencies were generated ~~different transmit-receive pairs were averaged together to yield new estimates~~ the signal amplitude and frequency for each of the 122 frequencies in the tuning sequence ~~for each particular tuned frequency~~

4. Interpretation of Measurements

ATOMMS observations of R, defined in Eq. (2), are sensitive to *changes* in the integrated water vapor along the path between the instruments. The retrieval algorithm discussed below determines changes in water vapor pressure relative to a reference period. We selected two reference periods that are identified in Fig. 2. The first period spanned 2:23 to 2:31 PM, shortly after data acquisition began, and the second spanned 4:51 to 4:56 PM, approximately 2.5 hours later. These are periods of relatively constant amplitude spectra due to relatively constant vapor pressure and temperature and relatively low optical depth, which maximizes the number of usable frequencies nearest line center. Comparing solutions derived using the two different reference periods provides some assessment of instrumental drift.

The retrieval algorithm determines the change in vapor pressure relative to the reference period by finding the best forward-calculated fit to each observed ATOMMS amplitude ratio spectrum (Eq. 2) using a least squares method. To forward model the clear sky atmospheric attenuation, we used an atmospheric propagation tool known as the Atmospheric Model (am), version 7.2 (Paine, 2011), which we will refer to as *am7.2*. This model ~~the *am* Atmospheric Model, version 7.2 [*Paine*, 2011] which~~ was shown to fit the ATOMMS measurements to the 0.3% level in previous work with the ground-based ATOMMS prototype system (~~[~~Kursinski et al., 2012)~~]~~. In operation, the ATOMMS ratio, R in Eq. (2), is determined from measurements at times, t and t_0, for a range of frequencies, f, which produces a frequency spectrum of the ratio. In forward calculations of

Eq. (2), we assume that the vapor pressure, air temperature, and air pressure are known at the reference time, t_0, and the air pressure and temperature are known at time, t. The solution is determined by finding the change in vapor pressure from the reference value that provides the best least squares fit between the forward-calculated and observed ATOMMS ratio spectra. During this experiment, we were able to accurately determine signal amplitudes up to total optical depths due to gas plus liquid water of 17.

For the purposes of determining the average water vapor along the path, we used 15 tuning frequencies spanning 187.861 GHz to 191.361 GHz to make the water vapor retrievals. Since the greatest sensitivity to changes in vapor pressure occurs at line center, it is desirable to utilize frequencies as close to line center as possible. For this field test, tuning tones with frequencies lower than 187.861 GHz were too attenuated to be measured accurately even during clear skies. During periods of lighter rain and clouds, the additional attenuation by liquid water caused the retrieval frequencies nearest line center to become too opaque to measure accurately, reducing the number of frequencies available for the fit. The liquid optical depth in Fig. 2 is the liquid optical depth measured by the calibration signal~~at the calibration tone~~, f_{CAL} = 198.5 GHz. The liquid optical depth subtracting the forward-calculated change in gaseous extinction relative to the reference period from the observed change in optical depth relative to the reference period, which includes changes in both liquid and gaseous extinction. During the heaviest rain period, none of the High-~~-~~Band signals could be measured due to strong liquid attenuation.

The retrieved path-averaged vapor pressure between the instruments is shown in Fig. 3A. The figure shows 12 different solutions that were used to estimate the random uncertainty in the retrieval of vapor pressure. The methodology used to compute the 12 solutions is described in Section 5.~~The figure shows 12 different solutions that were used to estimate the random uncertainty in the retrieval of vapor pressure as described in Section 5~~. The half range of the 12 solutions shown in Fig. 3B is generally less than 0.1 hPa. Most of the fractional uncertainties are well below 1% of the vapor pressure, indicating that the solution is highly constrained by the observations. The path averaged vapor pressure varied from 10.2 to 16.5 hPa over the nearly four hour observation period. The measured vapor pressure peaked in association with the rainy period before 15:00. Following that rain shower, there was a brief intrusion of drier air centered near 15:15 before the vapor pressure rapidly increased prior to the thunderstorm at 15:30. Immediately following the heavy rain after reacquisition of the High-~~-~~Band signals, the vapor pressure dropped to its lowest value. In Section 6~~5~~ we note that similar advection of dry air following summertime thunderstorms in this region have been observed in previously published work (Kursinski et al., 2008) and show that our estimation of the minimum vapor pressure was consistent with the nearby radiosonde observations from Tucson. During the brief cloud passage at 16:30, there was a sharp increase and peak in the vapor pressure that brought the relative humidity up to approximately 100%. The vapor pressure fell sharply following the passage of the cloud. There was one more peak in vapor pressure at 17:00 before the sharp rise associated with the rain that began at 17:30.

Determining temperature

Retrieving changes in water vapor versus time from the measured absorption spectra requires knowledge of atmospheric temperature and pressure. In the eventual LEO-LEO occultation measurements, ATOMMS will profile both the atmospheric Doppler shift and attenuation of the occulted signals, from which profiles of temperature, pressure and water vapor will be derived (~~[~~Kursinski et al., 2002)~~]~~. In the static mountaintop-to-mountaintop geometry, there is no Doppler shift and only the attenuation portion of the ATOMMS measurements is available. Pressure was determined using barometers on each mountaintop. Determining the atmospheric temperature along the signal path was more challenging.

During this experiment, three nearby thermometers measured the surface air temperature. An Arduino weather station was located next to each ATOMMS instrument and an automated weather station was located in the town of Summerhaven, about 300 m below Mt. Lemmon and 700 m to the north. Unfortunately, these surface temperature observations were not entirely representative of the air temperature aloft along the ATOMMS signal path because of their close proximity to the surface and a high bias in the Arduino temperatures due to heat generated by the ATOMMS instrumentation inside the protective tents.

To better estimate the temperature along the signal path, we derived the average air temperature along the path from the pressure scale height using the hypsometric equation and time-varying barometric pressure measured at the two ATOMMS instruments

$$\overline{T_V} = \frac{g\Delta Z}{R_d}\left[\ln\left(\frac{P_{Big}}{P_{Lem}}\right)\right]^{-1} \qquad (5)$$

where g is gravitational acceleration, ΔZ is the altitude difference between Mt. Lemmon and Mt. Bigelow, R_d is the gas constant for dry air, P_{Big} and P_{Lem} are the measured air pressures on Mt. Bigelow and Mt. Lemmon respectively, and $\overline{T_V}$ is the layer mean virtual temperature. ~~The uncertainty associated with this temperature estimation is discussed in Section 5. ~~The air

While Eq. (5) ideally provides the desired layer mean temperature needed for spectral calculations of R, there are issues with this approach. The sensitivity of Eq. (5) to small dynamic pressure variations made short term temperature estimates noisy. The horizontal separation between Mt. Lemmon and Mt. Bigelow caused the estimated temperature to be sensitive to propagating pressure perturbations. Finally, the assumption of hydrostatic balance in Eq. (5) is not true during thunderstorm activity. To alleviate these issues, we used a one hour running mean of the air pressure.

Temperatures derived in this manner are biased by small biases in barometric pressure. To minimize this bias, we shifted the entire temperature time series by 2.15 K so that the relative humidity was 100% at 16:30, when the cloud was present. Figure 4 shows the derived air temperature between the instruments that was used in the retrievals in black, as well as the nearby, in-situ thermometer observations, which are shown in red, green, and blue. The uncertainty associated with this temperature estimation is discussed in Section 5.

Water vapor spectra

Figure 5 shows four examples of fitted ATOMMS ratio spectra. The outstanding agreement between the measured and modeled spectra is immediately evident in that most of the individual ATOMMS amplitude ratio spectra fall within ±0.15 hPa (which is ±1%) of the calculated spectra. This is true for most of the individual retrievals.

Figure 5A shows a retrieval made during the clear period around 15:08, following the first rain period. All 15 frequencies spanning 187.861 to 191.361 GHz were available and closely fit the forward-calculated ATOMMS ratio. Figure 5B shows a retrieval made during the first rain period at 14:51. While the two frequencies nearest line center were lost due to the increase in optical depth caused by rain, the remaining 13 ATOMMS frequencies yielded accurate vapor pressure retrievals during the rain.

Panels C and D of Fig. 5 show retrievals made at 16:29, during the cloudy period. The solution in Panel C uses the first reference period while the solution in Panel D uses the second reference period, which is closer to the time of the cloudy period. The difference between the shape of the ATOMMS ratio spectrum in Fig. 5C and 5D is due to the use of the two different reference periods, which changes the amplitude ratio in the denominator of Eq. (2). The increased liquid optical depth due to the cloud eliminated the three frequencies nearest line center. Although scatter about the best fit forward calculation line is larger than that in Panels A and B, the fitted forward calculations constrain the water vapor solution quite well, despite the presence of the cloud and some light rain. The better fit that results when using the second reference period indicates that there was some subtle instrumental drift over the 2.5 hours between reference periods. Near the cloud peak, the Reference 1 water vapor solutions are greater than the Reference 2 solutions by only 0.03 hPa (0.2%), indicating the level of robustness of these vapor pressure retrievals.

5. Sources of Uncertainty and Validation of Results

There are a number of sources of uncertainty in the ATOMMS mountaintop water vapor retrievals that include

(1) Measurement errors including signal-~~–~~to-~~–~~noise-~~–~~ratio (SNR) and instrument drift,
(2) Undesired environmental effects such as scintillations due to turbulence,
(3) Errors in modeling including gaseous spectroscopy and particulate scattering,
(4) Biases due to errors in the reference period air temperature and water vapor estimates, and
(5) Errors in the estimated time varying, path-averaged, air temperature
(6) Uncertainty in spectral fitting

In terms of measurement errors (Category 1), the high SNR that enabled penetration and water vapor retrievals up to optical depths of 17 is not a significant source of error, except, of course, when optical depths exceeded 17 and became impenetrable. As noted, we did see signs of subtle instrument drift over approximately 2.5 hours, which is 9,000 seconds, ~~–~~that shifted the retrieved water vapor amount by 0.2%. However, because the duration of a LEO occultation is only about 100 seconds, errors due to instrument drift in LEO should be very small.

Turbulence-induced amplitude scintillations (Category 2) were quite significant during the periods of strong convection. These were reduced by almost an order of magnitude via amplitude ratioing with the calibration ~~tone~~ signal (~~[~~Kursinski et al., 2016b)~~]~~. The strong peaks near 14.6 hours in Fig. 3B are caused by momentary noise in the calibration which influences the frequency ratioing. Outside of this peak the largest fractional uncertainty is about 1.8% of the vapor pressure (green line). We attribute most of this to turbulent-induced scintillations that remain after the frequency ratioing. Thus, for the conditions of this field experiment, the upper bound for the random error in the vapor pressure retrieval due to turbulence is about 1.8% of the vapor pressure. ~~Residual amplitude scintillations may be the largest source of random error in the least square fits.~~

In terms of spectroscopic errors (Category 3), we again note that ATOMMS is itself a very high spectral resolution spectrometer such that the ATOMMS data can be used to refine the spectroscopic models and make them as accurate as the ATOMMS observations. Along these lines, we also note that in order to diagnose and reduce spectroscopic errors, Kursinski et al. (2009) recommended increasing the required number of Low-Band signals from 4 to 5 to make the solutions systematically over-determined in order to identify systematic errors in spectroscopic models and then refine those models.

Errors in the reference period temperature and water vapor estimates (Category 4) create unknown biases in our mountaintop estimates. These biases are not relevant to the eventual LEO system because, in the LEO-LEO occultation geometry, the reference period occurs when the signal path is above the detectable atmosphere where the atmospheric density is essentially zero.

The primary cause of temperature-related uncertainty is in the *change* in temperature between the reference period and the observation time (category 5). Errors in the absolute temperature are relatively insignificant, i.e., temperature biases are not a significant source of uncertainty in the water vapor retrievals in comparison to errors in estimating the change in temperature relative to the reference periods. For the conditions of this particular experiment, based on forward calculations made with *am7.2* for the range of temperature and vapor pressure conditions observed during the experiment~~based on the~~ of the change in derived water vapor due to a temperature change relative to the reference period temperature was approximately -0.17 hPa/°C. Examples of the sensitivity of the ATOMMS ratio, Eq. (2), to changes in vapor pressure, ~~and~~ ~~and~~ temperature, and air pressure relative to the reference conditions for this experiment are shown in Fig. 6. The figure plots forward-computed ATOMMS ratio spectrum for four ~~three~~ different changes relative to the reference conditions. For the of the field experiment, we were able to measure amplitudes for signal frequencies of 187.861 GHz and higher. Lower frequencies closer to line center were too attenuated to track. The figure shows the change in the ATOMMS ratio spectrum resulting from a change in air pressure of 10 hPa, which is much larger than the +2 hPa changes in air pressure that were observed during the experiment. Therefore, the sensitivity of the ATOMMS ratio to changes in air pressure is quite small relative to changes in vapor pressure. As the figure shows, for frequencies greater than 187.861 GHz, a one hPa decrease in vapor pressure produced approximately the same ATOMMS amplitude ratio spectrum as a 5.9° C increase in air temperature Larger changes in vapor pressure, such as the -3 hPa line in the figure, are easily distinguished from changes in air temperature.

was less than 3°C, which places an upper bound of a 0.5 hPa water vapor uncertainty due to the temperature uncertainty.

The misfit between the measured ATOMMS amplitude spectral ratios and the forward calculation of those spectral ratios (category 6) are sensitive to all of the error types noted above. To understand and characterize the robustness in the spectral fits, we varied the number of frequencies used in the fits. The baseline retrieval utilized the amplitudes of the 15 signals whose frequencies range from 187.861 to 191.361 GHz. Five additional retrievals were implemented using different subsets of these 15 frequencies. Specifically these subsets were the 10 lowest frequencies, the 10 highest frequencies, the 5 lowest frequencies, the 5 middle frequencies, and the 5 highest frequencies within the 187.861 to 191.361 GHz frequency range. We also ran the same 6 cases using the second reference period. The same temperature versus time was used for all 12 cases.

Figure 3A shows the resulting 12 solutions. The blue line in Fig. 3B shows the spread across the 12 retrievals, defined as the maximum minus the minimum vapor pressure divided by two. This half range represents a conservative estimate of the random uncertainty of the retrieved vapor pressure changes that includes both measurement and *am7.2* modeling errors~~am~~ average half range is 0.077 hPa which corresponds to a fractional uncertainty of approximately 0.6%. This small spread across the 12 cases indicates that instrument drift over the four hour observational period was quite small and that the ATOMMS spectral observations tightly constrained the vapor pressure with little ambiguity over a wide range of clear, cloudy and rainy conditions in optical depths up to 17.

The amplitude ratio in Eq. (2) reduces common mode sources of error and uncertainty. Ratioing of the amplitudes of two signals, as was done here, eliminates the effects of liquid particle extinction to the extent that the liquid extinction is spectrally flat over the ATOMMS tuning range and calibration frequencies. For raindrop-sized spheres of water, Mie theory predicts that the mm wavelength spectrum of extinction is nearly flat. For smaller cloud droplets, Mie theory combined with the dielectric model of liquid water indicate that the mm (and cm) wavelength extinction increases approximately linearly with frequency due to absorption by liquid water. Near 16:30, the passage of a cloud between the mountaintops coincided with an increase in the 198.5 GHz extinction but no increase in the 24.4 GHz extinction, indicating the presence of very small particles along the path. We adjusted the retrieval algorithm to account for this expected cloud droplet spectral dependence over the High-~~-~~Band frequency range which caused the retrieved vapor pressure to increase by 0.8%. The increase was necessary to compensate for the slight spectral variation in liquid water attenuation that resulted from using the Mie cloud model (Bohren and Huffman, 1983). Surprisingly, the spectral misfit to the ATOMMS observations increased slightly. The reason is not clear.

This small 0.8% change in the retrieved vapor pressure provides some indication of how effective the calibration ~~tone tone~~ signal ratioing is in minimizing the sensitivity of the ATOMMS water vapor retrievals to hydrometeors. In the future, High-~~-~~Band system will have 4 rather than its present 2 ~~tones~~ signals in order to place calibration signals ~~tones~~ on both the low frequency sides of the 183 GHz water vapor line to reveal and compensate for any overall spectral tilt caused by particle extinction as well as other effects. This should greatly reduce cloud ambiguity in the 183 GHz based water vapor retrievals.

6. Validation against in-situ measurements

In previously published work, we demonstrated the ability of the ATOMMS prototype system to accurately retrieve changes in water vapor along a relatively short 820 m path across the University of Arizona campus in clear conditions. In that experiment, the atmosphere was well mixed and nearly homogeneous along the observation path such that the retrieved changes in water vapor from ATOMMS matched those observed with an in situ sensor near one end of the path to 1-2% (~~[~~Kursinski et al., 2012)~~]~~. Based on these results, our intent had been to validate these ATOMMS moisture retrievals in the presence of clouds and rain via comparison with independent, in-situ moisture measurements analogous to the ~1% validation of clear sky ATOMMS retrievals along a shorter path demonstrated by Kursinski et al. (~~[~~2012)~~]~~. However, we came to realize that quantitative validation of the ATOMMS water vapor retrievals for this mountaintop experiment was limited by the substantial spatial inhomogeneity of the moisture field itself associated with a longer path, over mountainous terrain, during thunderstorm activity. The large variations of water vapor produced by the turbulent, moist, convective activity limited the level of agreement between the several in-situ sensors.

The spatial inhomogeneity of the water vapor field is evident in Fig. 7, which shows that ATOMMS water vapor retrieval and observations from three nearby in-situ sensors as well as the measurement from the Tucson radiosonde at the altitude of the ATOMMS experiment. The differences between the in-situ sensors are indicative of the magnitude of moisture variations along the 5.4 km path. The observation geometry in Fig. 1, shows that the ATOMMS-derived vapor pressure is an average over the 5.4 km path that runs above a valley between the mountaintops on which the instruments sit. The High-Band transmitter was located at the position marked and labeled as "Physics/Atmos bldg Radio Ridge" at an altitude of 2752 m and the High-Band receiver was located at the position marked and labeled as "Catalina Station Steward Observatory" at an altitude of 2515 m. In-situ sensors were located on the ground at the two instrument sites, with another at the location marked and labeled as "Summerhaven," which is about 830 m from the observation path in a valley at an elevation of 2439 m~~, while in-~~

The spatial variability of the water vapor during this experiment was large. A measure of the water vapor variability over the 5.4 km observation path is provided by computing the root mean square (RMS) differences for the three available in-situ sensors during the experiment, namely the two sensors at each end of the observation path and data from a sensor in the town of Summerhaven in the valley below the observation path. The RMS of the differences between the three in-situ sensors and the ATOMMS derived water vapor was approximately 8% during the period from 14:00 to 15:30, which preceded the first heavy rain period. Water vapor variations during the most active convective periods were likely larger. In the appendix, we discuss the difficulty and very high (prohibitive?) cost of designing and employing an in-situ observational network capable of verifying the ATOMMS retrievals for the conditions encountered during this experiment.

Cross correlations

Despite the inherent differences in the horizontal averaging of ATOMMS and the in-situ instruments, there is substantial cross-correlation between these water vapor measurements. We show this by examining the correlation between the ATOMMS-retrieved path-average water vapor and the in-situ water vapor sensor located on Mt. Bigelow. Figure 8A shows the ATOMMS retrieval for the path averaged vapor pressure in blue and the measured vapor pressure from the in-situ sensor on Mt. Bigelow in red. Substantial cross correlation is clearly evident between the two data sets. The other colored lines in Fig. 8A show time-shifted segments of the in-situ observations, as described below, that make the correlation between the datasets more visually apparent. In order to demonstrate and quantify the cross correlation between the ATOMMS-derived vapor pressure and the in-situ observations, we separated the datasets into several different time segments because the time lag between the two observations of water vapor varies as the wind conditions change. We discuss four particular time segments defined as follows

(1) 14.06 to 14.79 hours, which is approximately the first 45 minutes of data collection;
(2) 14.99 to 15.49 hours, which is the period leading up to the first heavy rain period when the ATOMMS High ~~-~~Band signals became too attenuated to track;
(3) 16.00 to 16.42 hours, which is the period when the High ~~-~~Band signals reappeared following the heavy rain; and
(4) 16.75 to 17.39 hours, which is the period immediately following the cloudy period.

Figure 8B shows the correlation coefficients as a function of sample time lag. Consecutive ATOMMS samples are separated by 48.8 s. The peak cross correlation coefficients range from 0.78 to 0.97, which indicate strong correlation between the ATOMMS-derived water vapor pressure and the in-situ observations of water vapor pressure on Mt Bigelow. Positive lags indicate periods when ATOMMS observed water vapor variations occurred earlier than those variations in the in-situ observations on Mt Bigelow. Although the winds were occasionally gusty, with variable direction due to shower and thunderstorm activity, there were two systematic shifts in the prevailing wind direction observed in the field: a shift from W to NNW around 15:48 and a shift from NNW to ENE around 16:55. These wind shifts were observed both from the motion of clouds in sequences of web camera images taken from Mt Bigelow and by the Tucson WSR-88D radar (Crum and Alberty, 1993). ~~RADAR.~~ The ATOMMS instruments were oriented along a NE to SW direction, with Mt. Bigelow on the SW end (Fig. 1). Figure 8B indicates that the first three time segments had positive lags, while the last time segment had a negative lag. This is consistent with our wind observations, in which the wind direction had a component from the observation path toward Mt. Bigelow for the first three time periods, and from Mt. Bigelow to the observation path for the fourth time period.

Moist bias in *in situ* sensor sampling

Another issue in validating the ATOMMS water vapor retrievals against the in-situ sensor results is a moist bias in the ground measurements relative to the overlying air after the period of heavy rain. The bias is due to evaporation from the wet surface moistening the near-surface air, which is the air whose properties are measured by the in-situ sensors. As a result, with the exception of the cloud around 16:30, the retrieved ATOMMS water vapor amounts over the 80 minutes following the heavy rain were systematically lower than the surface measurements. This continued until approximately 17:20 when the steady increase in water vapor and rain began and continued through the end of the experiment. The largest differences occurred shortly after the most intense rain, when ATOMMS measured a vapor pressure of 10.2 hPa, the smallest of the entire experiment. This value is approximately 25% lower than water vapor measured at the surface stations. Such behavior where moisture at the surface varies little while air aloft becomes significantly drier following summertime thunderstorms is common in this region (e.g., Fig. 4 in Kursinski et al. (~~[~~2008)~~]~~). It is also common in the Amazon (e.g., Fig. 7 in Schiro et al., 2016) and may be associated with mid-level inflow of drier air into the precipitating region that results in evaporative cooling and descent of this air (e.g., Leary, 1980 and Houze, 2004).

For the period of relatively dry air following the cloud, the 00 UTC~~Z~~ Tucson radiosonde profile provides perhaps the best validation of the ATOMMS results. The sonde launched between 16:30 and 16:45 from a location about 28 km southwest ~~20 km south~~ of the experiment and ascended through the Mt. Bigelow to Mt. Lemmon altitude interval between 16:35 and location approximately 20 km south of the observation path. According to the sonde, the average vapor pressure in the layer between Mt. Bigelow and Mt. Lemmon was about 12.3 hPa which is within a few percent of the ATOMMS water vapor retrievals following the cloud's passage. We also note that moisture concentrations measured on Mt. Lemmon decreased steadily through this period reaching a minimum of 12.7 hPa at 17:25, a value essentially identical to the ATOMMS moisture retrieval at this time (Fig. 7). This decrease, despite the evaporative moistening from the wet surface, suggests that dry air was indeed advecting over Mt. Lemmon. Thus, the combination of the sonde profile, the ATOMMS measurements and Mt Lemmon surface measurements all indicate passage of a relatively dry, horizontally extended, air layer following the heavy rain.

Further examination of the operational sonde profiles launched in Tucson that morning around 4:30 AM and particularly that afternoon, around 4:30 PM, provide additional clues as to what happened that afternoon. Figure 9 shows the specific humidity and potential temperature calculated from the Tucson August 19, 00 UTC sonde for the lowest 3000 m above Tucson. The green hatched region shows the altitude interval across the ATOMMS observation path. In the afternoon sonde profile, the potential temperature, θ, and specific humidity, q, are nearly constant between the surface and 2300 m above sea level (msl), indicating that the boundary layer (BL) near 16:30 local time extended to about 2300 msl. In contrast, cloud base at 3150 msl where the dew point equals the temperature in the sonde profile, and the 500 m near-adiabatic layer immediately below it, further indicate that earlier in the afternoon, the well mixed, dry adiabatic, sub-cloud BL very probably extended up to 3150 msl. Between 2300 and 2750 msl is a thermal inversion layer that is noticeably drier than the air immediately above and below it. The ATOMMS measurements were made within this altitude interval. The relatively low moisture concentrations in this layer measured by both ATOMMS and the afternoon sonde combined with the fact that the θ of this inversion layer is lower than the θ of the peak afternoon BL indicates this air was likely cooled diabatically by evaporation of precipitation falling through it during the turbulent period of heavy rain. The net effect of this process was to increase the q and reduce the θ of this air, causing it to descend from a higher altitude to where it was measured by ATOMMS. Similarly, the fact that the θ of the late afternoon boundary layer below the ATOMMS layer, is 2.5 K lower than that of the peak afternoon BL also indicates that that air has also been evaporative cooled and descended as a result. Such evaporative cooling and descent and moistening of dry air layers is a well-known feature of squall lines (e.g., Houze, 2004) and cause microbursts which are well known in Arizona (e.g. Willingham et al., 2010). Further understanding of the details of what happened that afternoon will require detailed modeling with a convection resolving model, which is beyond the scope of the present research.

7. Discussion

The results of this ATOMMS field test demonstrate that the differential absorption concept using an active microwave spectrometer works very well, yielding performance consistent with theoretical expectations that is well beyond the capabilities and performance of passive radiometers. Using a prototype ATOMMS instrument we developed~~ with funding from NSF~~, we measured differential absorption spectra and then forward modeled those spectra, achieving better than 1% agreement, through clear air, clouds and rain to determine the changes in the path-averaged water vapor pressure between the ATOMMS instruments. We demonstrated water vapor retrievals made during cloudy and rainy periods that were only slightly noisier than those made during clear sky periods. Accurate retrievals of water vapor pressure were made through optical depths up to 17, thus demonstrating the exceptionally wide dynamic range achievable via the differential absorption approach. The fact that this performance was achieved under turbulent conditions associated with intense, local thunderstorms also indicates the effectiveness of the differential approach in reducing the impact of turbulence.

While the variable, turbulent conditions associated with convective activity together with passing clouds and rain provided an excellent test of the ATOMMS system's ability to function and perform in very challenging conditions, it also limited the level of validation that could be achieved against in-situ surface sensors. The disagreement amongst the three nearby in-situ sensors revealed the substantial inhomogeneity in the water vapor field in the vicinity of the 5.4 km observation path. Prior to the first heavy rain period, the RMS of the differences between the in-situ sensors was approximately 8%, which set an upper bound to which the ATOMMS retrieved changes in water vapor pressure could be validated by the in-situ sensors. It is also important to note that ATOMMS measured the change in the *path-averaged* vapor pressure which will differ somewhat from point measurements along the path with a magnitude that depends on the inhomogeneity of the water vapor along the path.

During the period following the heavy rain, the ATOMMS measurements revealed systematically drier conditions than the nearby in-situ sensors. These differences were likely due to the fact that the in situ sensors were located at the surface while the path between the ATOMMS instruments was aloft. As a result, the in-situ sensors measured the humidity of air moistened by evaporation from the rain soaked surface, while ATOMMS measured the humidity of air aloft above the valley between the two instruments. The nearby Tucson radiosonde indeed indicated that, following the thunderstorm, a layer of drier air passed through the area. Thus, direct validation the ATOMMS retrievals against the in-situ sensors was limited to about 8%. In the appendix we discuss why it would have been extremely difficult to validate our retrievals at the 1% level with in-situ observations for the conditions encountered during this field experiment.

The better than 1% agreement achieved between the measured ATOMMS spectra and a forward microwave propagation model was substantially better than the comparisons with in situ sensors and indicates the very small level of uncertainty associated with the changes in water vapor that ATOMMS measured. Despite our varying both the combinations of signal frequencies used in the retrievals and the reference times, the agreement remained better than 1%, indicating that there is simply very little ambiguity in the retrievals of changes in the path-averaged vapor pressure. This essentially brings laboratory-quality measurements out into the field, a very desirable and sought-after property of any measurement system.

In terms of the number of signal frequencies required to accurately determine the water vapor, we used between ~~from~~ and ~~to~~ 15 tuned signal frequencies plus a calibration signal at a fixed frequency ~~frequency~~ for the water vapor spectral fits. and consistency of these results indicate that the amplitudes from just a few tuned frequencies and a fixed frequency amplitude calibration signal ~~calibration frequency~~ are needed to produce water vapor retrievals with very small random and absolute note that the spectral sweeps used in the mountaintop experiment were intentionally finely spaced in frequency, and therefore slow as well as redundant in order to assess instrument performance, the absorption and scattering spectra and the performance of the retrievals. Faster spectral sampling, as required for LEO-LEO occultations, is readily achievable using a combination of faster switching synthesizers and a smaller number of frequencies to sample the spectrum.

These field measurements of attenuation made near the 183 GHz water vapor absorption line in the presence of rain and liquid clouds enabled us to assess the attenuation due to liquid hydrometeors and the ambiguities associated with them. In terms of *raindrop-sized* liquid hydrometeors, Mie theory predicts that their attenuation across the 183 GHz band has little dependence on signal frequency. As a result, the attenuation due to rain largely ratioed out when we applied the differential absorption technique to determine the changes in water vapor. According to Mie theory, the attenuation of *cloud droplet-sized* liquid hydrometeors in the 183 GHz band has a spectral dependence that increases approximately linearly with frequency. However, when we accounted for this anticipated dependence, the fit between the observations and forward calculations from a microwave propagation model became slightly worse. The reasons for this are as yet unclear.

In the eventual LEO configuration, the ATOMMS signals will encounter a wider range of hydrometeors and spectral dependencies across both the High and Low-Band frequency bands. For example, the 183 GHz band will profile water vapor at high altitudes through ice clouds that will attenuate the signals via Rayleigh scattering which depends approximately on the fourth power of the signal frequency~~ to the fourth power~~. The LEO version of ATOMMS will provide the information necessary to observe and account for such non-vapor effects using at least three simultaneous signal frequencies to place amplitude calibration signals ~~calibration tones~~ on both the low and high sides of the absorption line and the third frequency on altitudes where most *liquid* hydrometeors are encountered, observations in the 22 GHz band will be used to make water vapor retrievals. The liquid water absorption spectrum across the L~~l~~ow-B~~ b~~and frequencies is generally more complex than the ice particle scattering across the H~~h~~igh-B~~ b~~and frequencies. Thus, in order to separate the water vapor absorption from the cloud liquid water absorption, we must observe the amplitudes from at least four L~~l~~ow-B~~ b~~and frequencies, with at least one of the signal frequencies on the high frequency side of the 22 GHz absorption line, since the liquid water absorption increases with frequency across the entire low frequency band, while the water vapor absorption is greatest at line center and will have the opposite frequency dependence on the high frequency side of the line. Under clear sky conditions, measurements of three to four simultaneously frequencies will allow evaluation and possibly refinement of the spectroscopy of the 22 and 183 GHz water lines. At least one additional frequency would be required to evaluate and improve spectroscopy when clouds are present.

The ability of ATOMMS signals to penetrate though optical depths up to 17 demonstrated here (which would have reached 19 with more stable synthesizers) and retrieve water vapor to 1% under a wide range of atmospheric conditions ranging from clear to cloudy to rain is well beyond the capability of radiometric systems whose penetration is typically limited to optical depths around unity. This large dynamic range allows ATOMMS to retrieve water vapor from the mesosphere into the lower troposphere as its concentration varies by many orders of magnitude. It is also necessary to be able to retrieve water vapor when there is increased attenuation from clouds. The stronger 183 GHz line is used at higher altitudes and the weaker 22 GHz line is used at lower altitudes. A design goal for ATOMMS is to have sufficient dynamic range to achieve a large vertical overlap of the High and Low-~~-~~Band measurements and retrieved profiles. A vertical overlap will provide a valuable crosscheck since the errors in the Low-~~-~~Band and High-~~-~~Band systems will be largely independent. The two bands will have different dependencies and sensitivities to turbulence and spectroscopic uncertainty. In the vertical overlap region the observable High-~~-~~Band frequencies will be far from line center, while the information from the Low-~~-~~Band signals will be from frequencies closer to line center.

A fundamental goal for weather and climate monitoring, prediction and understanding is all-weather unbiased global sampling. IR systems have substantial biases in their coverage due to the limited ability of IR photons to penetrate through clouds (~~[~~e.g., Hearty et al., 2013)~~]~~ and its ~2 km vertical resolution is poor in comparison to the verticals scales at which water varies in the atmosphere. While downward-viewing passive microwave systems penetrate through clouds, their vertical resolution is very coarse and their retrievals over land are significantly less accurate than over oceans. GPS RO does provide unbiased global coverage, but is limited by the inability to separate the wet and dry gas contributions to the index of refraction.

Given this present situation, ATOMMS' precise, all-weather retrieval capability, as demonstrated here, would achieve ~~offers~~ a major advance in remote sensing of the atmosphere. These results support the prediction that an ATOMMS system in LEO would be a major advance toward achieving the fundamental satellite observing system goals of very high vertical resolution, all-weather temperature and water vapor sounding with very small random and absolute uncertainties, across the entire globe in support of weather prediction, climate monitoring and the quantitative constraints on process needed to improve models. A mission design concept using a constellation of very small ATOMMS satellites using cubesat technology is given in Kursinski et al., 2016b. ATOMMS has the potential to provide global observations from space that approach, and in some ways exceed, the performance of sondes.

Appendix A: In-Situ Observational Network Required for Validation of ATOMMS Retrievals

We now discuss the question regarding the quality, quantity and spacing of in-situ observations that would be required to validate the ATOMMS retrievals of changes in vapor pressure with time, which we believe are accurate to within 1%. Chilled mirror hygrometers can reach accuracies of 1%, at least in the laboratory. However, when we discussed validating ATOMMS instruments to 1% with a chilled mirror hygrometer expert at NCAR, we were told that no in-situ measurements can reliably achieve 1% accuracy out in the field (Holger Vömel, personal communication). ~~Holger Vömel, a chilled mirror hygrometer expert at NCAR, he indicated that no in-situ measurements can reliably achieve 1% accuracy out in the field.~~ Chilled mirrors are also expensive. We purchased one for $9000 and even the less accurate miniature ones used on balloons are more than $1000 apiece. Therefore, while a series of chilled mirrors could be placed along the path, their accuracy might not be as good as required to achieve 1%. They would likely be the closest to 1% that is available.

The next consideration is how to satisfy the constraints imposed by the ATOMMS measurements which include (1) a raised observational path between the instruments sufficiently high above the ground surface to avoid surface reflections and (2) a sufficiently long path length to produce enough absorption to enable precise and accurate water vapor retrievals. To avoid contamination of the water vapor observations by the ground surface, the in-situ sensors must be located well above the surface (~50 m) and close to the signal path, but not so close that they interfere with the ATOMMS signal transmission.

Given the variability of the water vapor along the path, the next question is how closely must the in-situ instruments be spaced along the signal path to achieve a specified level of accuracy.~~?~~ We estimated the water vapor variability over the 5.4 km observation path by computing the root mean square (RMS) differences for the three available in-situ sensors during the experiment, namely the two sensors at each end of the observation path and data from a sensor in the town of Summerhaven in the valley below the observation path. The RMS of the differences between the three in-situ sensors and the ATOMMS measurements was approximately 8% during the period from 14:00 to 15:30, which preceded the first period of heavy rain.

To determine how many in-situ sensors would be required to achieve 1% agreement, we turn to the results of Otarola et al. (2011) who used aircraft measurements to determine how the ratio of the standard deviation of humidity point measurements divided by the path averaged humidity varies with the path length over which the point measurements are averaged. The Otarola et al. (2011) findings are shown in Fig. A1. The straight line segments in the figure represent power law type behavior. The power law exponent of the lines of std(q)/mean(q) in Figure 9 that pass near the point of stdev/mean = 8% for a path of 5 km is approximately 0.35. Given this power-law exponent and the requirement to keep uncertainties smaller than 1%, the path length required to achieve std(q)/mean(q) = 1% is approximately 10~~13~~ m. This result is shown graphically in Fig. A1 by the dashed blue line that passes through the ATOMMS conditions of stdev/mean = 8% for a path of 5 km.

Thus, in situ sensors, accurate to 1% each, would need to be placed every 10~~13~~ m along a 5.4 km path to achieve an situ-based path average consistent with the ATOMMS measurements to the 1% level. This would require approximately 400 total in-situ instruments, a very large number of laboratory quality sensors. It would be difficult, if not impossible, to locate these sensors close enough to the signal propagation path without interfering with signal itself. Furthermore, if the water vapor variations during the heavy rainfall were still larger than the 8% variations preceding the heavy rainfall, then still denser in-situ sampling would be required.

This immediately raises the question of whether one could actually develop, deploy, operate, maintain and protect such a large number of instruments along an elevated path during the kind of severe weather that was required to achieve the high opacities that were observed. We considered using one or more unmanned aerial vehicles (UAV) carrying precise humidity, temperature and pressure sensors making measurements along the path during the ATOMMS measurements. This solution has advantages of flexibility and relatively low cost, but it is not clear that any existing UAV humidity instrumentation can meet our performance needs. Furthermore, the biggest problem with an UAV approach is simply that the UAVs may not survive the intense convective activity that produced the high optical depths observed during our experiment.

We also considered deploying a series of tethered balloons along the 5.4 km path. However, the problem again is that during intense convective activity, with heavy rain, lighting, severe winds and downdrafts, the balloons would have been dangerous, potentially starting fires when struck by lightning, with at least a subset being destroyed, and the likelihood that the measurement accuracy required to validate ATOMMS would have been low. Given that sonde humidity sensors are notorious for getting wet during rain which yields positively biased humidity during and following rain, just the rainfall itself would likely have degraded the balloons' measurement accuracy.

We discussed using instrumented towers with experts at NCAR, with experience deploying in situ sensors for field experiments. Towers appear to offer the approach most likely capable of successful, accurate measurements aloft during such extreme weather conditions. However, issues of safety for both the instruments and personnel and environment remain as the towers would certainly act as lightning rods, with the potential to start fires. Furthermore, purchasing and deploying the hundreds of towers of sufficient height required to achieve confirmation at 1% would be quite expensive.

Assuming an approximate cost of $2,500 per chilled mirror hygrometer, 400 such instruments would cost one million dollars. Each would require a data collection system and should be monitored somehow during data collection. The instruments would then need to be placed at the altitude of the ATOMMS signal path where they would have to be protected from heavy rain, winds and lightning. It is also not clear how many personnel would be required to implement, maintain and operate such an array.

The point of the preceding discussion is that verification by in situ measurements at the level of 1% uncertainty achieved by the ATOMMS measurements and retrievals out in the field is very difficult (if even possible). As noted, we have not yet identified any practical, cost-effective way to make a sufficient number of *in-situ* observations along the beam path that could have been used to evaluate the ATOMMS retrievals at their level of 1% precision during periods of intense convection.

Acknowledgments

We want to thank Jeff Kingsley for his support in making critical resources available at the University of Arizona’s Steward Observatory needed to complete the ATOMMS instrumentation, and Chris Walker for sharing the Steward Observatory Radio Astronomy Laboratory (SORAL) facilities with us during development of the prototype ATOMMS instrument. We also want to thank Jim Grantham for providing access and modifications to the Mt Bigelow and Mt Lemmon facilities to support these observations. We thank David Adams and two anonymous reviewers whose constructive criticism improved the presentation of this paper considerably. This work was supported by the National Science Foundation Major Research Instrumentation (MRI) Program grant 0723239 and the National Science Foundation, Division of Atmospheric and Geospace Sciences (GEO/AGS) grants 0946411 and 1313563. In particular, we want to thank Jay Fein, program scientist and manager at NSF, who passed away in 2016. Without Jay’s insight and relentless effort and support, this research would never have been funded and taken place.

References

Allan, R.P., and B.J. Soden (2008), Atmospheric warming and the amplification of precipitation extremes. Science, 321, 1481-1484, doi: 10.1126/science.1160787.

Bohren, Craig F., and Donald R. Huffman. 1983. *Absorption and scattering of light by small particles*. New York: Wiley.

Bony, S., B. Stevens, D. M. W. Frierson, C. Jakob, M. Kageyama, and R. Pincus (2015), Clouds, circulation and climate sensitivity, Nature Geosci 8, 261–268, doi:10.1038/ngeo2398.

Brogniez, H., S. English, J.-F. Mahfouf, A. Behrendt, W. Berg, S. Boukabara, S. A. Buehler, P. Chambon, A. Gambacorta, A. Geer, W. Ingram, E. R. Kursinski, M. Matricardi, T. Odintsova, V. Payne, P. Thorne, M. Tretyakov, and J. Wang (2016), A review of sources of systematic errors and uncertainties in water vapor information derived from observations at 183 GHz, *Atmospheric Measurement Techniques* 9, no. 5 (2016): 2207-2221, doi:10.5194/amt-9-2207-2016.

Calbet, X., N. Peinado-Galan, S. DeSouza-Machado, E.R. Kursinski, P. Oria, D. Ward, A. Otarola, P. Rípodas, and R Kivi (2018), Can turbulence within the field of view cause significant biases in radiative transfer modelling at the 183 GHz band? *Submitted to Atmos. Meas. Tech.*, doi.org/10.5194/amt-2018-181.

Cardinali, C. and S. Healy (2014), Impact of GPS radio occultation measurements in the ECMWF system using adjoint-based diagnostics. Q.J.R. Meteorol. Soc., 140: 2315–2320. doi: 10.1002/qj.2300.

Chen, J., A. D. del Genio, B. E. Carlson and M. G. Bosilovich, (2008), The Spatiotemporal Structure of Twentieth-Century Climate Variations in Observations and Reanalyses. Part I: Long-Term Trend. *J. Climate*, *21(11)*, 2611-2633.

Crum, T.D. and R.L. Alberty, 1993: The WSR-88D and the WSR-88D Operational Support Facility. *Bull. Amer. Meteor. Soc.*, **74**, 1669–1688, doi.org/10.1175/1520-0477(1993)074<1669:TWATWO>2.0.CO;2

Durran, D. R., and J. A. Weyn (2016), Thunderstorms Do Not Get Butterflies, *Bull. Amer. Met. Soc.*, February 2016, P. 237-244, doi.org/10.1175/BAMS-D-15-00070.1.

Field Code Changed

Formatted: Font: 10 pt

Formatted: Font: 10 pt

Formatted: Font: 10 pt

Esau, I. and S. Sorokina (2010), Climatology of the Arctic Planetary Boundary Layer, in Atmospheric Turbulence, Meteorological Modeling and Aerodynamics, Editors: P. R. Lang and F. S. Lombargo, 2009 Nova Science Publishers, Inc., ISBN 978-1-60741-091-1.

Guan, B., and D. E. Waliser (2015), Detection of atmospheric rivers: Evaluation and application of an algorithm for global studies. *J. Geophys. Res. Atmos.*, **120**, 12 514–12 535, doi:10.1002/2015JD024257.

Hajj, G. A., E. R. Kursinski, and S. J. Walter. "Examining the Appropriate GPS Science Signal Suitable for Radio Occultation Measurements of Atmospheric Water Vapor." *Fall AGU* (1997): G22C-04.

Hardy, K. R., Hajj, G. A. and Kursinski, E. R. (1994), Accuracies of atmospheric profiles obtained from GPS occultations. Int. J. Satell. Commun., 12: 463-473. doi:10.1002/sat.4600120508.

Hearty, T. J., A. Savtchenko, B. Tian, E. Fetzer, Y. L. Yung, M. Theobald, B. Vollmer, E. Fishbein, and Y.-I. Won (2014), Estimating sampling biases and measurement uncertainties of AIRS/AMSU-A temperature and water vapor observations using MERRA reanalysis, J. Geophys. Res. Atmos., 119, 2725–2741, doi:10.1002/2013JD021205.

Held, Isaac M. and Soden, Brian J. (2000), Water vapor feedback and global warming, Annu Rev Energy Environ., 25, 441 – 475, doi: 10.1146/annurev.energy.25.1.441.

Herman, B., D. Feng, and X. Xun. "GPS Remote Sensing Using a Third Frequency for Water Vapor Profiles of the Atmosphere." *Fall AGU* (1997).

Houze, R. A., Jr. (2004), Mesoscale convective systems, *Rev. Geophys*., 42, RG4003, doi:10.1029/2004RG000150.

Itterly, K. F., P. C. Taylor, J. B. Dodson, and A. B. Tawfik (2016), On the sensitivity of the diurnal cycle in the Amazon to convective intensity, J. Geophys. Res. Atmos., 121, 8186–8208, doi:10.1002/2016JD025039.

Kay, J. E., and A. Gettelman (2009), Cloud influence on and response to seasonal Arctic sea ice loss, *J. Geophys. Res*., **114**, D18204, doi:10.1029/2009JD011773.

Klingebiel, M., A. de Lozar, S. Molleker, R. Weigel, A. Roth, L. Schmidt, J. Meyer, A. Ehrlich, R. Neuber, M. Wendisch, and S. Borrmann (2015), Arctic low-level boundary layer clouds: in situ measurements and simulations of mono- and bimodal supercooled droplet size distributions at the top layer of liquid phase clouds, *Atmos. Chem. Phys*., **15**, 617–631, doi:10.5194/acp-15-617-2015.

Kuo, Y.-H., et al. (1998), A GPS/MET Sounding through an Intense Upper-Level Front, *Bull. Amer. Meteor. Soc.*, **79**, 617-626.

Kursinski, E. R., G. A. Hajj, J. T. Schofield, R. P. Linfield and K. R. Hardy (1997), Observing Earth's atmosphere with radio occultation measurements using the Global Positioning System, Journal of Geophysical Research: Atmospheres, (1984-2012), 102.D19 (1997): 23429-23465.

Kursinski, E. R., D. Feng, D. Flittner, G. Hajj, B. Herman, S. Syndergaard, D. Ward and T. Yunck (2002), A microwave occultation observing system optimized to characterize atmospheric water, temperature and geopotential via absorption, J. Atmos. Oceanic Technol., 19, 1897-1914.

Field Code Changed

Formatted: No underline

Formatted: No underline

Kursinski, E. R., D. Feng, D. Flittner, G. Hajj, B. Herman, F. Romberg, S. Syndergaard, D. Ward, and T. Yunck (2004), An Active Microwave Limb Sounder for Profiling Water Vapor, Ozone, Temperature, Geopotential, Clouds, Isotopes and Stratospheric Winds, in *Occultations for Probing Atmosphere and Climate* (OPAC-1), Springer-Verlag, Berlin, ISBN 978-3-540-22350-4, p. 173-188.

Kursinski, E.R., R. A. Bennett, D. Gochis, S. I. Gutman, K. L. Holub, R. Mastaler, C. Minjarez Sosa, I. Minjarez Sosa, and T. van Hove (2008), Water vapor and surface observations in northwestern Mexico during the 2004 NAME enhanced observing period, Geophys. Res. Lett., 35, L03815, doi:10.1029/2007GL031404.

Kursinski, E. R., D. Ward, A. Otarola, R. Frehlich, Christopher Groppi, S. Albanna, M. Shein, W. Bertiger, H. Pickett, and M. Ross (2009), The active temperature, ozone and moisture microwave spectrometer (ATOMMS), In *New Horizons in Occultation Research*, pp. 295-313. Springer Berlin Heidelberg.

Kursinski, E. R., Ward, D., Stovern, M., Otarola, A. C., Young, A., Wheelwright, B., Stickney, R., Albanna, S., Duffy, B., Groppi, C., and Hainsworth, J. (2012), Development and testing of the Active Temperature, Ozone and Moisture Microwave Spectrometer (ATOMMS) cm and mm wavelength occultation instrument, Atmos. Meas. Tech., 5, 439-456, doi:10.5194/amt-5-439-2012.

Kursinski, E.R., and T. Gebhardt (2014). A Method to Deconvolve Errors in GPS RO-Derived Water Vapor Histograms. *J. Atmos. Ocean. Technol.*, **31**(12):2606–2628, *https://doi.org/10.1175/JTECH-D-13-00233.1*

Kursinski, E. R., D. Ward, A. C. Otarola, A. L. Kursinski and C. McCormick (2016a), Reducing Climate and Weather Prediction Uncertainty via cm- and mm-Wavelength Satellite to Satellite Occultations, *White Paper Submitted to 2017 ESAS Decadal Survey In Applications\ of\ ATOMMS\ 072118.docx response to RFI#1, January 2016,* http://surveygizmoresponseuploads.s3.amazonaws.com/fileuploads/15647/2289356/183-ea6d9954df8cfcbdb60a500c254348c4_KursinskiEmilR.pdf

Kursinski, E. R., D. Ward, A. C. Otarola, J. McGhee, M. Stovern, K. Sammler, H. Reed, D. Erickson, C. McCormick and E. Griggs (2016b). Atmospheric profiling via satellite to satellite occultations near water and ozone absorption lines for weather and climate. Proc. SPIE 9881, Earth Observing Missions and Sensors: Development, Implementation, and Characterization IV, 98810Z (May 2, 2016); doi:10.1117/12.2224038.

Leary, C. A. (1980), Temperature and humidity profiles in mesoscale unsaturated downdrafts, *J. Atmo. Sci.*, 37, p. 1005-1012.

Liebe, H.J., G.A. Hufford, and M.G. Cotton (1993), Propagation Modeling of Moist Air and Suspended Water/Ice Particles at Frequencies Below 1000 GHz. AGARD Conference Proc. 542, Atmospheric Propagation Effects through Natural and Man-Made Obscurants for Visible to MM-Wave Radiation, pp.3.1-3.10.

Liu, C. L., G. Kirchengast, S. Syndergaard, E. R. Kursinski, Y. O. Sun, W. H. Bai and Q. F. Du (2017), A review of LEO-LEO occultation techniques using microwave and infrared-laser signals, *Advances in Space Research.*

Otarola, A.C., Querel, R., and Kerber, F., (2011), "Precipitable Water Vapor: Considerations on the water vapor scale height, dry bias of the radiosonde humidity sensors, and spatial and temporal variability of the humidity field", Contribution in

Field Code Changed

Formatted: Font: 10 pt

Formatted: Font: 10 pt

Formatted: Font: 10 pt

conference "Comprehensive characterization of astronomical sites", held October 4-10, 2010, in Kislovodsk, Russia, arXiv:1103.3025v1 [astro-ph.IM].

Paine, S. (2011), Atmospheric Model am 7.2, http://www.cfa.harvard.edu/~spaine/am/, Harvard-Smithsonian Center for Astrophysics, Cambridge, MA, 02138.

Rodgers, C. D. (2000). *Inverse methods for atmospheric sounding: theory and practice* (Vol. 2). World Scientific.

Schiro, K. A., J. D, Neelin, D. K. Adams and B. R. Lintner (2016), Deep Convection and Column Water Vapor over Tropical Land versus Tropical Ocean: A Comparison between the Amazon and the Tropical Western Pacific, *J. Atmos. Sci*., 73, p. 4043-4063, DOI: 10.1175/JAS-D-16-0119.1.

Sherwood, S. C., R. Roca, T. M. Weckwerth, and N. G. Andronova (2010~~2010~~), Tropospheric water vapor, convection, and Rev. Geophys., 48, RG2001, doi:10.1029/2009RG000301.

Uttal, T., et al. (2002), Surface heat budget of the Arctic Ocean. *Bull. Amer. Meteor. Soc.*, **83,** 255–275.

Wallace, J. M., and P. V. Hobbs (1977), Atmospheric Science: An Introductory Survey, Academic, New York.

Wang, J., A. Dai and C. Mears (2016), Global Water Vapor Trend from 1988 to 2011 and Its Diurnal Asymmetry Based on GPS, Radiosonde, and Microwave Satellite Measurements, *J. Clim*., **29**, p. 5205-5222, DOI: 10.1175/JCLI-D-15-0485.1.

Willingham, K. M. , E. J. Thompson, K. W. Howard and C. L. Demspey (2010), Characteristics of Sonoran Desert Microbursts, *Weather and Forecasting*, 26, p. 94-108, DOI: 10.1175/2010WAF2222388.1.

Wong, S., E. J. Fetzer, M. Schreier, G. Manipon, E. F. Fishbein, B. H. Kahn, Q. Yue, and F. W. Irion (2015), Cloud-induced uncertainties in AIRS and ECMWF temperature and specific humidity, J. Geophys. Res. Atmos., 120, 1880–1901, doi:10.1002/2014JD022440.

~~Yue, Q., Fetzer, E. J., Kahn, B. H., Wong, S., Manipon, G., Guillaume, A., & Wilson, B. (2013). Cloud-state-dependent sampling in AIRS observations based on CloudSat cloud classification. Journal of Climate, 26(21), 8357-8377.~~

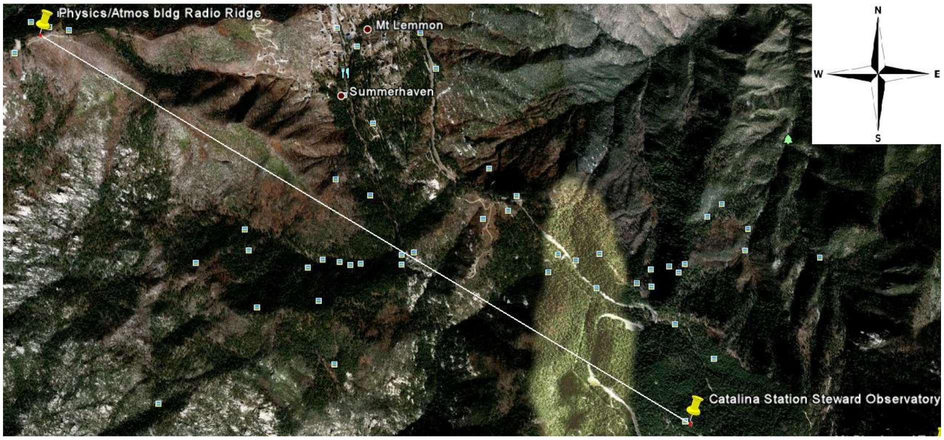

Figure 1: Geometry for the ATOMMS ground-based prototype instrument tests. The H~~h~~igh-B ~~b~~and transmitter was located on Ridge near Mt. Lemmon at an altitude of 2752 m, and the H~~h~~igh-B ~~b~~and receiver was located 5.4 km away at the Catalina Station Observatory near Mt. Bigelow at an altitude of 2515 m. The signal propagation path lies along a northwest to southeast line.

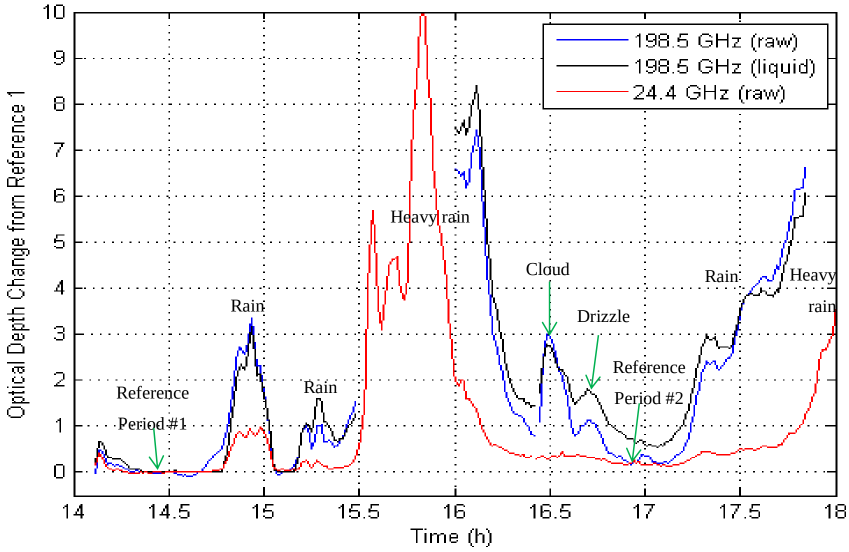

Figure 2: Blue and red lines show observed changes in optical depth at 198.5 GHz and 24.4 GHz relative to reference period 1. The black line shows changes in optical depth at 198.5 GHz due to changes in liquid water after removing the contribution from changes in vapor pressure and temperature.

black line shows changes in optical depth at 198.5 GHz due to changes in liquid water after removing the contribution from changes in vapor pressure and temperature.

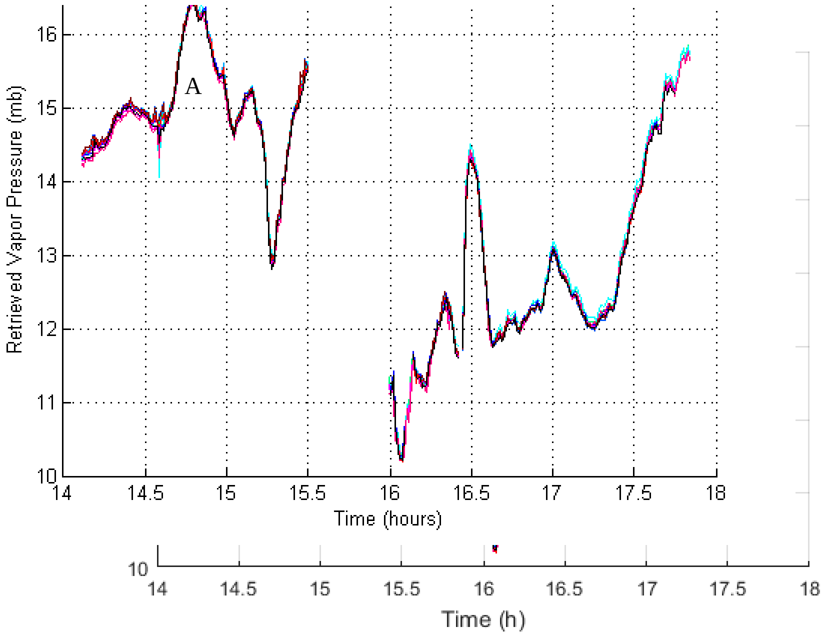
Retrieved Vapor Pressure (mb)
16
15
14
13
12
11
10
A
14
14.5
15
15.5
16
16.5
17
17.5
18
Time (hours)
10
14
14.5
15
15.5
16
16.5
17
17.5
18
Time (h)

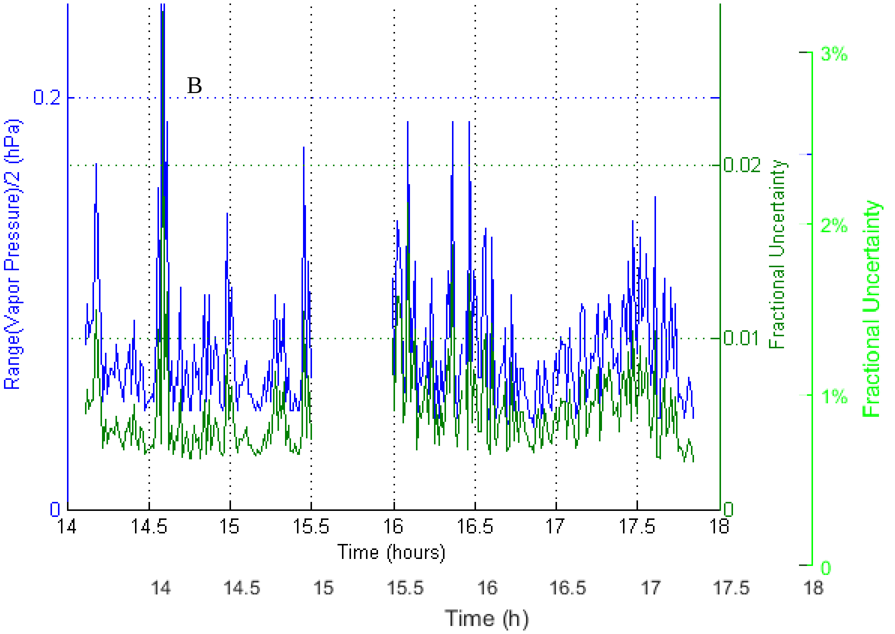

Figure 3: A. Retrieved vapor pressure for the 12 retrieval test cases described in the text. Each line is a different color. B. Blue line and left axis indicate the half range, which is one half of the maximum minus minimum vapor pressure from the 12 retrieval cases; green line and right axis is the half range divided by the absolute vapor pressure at each retrieval point expressed in percent. The strong peaks near 14.6 hours are due to momentary noise in the calibration signal.

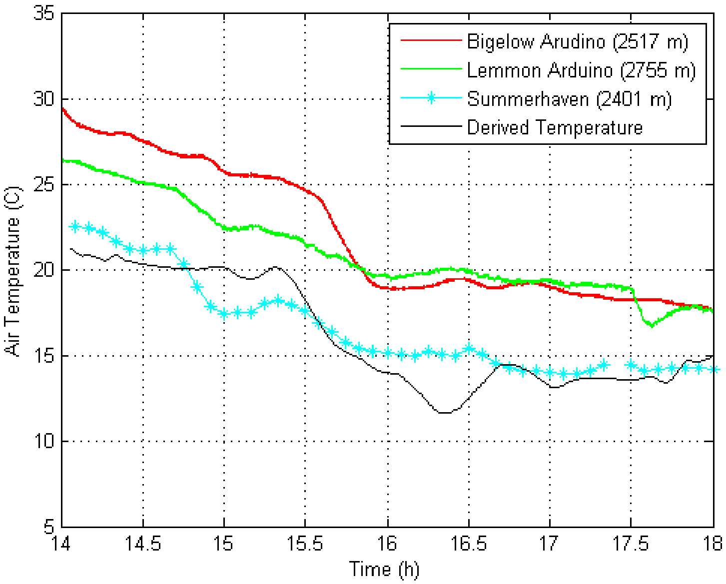

Figure 4: Observed and derived air temperatures during the ATOMMS ground-based experiment.

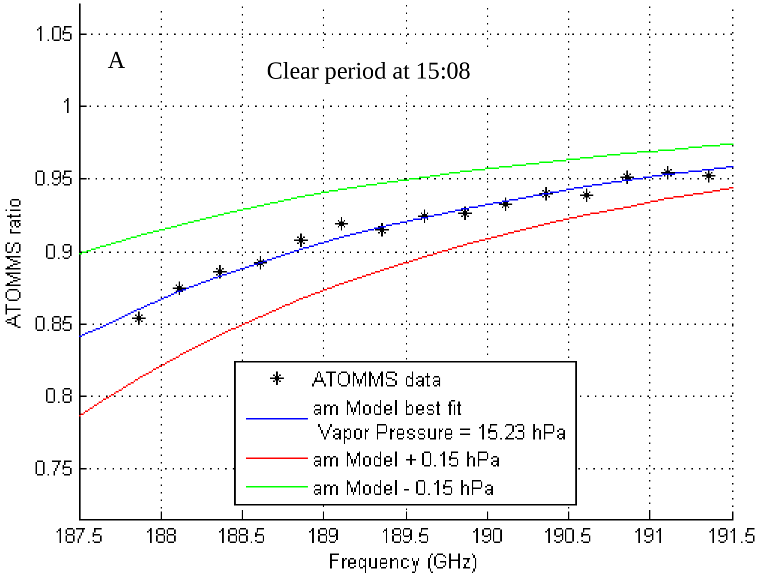
A
Clear period at 15:08
ATOMMS ratio
Frequency (GHz)
1.05
1
0.95
0.9
0.85
0.8
0.75
187.5
188
188.5
189
189.5
190
190.5
191
191.5
ATOMMS data
am Model best fit
Vapor Pressure = 15.23 hPa
am Model + 0.15 hPa
am Model - 0.15 hPa

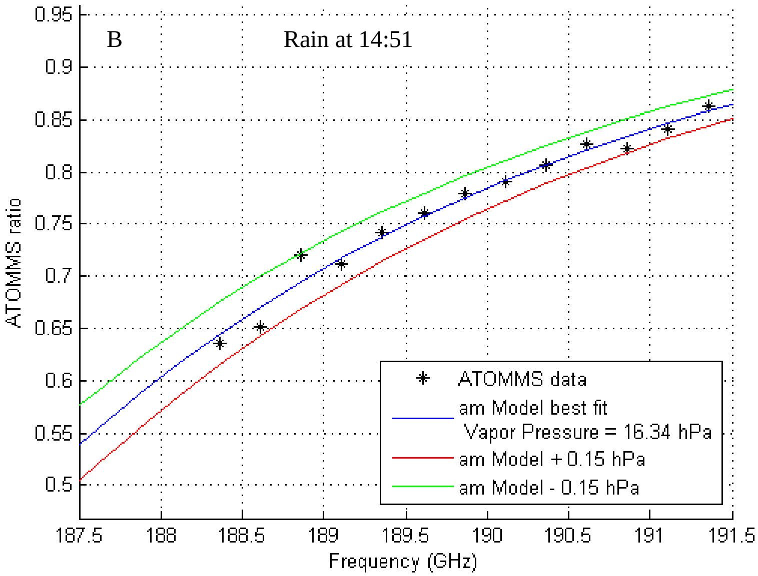
B
Rain at 14:51
ATOMMS ratio
0.95
0.9
0.85
0.8
0.75
0.7
0.65
0.6
0.55
0.5
187.5
188
188.5
189
189.5
190
190.5
191
191.5
Frequency (GHz)
ATOMMS data
am Model best fit
Vapor Pressure = 16.34 hPa
am Model + 0.15 hPa
am Model - 0.15 hPa

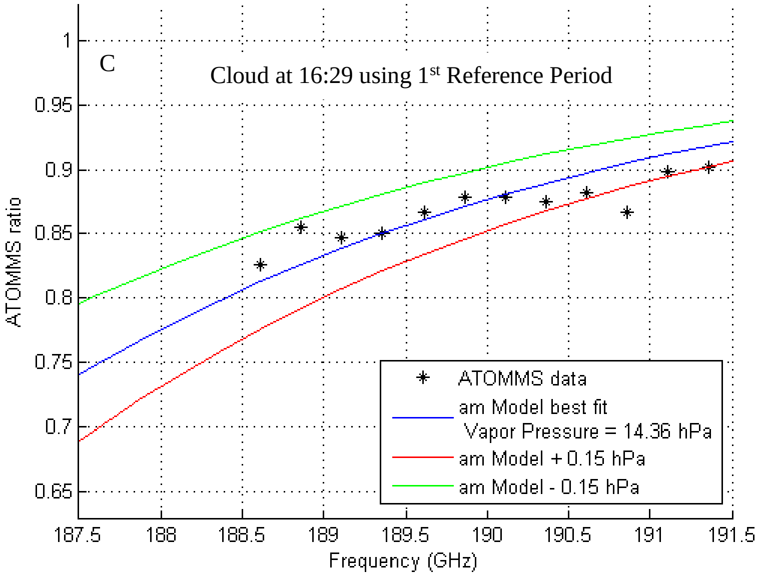
C
Cloud at 16:29 using 1st Reference Period
ATOMMS ratio
1
0.95
0.9
0.85
0.8
0.75
0.7
0.65
187.5
188
188.5
189
189.5
190
190.5
191
191.5
Frequency (GHz)
ATOMMS data
am Model best fit
Vapor Pressure = 14.36 hPa
am Model + 0.15 hPa
am Model - 0.15 hPa

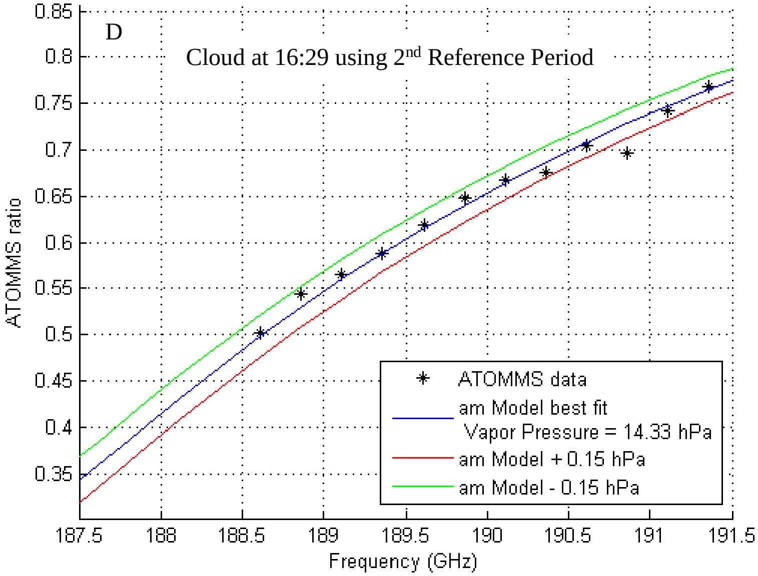

Figure 5: Examples of fitting the observed ATOMMS amplitude ratio, Eq. (2) (black asterisks), to the forward calculated ATOMMS ratio using using *am7.2*~~the am Model, version 7.2~~. Blue line is the best fit line for the indicated vapor pressure. Red line is am forward pressure 0.15 hPa greater than the best fit vapor pressure. Green line is forward calculation for a vapor pressure 0.15 hPa less than the best fit vapor pressure. The solutions shown in panels A, B, and C used reference period 1, while the solution in panel D used reference period 2.

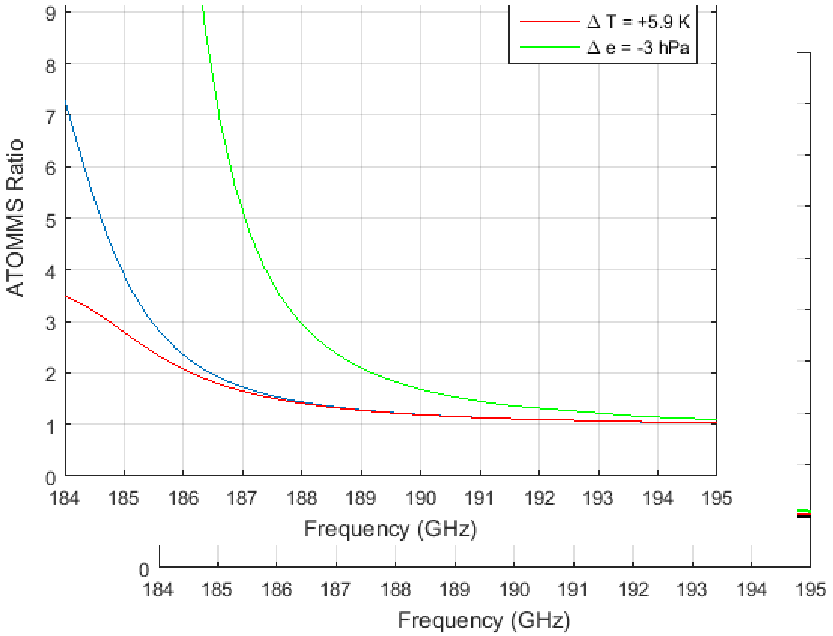

~~Figure 6: ATOMMS ratio for three atmospheric changes along the 5.4 km observation path relative to reference conditions:~~ **conditions: vapor pressure decreased by 1 hPa (blue), temperature increased by 5.9 K (red), vapor pressure decreased by 3 hPa (green), and air pressure increased by 10 hPa (black). The reference conditions were air pressure = 743 hPa, air temperature = 20° C, and vapor pressure = 15 hPa.**

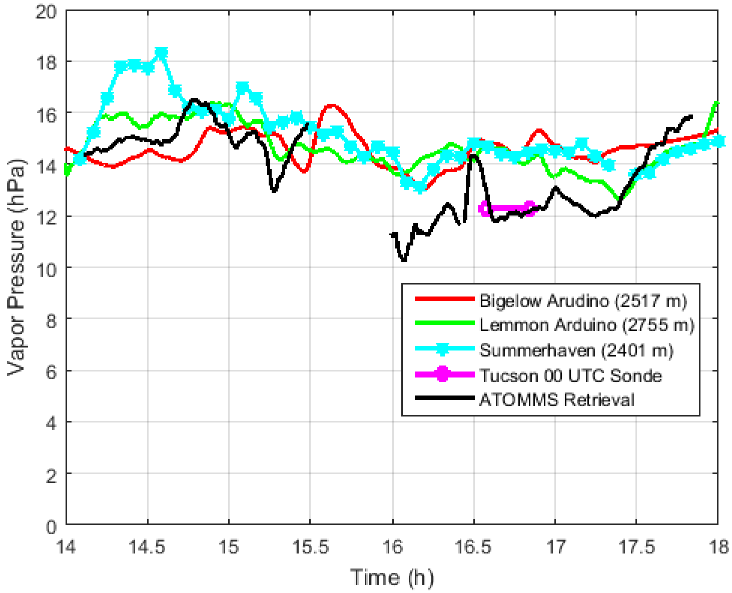

Figure 7: Observed and retrieved vapor pressures. The sonde line indicates the average vapor pressure over the altitude range of the ATOMMS instruments as reported in the 00 UTC Tucson sonde for August 19.

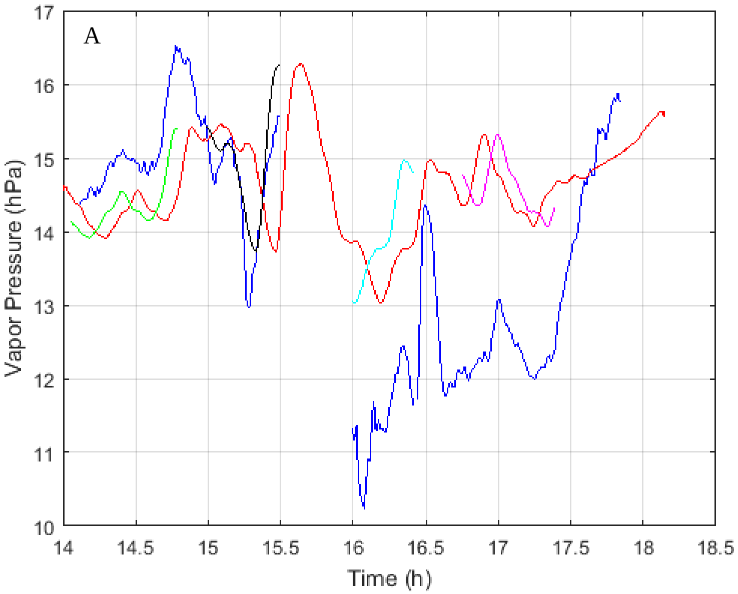
A
17
16
15
14
13
12
11
10
Vapor Pressure (hPa)
14
14.5
15
15.5
16
16.5
17
17.5
18
18.5
Time (h)

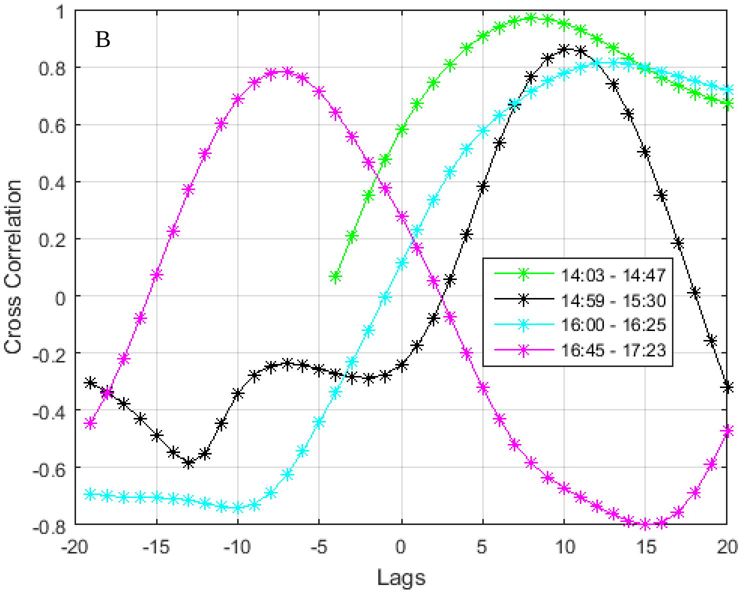

Figure 8: A. Vapor pressure derived from ATOMMS observations (blue) and measured with an in-situ sensor on Mt. Bigelow (red). Also shown in other colors are four time segments of the in-situ observations shifted in time (as described in text) to highlight correlation between the two vapor pressure data sets. The time shift for each colored line is indicated in panel (B). B. Cross-correlation coefficients as a function of sample lags between the ATOMMS-derived vapor pressure and in-situ measurements of water vapor taken on Mt. Bigelow. The four lines correspond with the four time segments described in the text: green (14:03 – 14.47 hours), black (14:59 to 15:30 hours), cyan (16:00 to 16:25 hours), and magenta (16:45 to 17:23 hours)~~(14.06 – 14.79 hours), black (14.99 to 15.49 hours), cyan (16.00 to 16.42 hours), and magenta (16.75 to 17.39 hours)~~.

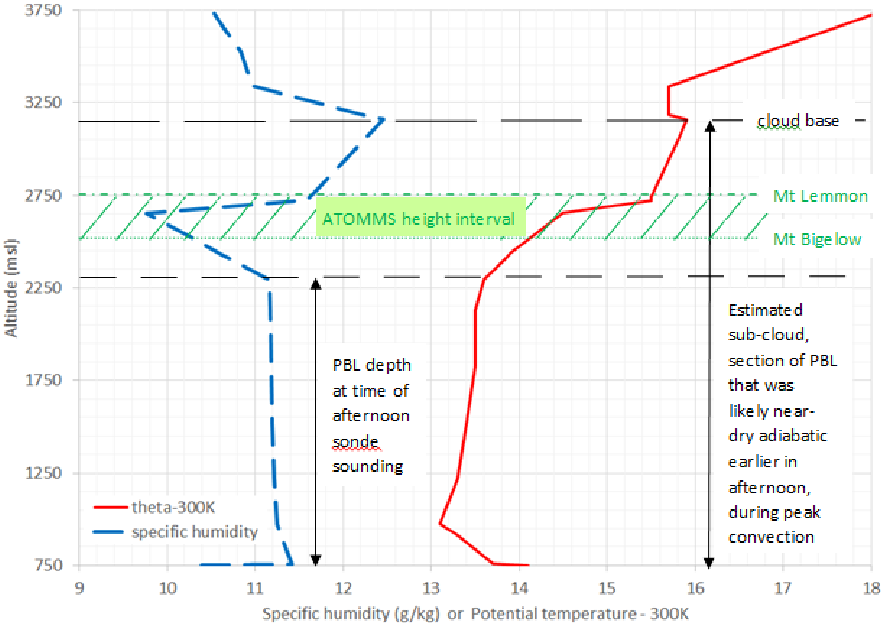

Figure 9: Vertical profiles of specific humidity and potential temperature minus 300 K calculated from the 00 UTC Tucson sonde. The local time of the sonde launch was approximately 16:30 on August 18. Theta label for the red line stands for potential temperature and PBL stands for planetary boundary layer. 5

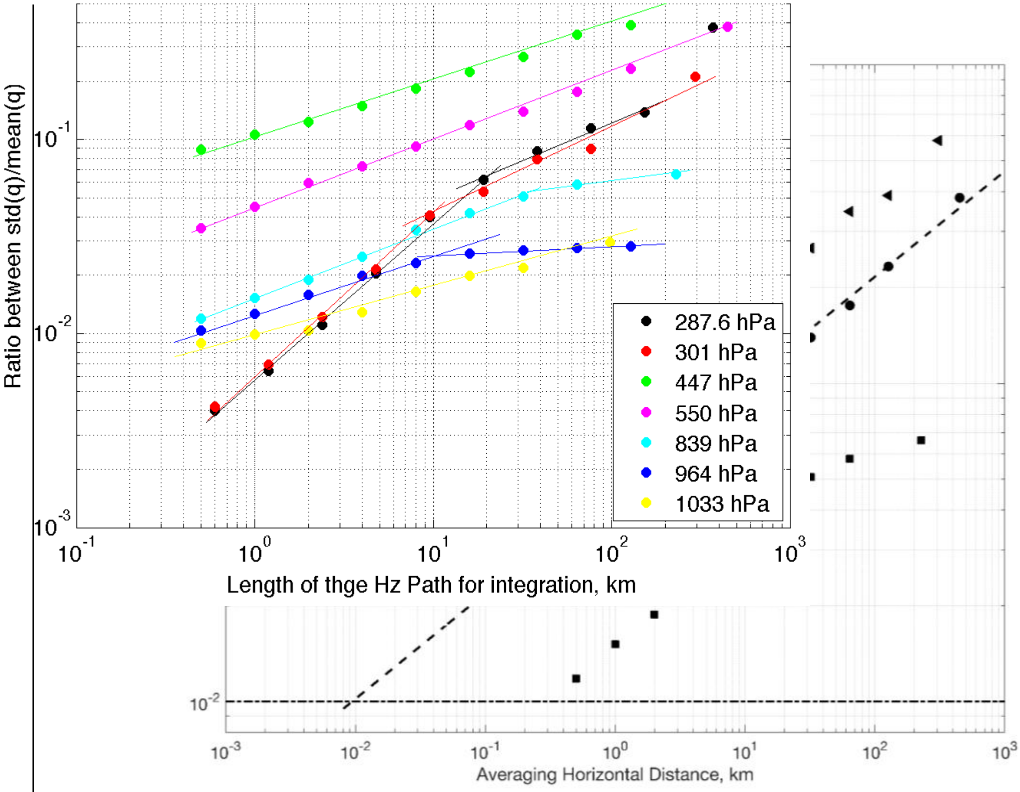

Figure A1: Ratio of the standard deviation of absolute humidity to the mean absolute humidity based on aircraft data taken at different altitudes, which is indicated by the air pressure along different flight paths. The red star on the dashed line constructed for the 550 hPa altitude observations corresponds with the value calculated from the three in-situ sensors operating during the ATOMMS mountaintop experiment (ratio of 8% for a 5 km path). The slope of the dashed line corresponds with a power law exponent of 0.35 for the dependence of std(q)/mean(q) with the length of the path, which is consistent with Kolomogorov turbulence. Extrapolation of this line to a std(q)/mean(q) value equal to 1% indicates that in-situ observations are required every 10 m in order to validate the 1% accuracy of the ATOMMS retrievals. Adapted from Otarola et al. (2011).

~~**Figure A1: Solid lines with dots show the ratio of the standard deviation of absolute humidity to the mean absolute humidity based on aircraft data taken at different altitudes, which is indicated by the air pressure along different flight paths. The blue dot on the dashed blue line corresponds with the value calculated from the three in-situ sensors operating during the experiment (ratio of 8% for a 5 km path). The slope of the dashed blue line corresponds with a power law exponent of 0.35 for the dependence of std(q)/mean(q) with the length of the path, which is consistent with Kolomogorov turbulence. Extrapolation of this line to std(q)/mean(q) to 1% would indicate that in-situ observations are required every 13 m in order to validate the 1% accuracy of the ATOMMS retrievals. Adapted from *Otarola et al.* (2011).**~~